crystals

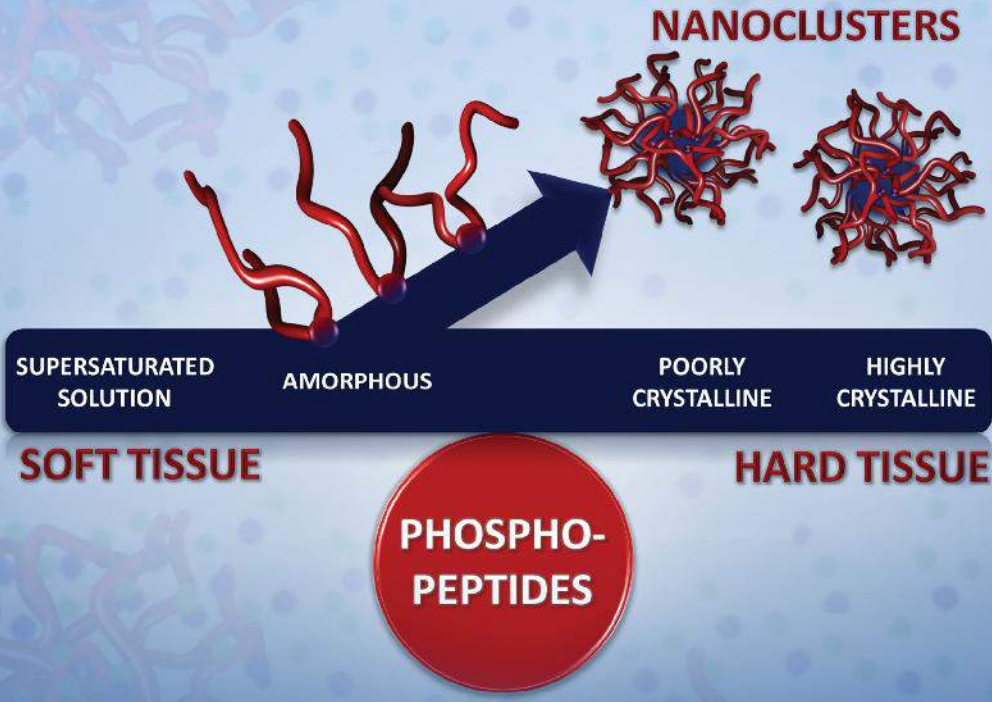

Structural Biology of Calcium Phosphate Nanoclusters Sequestered by Phosphoproteins

Volume 10 · Issue 9 | September 2020

MDPI

mdpi.com/journal/crystals
ISSN 2073-4352

Editorial Board

Editors (10)

Prof. Dr. Helmut Cölfen Website SciProfiles
Editor-in-Chief
Physical Chemistry, Universität Konstanz, Germany
Interests: nucleation; nanoparticle self organization; non classical crystallization; mesocrystals; biomineralization; nanoparticle analysis by fractionating methods
Special Issues and Collections in MDPI journals

Prof. Dr. Leonid Kustov * Website SciProfiles
Section Editor-in-Chief
1. National University of Science and Technology «MISIS», Moscow 119049, Russia
2. Department of Chemistry, M. V. Lomonosov Moscow State University, Moscow 119992, Russia
3. N. D. Zelinsky Institute of Organic Chemistry, Russian Academy of Sciences, Moscow 119991, Russia
Interests: catalysis; nanomaterials; renewables; green chemistry
* Section: Hybrid and Composite Crystalline Materials
Special Issues and Collections in MDPI journals

Prof. Dr. Jesús Sanmartín-Matalobos * Website SciProfiles
Section Editor-in-Chief
Inorganic Chemistry Department, University of Santiago de Compostela, 15782 Santiago de Compostela, Spain
Interests: supramolecular chemistry; coordination chemistry; single crystal X-ray crystallography; H-bonding; chirality; fluorescence
* Section: Macromolecular Crystals
Special Issues and Collections in MDPI journals

Prof. Dr. Wolfgang W. Schmahl * Website SciProfiles
Section Editor-in-Chief
Department of Earth and Environmental Sciences, Ludwig Maximilian University of Munich, 80333 Munich, Germany
Interests: biomineralization; microstructures; functional Materials; electron microscopy; high resolution diffraction methods
* Section: Crystalline Minerals and Biominerals
Special Issues and Collections in MDPI journals

Prof. Dr. Neil Champness * ★ Website
Section Editor-in-Chief
School of Chemistry, University of Nottingham, Nottingham, UK
Interests: supramolecular chemistry; crystal engineering; chemical nanoscience; molecular organisation from solid-state and solution-based self-assembly of nanoscale molecular architectures to success in surface molecular organisation
* Section: Organic Crystalline Materials

Prof. Dr. Heike Lorenz * Website SciProfiles
Section Editor-in-Chief
Max Planck Institute for Dynamics of Complex Technical Systems, 39106 Magdeburg, Germany
Interests: phase equilibria; crystallization kinetics; process monitoring & design; separation of fine chemicals, large scale industrial products and renewable resources; innovative crystallization-based separation concepts; enantiomers; natural products; multi-component mixtures
* Section: Industrial Crystallization
Special Issues and Collections in MDPI journals

Prof. Dr. Slawomir J. J. Grabowski * Website SciProfiles
Section Editor-in-Chief
Kimika Fakultatea, Euskal Herriko Unibertsitatea UPV/EHU, Donostia International Physics Center (DIPC), P.K. 1072, 20080, Donostia, Euskadi, Spain
Interests: hydrogen bond; Lewis acid–Lewis base interactions; atoms in molecules theory; ab initio calculations
* Section: "Crystal Engineering"
Special Issues and Collections in MDPI journals

Prof. Dr. Abel Moreno * Website SciProfiles
Section Editor-in-Chief
Instituto de Química, Universidad Nacional Autónoma de México. Av. Universidad 3000, Cd.Mx. 04510, Mexico
Interests: protein crystals; biocrystals; crystal growth; protein crystallography; crystal chemistry; biomineralization; biomimetics; biological macromolecules
* Section: "Biomolecular Crystals"
Special Issues and Collections in MDPI journals

Prof. Dr. Charles Rosenblatt * Website
Section Editor-in-Chief
Ohio Eminent Scholar and Professor of Physics, Department of Physics, Case Western Reserve University Cleveland, OH 44106-7079, USA
Interests: liquid crystals and complex fluids (electric and magnetic field effects, interfaces, phase transitions, colloidal inclusions); fluid interface instabilities; microgravity
* Section: "Liquid Crystals"
Special Issues and Collections in MDPI journals

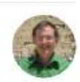

Prof. Dr. Shujun Zhang * Website SciProfiles
Section Editor-in-Chief
ISEM/AIIM, University of Wollongong, Wollongong, NSW 2500, Australia
Interests: piezoelectricity; ferroelectricity; crystals; ceramics; transducers
* Section: "Crystalline Materials"
Special Issues and Collections in MDPI journals

Previous Editor

Prof. Dr. Gerd Meyer * Website
Former Editor-in-Chief
Institut für Anorganische Chemie, Universität zu Köln, Greinstraße 6, D-50939 Köln, Germany
Interests: rare-earth and transition metal; solid state; coordination chemistry
* Founding Editor-in-Chief
Special Issues and Collections in MDPI journals

Advisory Board (9)

Prof. Dr. Masakazu Anpo SciProfiles
1. State Key Laboratory of Photocatalysis on Energy and Environment, Fuzhou University, Fuzhou 350117, China
2. Department of Applied Chemistry, Osaka Prefecture University, Osaka 599-8531, Japan
Interests: photocatalysis; heterogeneous catalysis; photoluminescence spectroscopy; reaction mechanism; clean energy and environment; metal oxide semiconducting materials
Special Issues and Collections in MDPI journals:
Special Issue in Crystals: Photocatalytic Performance of Inorganic and Organic Crystalline Materials

water electrolysis, solar cells, photoelectrochemical water splitting, solar fuels
Special Issues and Collections in MDPI journals:
Special Issue in *Processes: Electrochemical Energy Conversion and Storage Processes*

Prof. Dr. Mohamed Balli Website SciProfiles
International University of Rabat, ParcTechnopolis Rabat, Morocco
Interests: magnetic materials; magnetocaloric materials; caloric materials; magnetic refrigeration; multiferroics; nanomagnetic materials; thin films; single crystals; frustrated magnetism; permanent magnets; soft magnetic materials; structural and physical properties; energy conversion
Special Issues and Collections in MDPI journals:
Special Issue in *Crystals: Advances in Caloric Materials*
Special Issue in *Crystals: Advances in Magnetocaloric Effect Materials*

Dr. Bidhan C. Bandyopadhyay Website
Medicine (GWU) and Biomedical Engineering, Catholic University of America(CUA), DCVA Medical Center, Research Service (151), 50 Irving Street, NW, Washington, DC 20422, USA
Interests: Ca^{2+} signaling; Calcium crystals; calcification; cell injury and cell death

Prof. Dr. Peter Baran Website
Department of Chemistry and Biochemistry, Juniata College, von Liebig Science Center 2035, 1700 Moore Street, Huntingdon, PA 16652, USA
Interests: synthesis of coordination compounds; spectroscopic characterization of coordination compounds; X-ray crystallography of small molecules; crystal growing techniques; coordination compounds with biological activity; coordination polymeric networks

Prof. Dr. Rajratan Basu Website SciProfiles
Department of Physics, The United States Naval Academy, Annapolis, MD 21402, USA
Interests: directed self-assembly of nanomaterials (carbon nanotubes, quantum dots, ferroelectric nanoparticles, graphene, ferromagnetic nanoparticles, gold nanoparticles, nanodiamonds etc.) in liquid crystals; development of liquid crystal / nanomaterials based nano- electromechanical systems; electro-optic devices; micro-switching devices; and electromechanical memory functions; order-disorder phenomena in soft matter systems; liquid crystal phases and phase transitions

IMPACT FACTOR 2.589
CITESCORE 3.2 SCOPUS

Special Issue "Numerical Study of Concrete"

- Print Special Issue Flyer
- Special Issue Editors
- Special Issue Information
- Keywords
- Published Papers

A special issue of *Crystals* (ISSN 2073-4352). This special issue belongs to the section "Industrial Crystallization".

Deadline for manuscript submissions: **closed (31 July 2020)**.

Share This Special Issue

Special Issue Editor

Dr. Vipul Patel E-Mail Website
Guest Editor
School of Engineering and Mathmatical Sciences, La Trobe University, Bendigo, VIC 3552, Australia
Interests: steel–concrete composite strucutres

Special Issue Information

Dear Colleagues,

Concrete is one of the most widely used construction materials in the word today. Research in concrete follows the environment impact, economy, population, and advanced technology. This Special Issue invites recent numerical studies for research in concrete. Some of the topics of interest include finite element analysis, digital concrete, the reinforcement technique without rebars, and 3D printing.

Dr. Vipul Patel
Guest Editor

Manuscript Submission Information

Manuscripts should be submitted online at www.mdpi.com by registering and logging in to this website. Once you are registered, click here to go to the submission form. Manuscripts can be submitted until the deadline. All papers will be peer-reviewed. Accepted papers will be published continuously in the journal (as soon as accepted) and will be listed together on the special issue website. Research articles, review articles as well as short communications are invited. For planned papers, a title and short abstract (about 100 words) can be sent to the Editorial Office for announcement on this website.

Submitted manuscripts should not have been published previously, nor be under consideration for publication elsewhere (except conference proceedings papers). All manuscripts are thoroughly refereed through a single-blind peer-review process. A guide for authors and other relevant information for submission of manuscripts is available on the Instructions for Authors page. *Crystals* is an international peer-reviewed open access monthly journal published by MDPI.

Please visit the Instructions for Authors page before submitting a manuscript. The Article Processing Charge (APC) for publication in this open access journal is 1800 CHF (Swiss Francs). Submitted papers should be well formatted and use good English. Authors may use MDPI's English editing service prior to publication or during author revisions.

Keywords

- Analysis
- Concrete
- Recycle materials
- Compression strength

Published Papers (23 papers)

Download All Papers

Order results: Content type
Result details: Normal

Show export options

Editorial

Jump to: Research

Open Access Editorial

Numerical Study of Concrete

by Vipulkumar Ishvarbhai Patel

Crystals **2021**, *11*(1), 74; https://doi.org/10.3390/cryst11010074 - 18 Jan 2021

Viewed by 526

Abstract This Special Issue, "Numerical Study of Concrete", consists of 22 research articles [...] Full article

(This article belongs to the Special Issue Numerical Study of Concrete)

Research

Jump to: Editorial

Open Access Article

Numerical Analysis of a Novel Shaft Lining Structure in Coal Mines Consisting of Hybrid-Fiber-Reinforced Concrete

by Xuesong Wang, Hua Cheng, Taoli Wu, Zhishu Yao and Xianwen Huang

Crystals **2020**, *10*(10), 928; https://doi.org/10.3390/cryst10100928 - 12 Oct 2020

Cited by 3 | Viewed by 643

Abstract To address the temperature cracking of concrete in frozen shaft linings in extra-thick alluvial layers in coal mines, a novel shaft lining structure of coal mines consisting of hybrid-fiber-reinforced concrete (HFRC) was developed. Using the Finite Element Method (FEM), a numerical simulation test [...] Read more.

(This article belongs to the Special Issue Numerical Study of Concrete)

▶ Show Figures

Open Access Article

Analysis of Concrete Failure on the Descending Branch of the Load-Displacement Curve

by Gennadiy Kolesnikov

Crystals **2020**, *10*(10), 921; https://doi.org/10.3390/cryst10100921 - 12 Oct 2020

Cited by 3 | Viewed by 883

Abstract In this paper, load-displacement and stress-strain diagrams are considered for the uniaxial compression of concrete and under three-point bending. It is known that the destruction of such materials occurs on the descending branch of the load-displacement diagram. The attention of the presented research [...] Read more.

(This article belongs to the Special Issue Numerical Study of Concrete)

▶ Show Figures

Open Access Article

Compressive Strength Forecasting of Air-Entrained Rubberized Concrete during the Hardening Process Utilizing Elastic Wave Method

by Zhi Heng Lim, Foo Wei Lee, Kim Hung Mo, Jee Hock Lim, Ming Kun Yew and Kok Zee Kwong

Crystals **2020**, *10*(10), 912; https://doi.org/10.3390/cryst10100912 - 09 Oct 2020

Cited by 3 | Viewed by 776

Abstract Conventional compressive strength test of concrete involves the destruction of concrete samples or existing structures. Thus, the focus of this research is to ascertain a more effective method to assess the compressive strength of concrete, especially during the hardening process. One of the [...] Read more.

(This article belongs to the Special Issue Numerical Study of Concrete)

▶ Show Figures

Open Access Article

Capillary Water Absorption and Micro Pore Connectivity of Concrete with Fractal Analysis

by Xiangqun Ding, Xinyu Liang, Yichao Zhang, Yanfeng Fang, Jinghai Zhou and Tianbei Kang

Crystals **2020**, *10*(10), 892; https://doi.org/10.3390/cryst10100892 - 01 Oct 2020

Cited by 4 | Viewed by 606

Abstract This study focuses on the relationship between the complexity of pore structure and capillary water absorption of concrete, as well as the connection behavior of concrete in specific directions. In this paper, the water absorption of concrete with different binders was tested during [...] Read more.

(This article belongs to the Special Issue Numerical Study of Concrete)

▶ Show Figures

Open Access Article

Numerical Investigation on Dynamic Response of RC T-Beams Strengthened with CFRP under Impact Loading

by Huiling Zhao, Xiangqing Kong, Ying Fu, Yihan Gu and Xuezhi Wang

Crystals **2020**, *10*(10), 890; https://doi.org/10.3390/cryst10100890 - 01 Oct 2020

Cited by 1 | Viewed by 557

Abstract To precisely evaluate the retrofitting effectiveness of Carbon Fiber Reinforced Plastic (CFRP) sheets on the impact response of reinforced concrete (RC) T-beams, a non-linear finite element model was developed to simulate the structural response of T-beams with CFRP under impact loads. The numerical [...] Read more.

(This article belongs to the Special Issue Numerical Study of Concrete)

► Show Figures

Open Access Article

Constitutive Modeling of New Synthetic Hybrid Fibers Reinforced Concrete from Experimental Testing in Uniaxial Compression and Tension

by S. M. Iqbal S. Zainal, Farzad Hejazi, Farah N. A. Abd. Aziz and Mohd Saleh Jaafar

Crystals **2020**, *10*(10), 885; https://doi.org/10.3390/cryst10100885 - 01 Oct 2020

Abstract Hybridization of fibers in concrete yields a variety of applications due to its benefits compared to conventional concrete or concrete with single type-fiber. However, the Finite Element (FE) modeling of these new materials for numerical analyses are very challenging due to the lack [...] Read more.

(This article belongs to the Special Issue Numerical Study of Concrete)

► Show Figures

Open Access Article

Prediction of Properties of FRP-Confined Concrete Cylinders Based on Artificial Neural Networks

by Afaq Ahmad, Vagelis Plevris and Qaiser-uz-Zaman Khan

Crystals **2020**, *10*(9), 811; https://doi.org/10.3390/cryst10090811 - 14 Sep 2020

Abstract Recently, the use of fiber-reinforced polymers (FRP)-confinement has increased due to its various favorable effects on concrete structures, such as an increase in strength and ductility. Therefore, researchers have been attracted to exploring the behavior and efficiency of FRP-confinement for concrete structural elements [...] Read more.

(This article belongs to the Special Issue Numerical Study of Concrete)

► Show Figures

Open Access Article

Determination of Mohr-Coulomb Parameters for Modelling of Concrete

by Selimir Lelovic and Dejan Vasovic

Crystals **2020**, *10*(9), 808; https://doi.org/10.3390/cryst10090808 - 13 Sep 2020

Abstract Cohesion is defined as the shear strength of material when compressive stress is zero. This article presents a new method for the experimental determination of cohesion at pre-set angles of shear deformation. Specially designed moulds are created to force deformation (close to τ-axis) [...] Read more.

(This article belongs to the Special Issue Numerical Study of Concrete)

► Show Figures

Open Access Article

The Impact Resistance and Deformation Performance of Novel Pre-Packed Aggregate Concrete Reinforced with Waste Polypropylene Fibres

by Fahed Alrshoudi, Hossein Mohammadhosseini, Rayed Alyousef, Mahmood Md. Tahir, Hisham Alabduljabbar and Abdeliazim Mustafa Mohamed

Crystals **2020**, *10*(9), 788; https://doi.org/10.3390/cryst10090788 - 06 Sep 2020

Abstract Pre-packed aggregate fibre-reinforced concrete (PAFRC) is an innovative type of concrete composite using a mixture of coarse aggregates and fibres which are pre-mixed and pre-placed in the formwork. A flowable grout is then injected into the cavities between the aggregate mass. This study [...] Read more.

(This article belongs to the Special Issue Numerical Study of Concrete)

► Show Figures

Open Access Article

Thermal Performance of Alginate Concrete Reinforced with Basalt Fiber

by Seyed Esmaeil Mohammadyan-Yasouj, Hossein Abbastabar Ahangar, Narges Ahevani Oskoei, Hoofar Shokravi, Seyed Saeid Rahimian Koloor and Michal Petrů

Crystals **2020**, *10*(9), 779; https://doi.org/10.3390/cryst10090779 - 03 Sep 2020

Abstract The sustainability of reinforced concrete structures is of high importance for practitioners and researchers, particularly in harsh environments and under extreme operating conditions. Buildings and tunnels are of the places that most of the fire cases take place. The use of fiber in [...] Read more.

(This article belongs to the Special Issue Numerical Study of Concrete)

► Show Figures

Open Access Article

Effects of Erosion Form and Admixture on Cement Mortar Performances Exposed to Sulfate Environment

by Peng Liu, Ying Chen and Zhiwu Yu

Crystals **2020**, *10*(9), 774; https://doi.org/10.3390/cryst10090774 - 01 Sep 2020

Abstract The effects of the admixtures, erosion age, concentration of sulfate solution, and erosion form of sulfate attack on the mechanical properties of mortar were investigated. Simultaneously, the microstructure, pore characteristics, kinds and morphologies of erosion products of mortar before and after sulfate attacks [...] Read more.

(This article belongs to the Special Issue Numerical Study of Concrete)

► Show Figures

Open Access Article

A Coupled Modeling Simulator for Near-Field Processes in Cement Engineered Barrier Systems for Radioactive Waste Disposal

by Steven J. Benbow, Daisuke Kawama, Hiroyasu Takase, Hiroyuki Shimizu, Chie Oda, Fumio Hirano, Yusuke Takayama, Morihiro Mihara and Akira Honda

Crystals 2020, *10*(9), 767; https://doi.org/10.3390/cryst10090767 - 29 Aug 2020

Abstract Details are presented of the development of a coupled modeling simulator for assessing the evolution in the near-field of a geological repository for radioactive waste disposal where concrete is used as a backfill. The simulator uses OpenMI, a standard for exchanging data between [...] Read more.

(This article belongs to the Special Issue Numerical Study of Concrete)

▶ Show Figures

Open Access Article

The Prediction of Stiffness of Bamboo-Reinforced Concrete Beams Using Experiment Data and Artificial Neural Networks (ANNs)

by Muhtar, Amri Gunasti, Suhardi, Nursaid, Irawati, Ilanka Cahya Dewi, Moh. Dasuki, Sofia Ariyani, Fitriana, Idris Mahmudi, Taufan Abadi, Miftahur Rahman, Syarif Hidayatullah, Agung Nilogiri, Senki Desta Galuh, Ari Eko Wardoyo and Rofi Budi Hamduwibawa

Crystals 2020, *10*(9), 757; https://doi.org/10.3390/cryst10090757 - 27 Aug 2020

Abstract Stiffness is the main parameter of the beam's resistance to deformation. Based on advanced research, the stiffness of bamboo-reinforced concrete beams (BRC) tends to be lower than the stiffness of steel-reinforced concrete beams (SRC). However, the advantage of bamboo-reinforced concrete beams has enough [...] Read more.

(This article belongs to the Special Issue Numerical Study of Concrete)

▶ Show Figures

Open Access Article

Numerical Evaluation of the Perfobond (PBL) Shear Connector Subjected to Lateral Pressure Using Coupled Rigid Body Spring Model (RBSM) and Nonlinear Solid Finite Element Method (FEM)

by Muhammad Shoaib Karam, Yoshihito Yamamoto, Hikaru Nakamura and Taito Miura

Crystals 2020, *10*(9), 743; https://doi.org/10.3390/cryst10090743 - 24 Aug 2020

Abstract An analytical investigation focusing on the concrete damage progress of the PBL shear connector under the influence of various lateral pressures, employing a coupled RBSM and solid FEM model was carried out. The analytical model succeeded in simulating the test shear capacities and [...] Read more.

(This article belongs to the Special Issue Numerical Study of Concrete)

▶ Show Figures

Open Access Article

Numerical Simulation of Adsorption of Organic Inhibitors on C-S-H Gel

by Zijian Song, Huanchun Cai, Qingyang Liu, Xing Liu, Qi Pu, Yingjie Zang and Na Xu

Crystals 2020, *10*(9), 742; https://doi.org/10.3390/cryst10090742 - 23 Aug 2020

Abstract Corrosion inhibitors are one of the most effective anticorrosion techniques in reinforced concrete structures. Molecule dynamics (MD) was usually utilized to simulate the interaction between the inhibitor molecules and the surface of Fe to evaluate the inhibition effect, ignoring the influence of cement [...] Read more.

(This article belongs to the Special Issue Numerical Study of Concrete)

▶ Show Figures

Open Access Article

New Prediction Model for the Ultimate Axial Capacity of Concrete-Filled Steel Tubes: An Evolutionary Approach

by Muhammad Faisal Javed, Furqan Farooq, Shazim Ali Memon, Arslan Akbar, Mohsin Ali Khan, Fahid Aslam, Rayed Alyousef, Hisham Alabduljabbar and Sardar Kashif Ur Rehman

Crystals 2020, *10*(9), 741; https://doi.org/10.3390/cryst10090741 - 22 Aug 2020

Abstract The complication linked with the prediction of the ultimate capacity of concrete-filled steel tubes (CFST) short circular columns reveals a need for conducting an in-depth structural behavioral analyses of this member subjected to axial-load only. The distinguishing feature of gene expression programming (GEP) [...] Read more.

(This article belongs to the Special Issue Numerical Study of Concrete)

▶ Show Figures

Open Access Article

Applications of Gene Expression Programming and Regression Techniques for Estimating Compressive Strength of Bagasse Ash based Concrete

by Muhammad Faisal Javed, Muhammad Nasir Amin, Muhammad Izhar Shah, Kaffayatullah Khan, Bawar Iftikhar, Furqan Farooq, Fahid Aslam, Rayed Alyousef and Hisham Alabduljabbar

Crystals 2020, *10*(9), 737; https://doi.org/10.3390/cryst10090737 - 21 Aug 2020

Abstract Compressive strength is one of the important property of concrete and depends on many factors. Most of the concrete compressive strength predictive models mainly rely on available literature data, which are too simple to consider all the contributing factors. This study adopted a [...] Read more.

(This article belongs to the Special Issue Numerical Study of Concrete)

▶ Show Figures

Open Access Article

Use of Flue Gas Desulfurization Gypsum, Construction and Demolition Waste, and Oil Palm Waste Trunks to Produce Concrete Bricks

by Lalitsuda Phutthimethakul, Park Kumpueng and Nuta Supakata

Crystals **2020**, *10*(8), 709; https://doi.org/10.3390/cryst10080709 - 18 Aug 2020

Abstract This research aims to study the utilization of waste from power plants, construction and demolition, and agriculture by varying the ratios of flue-gas desulfurization (FGD) gypsum, construction and demolition waste (CDW), and oil palm trunks (OPT) in concrete production. This research used these [...] Read more.

(This article belongs to the Special Issue Numerical Study of Concrete)

▶ Show Figures

Open Access Article

A Comparative Study on Blast-Resistant Performance of Steel and PVA Fiber-Reinforced Concrete: Experimental and Numerical Analyses

by Le Chen, Weiwei Sun, Bingcheng Chen, Sen Xu, Jianguo Liang, Chufan Ding and Jun Feng

Crystals **2020**, *10*(8), 707; https://doi.org/10.3390/cryst10080707 - 16 Aug 2020

Abstract This paper deals with the blast-resistant performance of steel fiber-reinforced concrete (SFRC) and polyvinyl alcohol (PVA) fiber-reinforced concrete (PVA-FRC) panels with a contact detonation test both experimentally and numerically. With 2% fiber volumetric content, SFRC and PVA-FRC specimens were prepared and comparatively tested [...] Read more.

(This article belongs to the Special Issue Numerical Study of Concrete)

▶ Show Figures

Open Access Article

Enhanced Performance of Concrete Composites Comprising Waste Metalised Polypropylene Fibres Exposed to Aggressive Environments

by Rayed Alyousef, Hossein Mohammadhosseini, Fahed Alrshoudi, Mahmood Md. Tahir, Hisham Alabduljabbar and Abdeliazim Mustafa Mohamed

Crystals **2020**, *10*(8), 696; https://doi.org/10.3390/cryst10080696 - 12 Aug 2020

Abstract The utilisation of waste plastic and polymeric-based materials remains a significant option for clean production, waste minimisation, preserving the depletion of natural resources and decreasing the emission of greenhouse gases, thereby contributing to a green environment. This study aims to investigate the resistance [...] Read more.

(This article belongs to the Special Issue Numerical Study of Concrete)

▶ Show Figures

Open Access Article

Effect of Aggregate Type and Specimen Configuration on Concrete Compressive Strength

by Sherif Yehia, Akmal Abdelfatah and Doaa Mansour

Crystals **2020**, *10*(7), 625; https://doi.org/10.3390/cryst10070625 - 19 Jul 2020

Abstract In this paper, concrete mixes utilizing two sizes of natural aggregate and two sources of lightweight and recycled aggregates were used to investigate the effect of aggregate type and specimen size and shape on the compressive strength of concrete. In addition, samples from [...] Read more.

(This article belongs to the Special Issue Numerical Study of Concrete)

▶ Show Figures

Open Access Article

Durability Assessment of PVA Fiber-Reinforced Cementitious Composite Containing Nano-SiO_2 Using Adaptive Neuro-Fuzzy Inference System

by Ting-Yu Liu, Peng Zhang, Qing-Fu Li, Shao-Wei Hu and Yi-Feng Ling

Crystals **2020**, *10*(5), 347; https://doi.org/10.3390/cryst10050347 - 28 Apr 2020

Abstract In this study, the durability of polyvinyl alcohol fiber-reinforced cementitious composite containing nano-SiO_2 was evaluated using the adaptive neuro-fuzzy inference system (ANFIS). According to the structural characteristics of the cementitious composite material and some related standards, the classification criteria for the evaluation [...] Read more.

(This article belongs to the Special Issue Numerical Study of Concrete)

▶ Show Figures

Show export options

Displaying articles 1-23

crystals
Submit to Crystals
Review for Crystals

Journal Menu

- Crystals Home
- Aims & Scope
- Editorial Board
- Reviewer Board
- Topics Board
- Instructions for Authors
- Special Issues
- Sections & Collections
- Article Processing Charge
- Indexing & Archiving
- Editor's Choice Articles
- Most Cited & Viewed
- Journal Statistics
- Journal History
- Journal Awards
- Editorial Office

Journal Browser

volume
issue
Go

> Forthcoming issue
> Current issue

Vol. 11 (2021)
Vol. 10 (2020)
Vol. 9 (2019)
Vol. 8 (2018)
Vol. 7 (2017)
Vol. 6 (2016)
Vol. 5 (2015)
Vol. 4 (2014)
Vol. 3 (2013)
Vol. 2 (2012)
Vol. 1 (2011)

Crystals, Volume 10, Issue 9 (September 2020) – 134 articles

Cover Story (view full-size image): Nanoclusters of amorphous calcium phosphate sequestered by a shell of phosphopeptides have helped us to understand how soft and hard tissues can co-exist in the same organism with relative ease, even when permeated by the same supersaturated biofluid. They may be metastable intermediates in the formation of more crystalline forms of calcium phosphate, contributing to hard tissue mineralization, or constituents of thermodynamically stable biofluids in contact with soft tissues. The latter type of biofluid can contain high concentrations of calcium and phosphate, as in the milk of many species. Lenton et al. comprehensively review the structural biology of calcium phosphate nanocluster complexes formed with phosphopeptides from caseins and osteopontin and model studies with recombinant phosphopeptides. View this paper

- Issues are regarded as officially published after their release is announced to the table of contents alert mailing list.
- You may sign up for e-mail alerts to receive table of contents of newly released issues.
- PDF is the official format for papers published in both, html and pdf forms. To view the papers in pdf format, click on the "PDF Full-text" link, and use the free Adobe Reader to open them.

Order results: Publication Date
Result details: Normal

Show export options

Open Access Article

Single Source Precursor for PAD-$LaMnO_3$ Thin Films

by Ramona Bianca Sonher, Richard Attila Varga, Mircea Nasui, Traian Petrisor Jr., Mihai Sebastian Gabor, Marin Senila, Alessandro Rufoloni, Traian Petrisor and Lelia Ciontea

Crystals 2020, *10*(9), 851; https://doi.org/10.3390/cryst10090851 - 22 Sep 2020

Viewed by 558

Abstract A new lanthanum and manganese ethylenediaminetetraacetate (EDTA) coordination polymer ($EDTA^{4-}$ = [$(CH_2N)_2(CH_2$-$COOH)(CH_2COO)_4$]) was synthesized from $La(NO_3)_3$ and $Mn(NO_3)_2$ reagents, ethylenediaminetetraacetic acid, and water at room temperature. [...] Read more.

(This article belongs to the Section Crystal Engineering)

► Show Figures

Open Access Article

Grating Coupler Design for Vertical Light Coupling in Silicon Thin Films on Lithium Niobate

by Huangpu Han and Bingxi Xiang

Crystals 2020, *10*(9), 850; https://doi.org/10.3390/cryst10090850 - 22 Sep 2020

Viewed by 454

Abstract In this paper we provide a design for a vertical grating coupler for a silicon thin film on lithium niobate. The parameters-such as the cladding layer thickness of lithium niobate, fiber position, fiber angle, grating period, and duty cycle are analyzed and optimized [...] Read more.

► Show Figures

Open Access Article

A Multifaceted Kinetic Model for the Thermal Decomposition of Calcium Carbonate

by Jingxuo Zhong, Junchen Huang, Lin Tao, Zhi Li and Qi Wang

Crystals 2020, *10*(9), 849; https://doi.org/10.3390/cryst10090849 - 22 Sep 2020

Viewed by 459

Abstract The existing kinetic models often consider the influence of a single factor alone on the chemical reaction and this is insufficient to completely describe the decomposition reaction of solids. Therefore, the existing kinetic models were improved using the pore structure model. The proposed [...] Read more.

► Show Figures

Open Access Article

Effects of GaN Buffer Resistance on the Device Performances of AlGaN/GaN HEMTs

by Ki-Sik Im, Jae-Hoon Lee, Yeo Jin Choi and Sung Jin An

Crystals 2020, *10*(9), 848; https://doi.org/10.3390/cryst10090848 - 22 Sep 2020

Viewed by 572

Abstract We investigated the effects of GaN buffer resistance of AlGaN/GaN high-electron-mobility transistors (HEMTs) on direct current (DC), low-frequency noise (LFN), and pulsed I-V characterization performances. The devices with the highest GaN buffer resistance were grown on sapphire substrate using two-step growth [...] Read more.

(This article belongs to the Special Issue Nano/Micro and Bio-Inspired Materials on Wide-Bandgap-Semiconductor-Based Optoelectronic/Power Devices)

► Show Figures

Open Access Article

Characterization of Accumulated B-Integral of Regenerative Amplifier Based CPA Systems

by Stefan Bock, Franziska Marie Herrmann, Thomas Püschel, Uwe Helbig, René Gebhardt, Jakob Johannes Lötfering, Richard Pausch, Karl Zeil, Tim Ziegler, Arie Irman, Thomas Oksenhendler, Akira Kon, Mamiko Nishuishi, Hiromitsu Kiriyama, Kiminori Kondo, Toma Toncian and Ulrich Schramm

Crystals 2020, *10*(9), 847; https://doi.org/10.3390/cryst10090847 - 22 Sep 2020

Cited by 1 | Viewed by 679

Abstract We report on a new approach to measure the accumulated B-integral in the regenerative and multipass amplifier stages of ultrashort-pulse high-power laser systems by B-integral-induced coupling between delayed test post-pulses and the main pulse. A numerical model for such non-linear pulse coupling is [...] Read more.

(This article belongs to the Special Issue Development of High Intensity Crystal Laser and Its Applications)

► Show Figures

Open Access Article

Si Quantum Dots Assist Synthesized Microflower-Like Si/MoS_2 Composites for Supercapacitors

by Jishong Zhang, Kangkang Cheng, Runmei Zhang, Yamei Yang, Yuntao Wu and Pengfei Yu

Crystals 2020, *10*(9), 846; https://doi.org/10.3390/cryst10090846 - 22 Sep 2020

Viewed by 476

Abstract The microflower-like Si/MoS_2 composites were fabricated using Si quantum dots (QDs) to assist a facile hydrothermal method. The electrochemical performance of Si/MoS_2 composite in symmetric and asymmetric systems was studied. Electrochemical characterization revealed that the Si/MoS_2 composite electrode in a [...] Read more.

► Show Figures

Open Access Editor's Choice Article

Depth Profile Analysis of Deep Level Defects in 4H-SiC Introduced by Radiation

by Tomislav Brodar, Luka Bakrač, Ivana Capan, Takeshi Ohshima, Luka Snoj, Vladimir Radulović and Željko Pastuović

Crystals 2020, *10*(9), 845; https://doi.org/10.3390/cryst10090845 - 22 Sep 2020

Cited by 1 | Viewed by 1038

Abstract Deep level defects created by implantation of light-helium and medium heavy carbon ions in the single ion regime and

neutron irradiation in n-type 4H-SiC are characterized by the DLTS technique. Two deep levels with energies 0.4 eV (EH1) and 0.7 eV (EH3) below [...] Read more.
(This article belongs to the Special Issue Crystalline Materials for Radiation Detection: A New Perspectives)

► Show Figures

Open Access Article

Proton, UV, and X-ray Induced Luminescence in Tb^{3+} Doped $LuGd_2Ga_2Al_3O_{12}$ Phosphors

by U. Fawad, H. J. Kim, Ibrahim Gul, Mataullah Khan, Sajjad Tahir, Tauseef Jamal and Wazir Muhammad

Crystals 2020, 10(9), 844; https://doi.org/10.3390/cryst10090844 - 22 Sep 2020

Abstract The well-known solid-state reaction method is used for the synthesis of Tb doped $LuGd_2Ga_2Al_3O_{12}$ phosphor. XRD and SEM techniques are used for the phase and structural morphology of the synthesized phosphor. UV, X-ray and proton induced [...] Read more.
(This article belongs to the Special Issue Xene Materials and Biomedical Applications of Nanostructures)

► Show Figures

Open Access Review

Spin Crossover in New Iron(II) Coordination Compounds with Tris(pyrazol-1-yl)Methane

by Olga G. Shakirova and Ludmila G. Lavrenova

Crystals 2020, 10(9), 843; https://doi.org/10.3390/cryst10090843 - 22 Sep 2020

Abstract We review here new advances in the synthesis and investigation of iron(II) coordination compounds with tris(pyrazol-1-yl)methane and its derivatives as ligands. The complexes demonstrate thermally induced spin crossover accompanied by thermochromism. Factors that influence the nature and temperature of the spin crossover are [...] Read more.
(This article belongs to the Special Issue Spin-Crossover in Molecular Complexes and Coordination Polymers)

► Show Figures

Open Access Article

Development of Catalytic-CVD SiN_x Passivation Process for AlGaN/GaN-on-Si HEMTs

by Myoung-Jin Kang, Hyun-Seop Kim, Ho-Young Cha and Kwang-Seok Seo

Crystals 2020, 10(9), 842; https://doi.org/10.3390/cryst10090842 - 21 Sep 2020

Abstract We optimized a silicon nitride (SiN_x) passivation process using a catalytic-chemical vapor deposition (Cat-CVD) system to suppress the current collapse phenomenon of AlGaN/GaN-on-Si high electron mobility transistors (HEMTs). The optimized Cat-CVD SiN_x film exhibited a high film density of 2.7 [...] Read more.
(This article belongs to the Special Issue Nano/Micro and Bio-Inspired Materials on Wide-Bandgap-Semiconductor-Based Optoelectronic/Power Devices)

► Show Figures

Open Access Article

Gas-Dependent Reversible Structural and Magnetic Transformation between Two Ladder Compounds

by Jun Manabe, Kazuki Nishida, Xiao Zhang, Yuki Nakano, Masaru Fujibayashi, Goulven Cosquer, Katsuya Inoue, Seiya Shimono, Hiroki Ishibashi, Yoshiki Kubota, Misaki Shiga, Ryo Tsunashima, Yoko Tatewaki and Sadafumi Nishihara

Crystals 2020, 10(9), 841; https://doi.org/10.3390/cryst10090841 - 19 Sep 2020

Abstract We report reversible structural transformation that occurs in two ladder compounds: $Cu_2CO_3(ClO_4)_2(NH_3)_6$ (1) and $Cu_2CO_3(ClO_4)_2(NH_3)_5(H_2O)$ ([...] Read more.
(This article belongs to the Special Issue Organic Conductors)

► Show Figures

Open Access Article

Surface Stabilized Topological Solitons in Nematic Liquid Crystals

by Inge Nys, Brecht Berteloot and Guilhem Poy

Crystals 2020, 10(9), 840; https://doi.org/10.3390/cryst10090840 - 19 Sep 2020

Abstract Photo-alignment is a versatile tool to pattern the alignment at the confining substrates in a liquid crystal (LC) cell. Arbitrary alignment patterns can be created by using projection with a spatial light modulator (SLM) for the illumination. We demonstrate that a careful design [...] Read more.
(This article belongs to the Special Issue Micro and Nano Patterned Substrates for Liquid Crystal Alignment (Volume II))

► Show Figures

Open Access Article

A Nature's Curiosity: The Argonaut "Shell" and Its Organic Content

by Morgane Oudot, Ira Ben Shir, Asher Schmidt, Laurent Plasseraud, Cédric Broussard, Pascal Neige and Frédéric Marin

Crystals 2020, 10(9), 839; https://doi.org/10.3390/cryst10090839 - 19 Sep 2020

Abstract Molluscs are known for their ability to produce a calcified shell resulting from a genetically controlled and matrix-mediated process, performed extracellularly. The occluded organic matrix consists of a complex mixture of proteins, glycoproteins and polysaccharides that are in most cases secreted by the [...] Read more.
(This article belongs to the Special Issue Biominerals: Formation, Function, Properties)

► Show Figures

Open Access Article

Ti_3O_5 and Al_2TiO_5 Crystals Flotation Characteristics from Ti-bearing Blast Furnace Slag: A Density Functional Theory and Experimental Study

by Shan Ren, Zanghui Su, Weizao Liu, Yali Sun, Xiaoming Li and Jian Yang

Crystals 2020, 10(9), 838; https://doi.org/10.3390/cryst10090838 - 19 Sep 2020

Abstract Anosovite crystalline is an ideal mineral for flotation from the Ti-bearing blast furnace (TBBF) slag. Ti_3O_5 crystal and Al_2TiO_5 crystal are two kinds of anosovites, and the Al element significantly affects the electronic structure and flotation performance [...] Read more.
(This article belongs to the Special Issue Metallurgical Slag)

► Show Figures

Open Access Article

High-Intensity Laser-Driven Oxygen Source from CW Laser-Heated Titanium Tape Targets

by Kotaro Kondo, Mamiko Nishiuchi, Hironao Sakaki, Nicholas P. Dover, Hazel F. Lowe, Takumi Miyahara, Yukinobu Watanabe, Tim Ziegler, Karl Zeil, Ulrich Schramm, Emma J. Ditter, George S. Hicks, Oliver C. Ettlinger, Zulfikar Najmudin, Hiromitsu Kiriyama, Masaki Kando and Kiminori Kondo

Crystals 2020, 10(9), 837; https://doi.org/10.3390/cryst10090837 - 19 Sep 2020

Abstract The interaction of high-intensity laser pulses with solid targets can be used as a highly charged, energetic heavy ion source. Normally, intrinsic contaminants on the target surface suppress the performance of heavy ion acceleration from a high-intensity laser–target interaction, resulting in preferential proton [...] Read more.
(This article belongs to the Special Issue Development of High Intensity Crystal Laser and Its Applications)

► Show Figures

Open Access Article

Effect of Nitrogen Content on the Formation of Inclusions in Fe-5Mn-3Al Steels

by Michelia Alba, Muhammad Nabeel and Neslihan Dogan

Crystals 2020, 10(9), 836; https://doi.org/10.3390/cryst10090836 - 18 Sep 2020

Abstract The effect of N content on the characteristics and formation of inclusions in the Fe-5Mn-3Al steels was investigated in this study. Two synthetic steel melts were produced by two different methods—N_2 gas purging and injecting—to introduce nitrogen into the melt. The N [...] Read more.
(This article belongs to the Special Issue Liquid Steel Alloying Process)

► Show Figures

Open Access Article

Engineering Aspheric Liquid Crystal Lenses by Using the Transmission Electrode Technique

by José Francisco Algorri, Dimitrios C. Zografopoulos, Luis Rodríguez-Cobo, José Manuel Sánchez-Pena and José Miguel López-Higuera
Crystals 2020, *10*(9), 835; https://doi.org/10.3390/cryst10090835 - 18 Sep 2020
Viewed by 520

Abstract The transmission electrode technique has been recently proposed as a versatile method to obtain various types of liquid-crystal (LC) lenses. In this work, an equivalent electric circuit and new analytical expressions based on this technique are developed. In addition, novel electrode shapes are [...] Read more.
(This article belongs to the Special Issue Liquid Crystals Optical Devices (Volume II))

► Show Figures

Open Access Article

Dual-Energy X-ray Medical Imaging with Inverse Compton Sources: A Simulation Study

by Gianfranco Paternò, Paolo Cardarelli, Mauro Gambaccini and Angelo Taibi
Crystals 2020, *10*(9), 834; https://doi.org/10.3390/cryst10090834 - 18 Sep 2020
Viewed by 566

Abstract It has been long recognized that dual-energy imaging could help to enhance the detectability of lesions in diagnostic radiology, by removing the contrast of surrounding tissues. Furthermore, X-ray attenuation is material specific and information about the object constituents can be extracted for tissue [...] Read more.
(This article belongs to the Special Issue Development and Application of Novel Dual Energy X-ray Imaging Methods)

► Show Figures

Open Access Article

Microwave-Assisted Aldol Condensation of Furfural and Acetone over Mg–Al Hydrotalcite-Based Catalysts

by Alberto Tampieri, Mateo Lilic, Magda Constanti and Francesc Medina
Crystals 2020, *10*(9), 833; https://doi.org/10.3390/cryst10090833 - 18 Sep 2020
Cited by 1 | Viewed by 566

Abstract The depletion of fossil fuel resources has prompted the scientific community to find renewable alternatives for the production of energy and chemicals. The products of the aldol condensation between bio-based furfural and acetone have been individuated as promising intermediates for the preparation of [...] Read more.
(This article belongs to the Special Issue Layered Double Hydroxides (LDHs))

► Show Figures

Open Access Editorial

Cement-Based Composites: Advancements in Development and Characterization

by Pawel Sikora and Sang-Yeop Chung
Crystals 2020, *10*(9), 832; https://doi.org/10.3390/cryst10090832 - 17 Sep 2020
Viewed by 535

Abstract This Special Issue on "Cement-Based Composites: Advancements in Development and Characterization" presents the latest research and advances in the field of cement-based composites. This special issue covers a variety of experimental studies related to fibre-reinforced, photocatalytic, lightweight, and sustainable cement-based composites. Moreover, simulation [...] Read more.
(This article belongs to the Special Issue Cement-Based Composites: Advancements in Development and Characterization)
Printed Edition available

Open Access Article

High-Thermal-Conductivity SiC Ceramic Mirror for High-Average-Power Laser System

by Yasuhiro Miyasaka, Kotaro Kondo and Hiromitsu Kiriyama
Crystals 2020, *10*(9), 831; https://doi.org/10.3390/cryst10090831 - 17 Sep 2020
Viewed by 501

Abstract The importance of heat-resistant optics is increasing together with the average power of high-intensity lasers. A silicon carbide (SiC) ceramic with high thermal conductivity is proposed as an optics substrate to suppress thermal effects. The temperature rise of the substrate and the change [...] Read more.
(This article belongs to the Special Issue Development of High Intensity Crystal Laser and Its Applications)

► Show Figures

Open Access Article

Low-Frequency Noise Behavior of AlGaN/GaN HEMTs with Different Al Compositions

by Yoo Jin Choi, Jae-Hoon Lee, Sung Jin An and Ki-Sik Im
Crystals 2020, *10*(9), 830; https://doi.org/10.3390/cryst10090830 - 17 Sep 2020
Viewed by 454

Abstract $Al_xGa_{1-x}N$/GaN heterostructures with two kinds of Al composition were grown by metal organic chemical vapor deposition (MOCVD) on sapphire substrates. The Al compositions in the AlGaN barrier layer were confirmed to be 13% and 28% using high resolution X-ray [...] Read more.
(This article belongs to the Special Issue Nano/Micro and Bio-Inspired Materials on Wide-Bandgap-Semiconductor-Based Optoelectronic/Power Devices)

► Show Figures

Open Access Editorial

Synthesis and Characterization of Ferroelectrics

by Jan Dec
Crystals 2020, *10*(9), 829; https://doi.org/10.3390/cryst10090829 - 17 Sep 2020
Viewed by 358

Abstract
Ferroelectrics belong to one of the most studied groups of materials in terms of research and applications [...] Full article
(This article belongs to the Special Issue Synthesis and Characterization of Ferroelectrics) Printed Edition available

Open Access Article

Guided Crystallization of Zeolite Beads Composed of ZSM-12 Nanosponges

by Kassem Moukahhal, Ludovic Josien, Habiba Nouali, Joumana Toufaily, Tayssir Hamieh, T. Jean Daou and Bénédicte Lebeau
Crystals 2020, *10*(9), 828; https://doi.org/10.3390/cryst10090828 - 17 Sep 2020
Viewed by 530

Abstract The direct route using a bifunctional amphiphilic structuring agent for the synthesis of hierarchical nanozeolites coupled with pseudomorphic transformation was used for the crystallization of hierarchized zeolite beads/hollow spheres composed of ZSM-12 (MTW structural-type) with nanosponge morphology. These beads/hollow spheres have the same [...] Read more.
(This article belongs to the Special Issue Zeolites)

► Show Figures

Open Access Article

Crystal Growth by the Floating Zone Method of Ce-Substituted Crystals of the Topological Kondo Insulator SmB_6

by Monica Ciomaga Hatnean, Talha Ahmad, Marc Walker, Martin R. Lees and Geetha Balakrishnan
Crystals 2020, *10*(9), 827; https://doi.org/10.3390/cryst10090827 - 17 Sep 2020
Viewed by 538

Abstract SmB_6 is a mixed valence topological Kondo insulator. To investigate the effect of substituting Sm with magnetic Ce ions on the physical properties of samarium hexaboride, Ce-substituted SmB_6 crystals were grown by the floating zone method for the first time as [...] Read more.
(This article belongs to the Special Issue Advances in Topological Materials)

► Show Figures

Open Access Article

Thermal Stability of PS-PVD YSZ Coatings with Typical Dense Layered and Columnar Structures

by Zefei Cheng, Jiasheng Yang, Fang Shao, Xinghua Zhong, Huayu Zhao, Yin Zhuang, Jing Sheng, Jinxing Ni and Shunyan Tao
Crystals 2020, *10*(9), 826; https://doi.org/10.3390/cryst10090826 - 17 Sep 2020
Cited by 1 | Viewed by 439

Abstract Yttria-stabilized zirconia (YSZ) coatings with typical pyramid columnar and dense layered structure were prepared by plasma spray-physical vapor deposition (PS-PVD). The evolution behavior of microstructure and crystallography of the coatings before and after thermal aging treatment were observed by electron backscatter diffraction (EBSD) [...] Read more.
(This article belongs to the Section Inorganic Crystalline Materials)

► Show Figures

Open Access Article

Effect of Transition Metals Oxides on the Physical and Mechanical Properties of Sintered Tungsten Heavy Alloys

by Ayman H. Elsayed, Mohamed A. Sayed, Osama M. Dewood and Walid M. Daoush
Crystals 2020, 10(9), 825; https://doi.org/10.3390/cryst10090825 - 17 Sep 2020
Viewed by 518

Abstract The addition of transition element oxides to tungsten heavy alloys (WHAs) fabricated by powder metallurgy technique provides new materials with higher density and electrical conductivity, which may be adequate in some applications such as kinetic energy penetrators. Additionally, materials with higher electrical conductivity [...] Read more.
(This article belongs to the Special Issue Recent Advances in Metallurgy and Properties of Superalloys)

► Show Figures

Open Access Review

Polymer-Derived Si-Based Ceramics: Recent Developments and Perspectives

by Aidong Xia, Jie Yin, Xiao Chen, Xuejian Liu and Zhengren Huang
Crystals 2020, 10(9), 824; https://doi.org/10.3390/cryst10090824 - 16 Sep 2020
Cited by 1 | Viewed by 610

Abstract Polymer derived ceramics (PDCs) are promising candidates for usages as the functionalization of inorganic Si-based materials. Compared with traditional ceramics preparation methods, it is easier to prepare and functionalize ceramics with complex shapes by using the PDCs technique, thereby broadening the application fields [...] Read more.
(This article belongs to the Special Issue Functionalization of Inorganic Silica-Based Materials)

► Show Figures

Open Access Article

Hardness, Young's Modulus and Elastic Recovery in Magnetron Sputtered Amorphous $AlMgB_{14}$ Films

by Alexander M. Grishin
Crystals 2020, 10(9), 823; https://doi.org/10.3390/cryst10090823 - 16 Sep 2020
Viewed by 884

Abstract We report optical and mechanical properties of hard aluminum magnesium boride films magnetron sputtered from a stoichiometric $AlMgB_{14}$ ceramic target onto Corning® 1737 Glass and Si (100) wafers. High target sputtering rf-power and sufficiently short target-to-substrate distance appeared to be critical [...] Read more.
(This article belongs to the Special Issue Hardmetal)

► Show Figures

Open Access Article

Statistical Crystal Plasticity Model Advanced for Grain Boundary Sliding Description

by Alexey Shveykin, Peter Trusov and Elvira Sharifullina
Crystals 2020, 10(9), 822; https://doi.org/10.3390/cryst10090822 - 16 Sep 2020
Cited by 1 | Viewed by 476

Abstract Grain boundary sliding is an important deformation mechanism, and therefore its description is essential for modeling different technological processes of thermomechanical treatment, in particular the superplasticity forming of metallic materials. For this purpose, we have developed a three-level statistical crystal plasticity constitutive model [...] Read more.
(This article belongs to the Special Issue Crystal Plasticity)

► Show Figures

Open Access Article

Enhancing Protein Crystallization under a Magnetic Field

by Sun Young Ryu, In Hwan Oh, Sang Jin Cho, Shin Ae Kim and Hyun Kyu Song
Crystals 2020, 10(9), 821; https://doi.org/10.3390/cryst10090821 - 16 Sep 2020
Viewed by 561

Abstract High-quality crystals are essential to ensure high-resolution structural information. Protein crystals are controlled by many factors, such as pH, temperature, and the ion concentration of crystalline solutions. We previously reported the development of a device dedicated to protein crystallization. In the current study, [...] Read more.
(This article belongs to the Special Issue Novel Strategies for Improved Protein Crystallization)

► Show Figures

Open Access Article

Relation between Fish Habitat and the Periodicity of Incremental Lines in the Fossil Otoliths

by Hiroyuki Mishima, Yasuo Kondo, Fumio Ohe, Yasuo Miake and Tohru Hayakawa
Crystals 2020, 10(9), 820; https://doi.org/10.3390/cryst10090820 - 16 Sep 2020
Viewed by 316

Abstract There are few research reports on the relationship between fish habitats and the periodicity of the fishes' incremental lines of otolith fossils. The present study examines this relationship through histological and analytical studies on otolith fossils from Nobori Formation, Pliocene, Japan. The specimens [...] Read more.
(This article belongs to the Special Issue Biominerals: Formation, Function, Properties)

► Show Figures

Open Access Article

Use of the Correlation between Grain Size and Crystallographic Orientation in Crystal Plasticity Simulations: Application to AISI 420 Stainless Steel

by Jesús Galán-López and Javier Hidalgo
Crystals 2020, 10(9), 819; https://doi.org/10.3390/cryst10090819 - 16 Sep 2020
Cited by 1 | Viewed by 553

Abstract Crystal plasticity models attempt to reproduce the complex deformation processes of polycrystalline metals based on a virtual representation of the real microstructure. When choosing this representation, a compromise must be made between level of detail at the local level and statistical significance of [...] Read more.
(This article belongs to the Special Issue Crystal Plasticity)

► Show Figures

Open Access Editor's Choice Review

Glycosylation: A "Last Word" in the Protein-Mediated Biomineralization Process

by John Spencer Evans
Crystals 2020, 10(9), 818; https://doi.org/10.3390/cryst10090818 - 16 Sep 2020
Viewed by 519

Abstract Post-translational modifications are one way that biomineral-associated cells control the function and fate of proteins. Of the ten different types of post-translational modifications, one of the most interesting and complex is glycosylation, or the covalent attachment of carbohydrates to amino acid sidechains Asn, [...] Read more.
(This article belongs to the Special Issue Proteins and Biomineralisation)

► Show Figures

Open Access Article

Effect of CeO_2-ZnO Nanocomposite for Photocatalytic and Antibacterial Activities

by Asad Syed, Lakshmi Sagar Reddy Yadav, Ali H. Bahkali, Abdallah M. Elgorban, Deshmukh Abdul Hakeem and Nagaraju Ganganagappa
Crystals 2020, 10(9), 817; https://doi.org/10.3390/cryst10090817 - 16 Sep 2020
Viewed by 492

Abstract The impact of a CeO_2-ZnO nanocomposite on the photocatalytic and antibacterial properties compared to bare ZnO was investigated. A CeO_2-ZnO nanocomposite was synthesized using Acacia nilotica fruit extract as a novel fuel by a simple solution combustion method. The [...] Read more.
(This article belongs to the Special Issue Zinc Oxide Nanomaterials and Based Devices)

► Show Figures

Open Access Article

Effects of Highly Crystalized Nano C-S-H Particles on Performances of Portland Cement Paste and Its Mechanism

by Yuli Wang, Huijuan Lu, Junjie Wang and Hang He
Crystals 2020, 10(9), 816; https://doi.org/10.3390/cryst10090816 - 15 Sep 2020
Viewed by 387

Abstract In order to improve the early age strength of ordinary Portland cement-based materials, many early strength agents were applied in different conditions. Different from previous research, the nano calcium silicate hydrate (C-S-H) particles used in this study were synthesized through the chemical reaction [...] Read more.

(This article belongs to the Special Issue Recycling Silicate-Bearing Waste Materials)

► Show Figures

Open Access Review

Viable Materials with a Giant Magnetocaloric Effect

by Nikolai A. Zarkevich and Vladimir I. Zverev

Crystals 2020, *10*(9), 815; https://doi.org/10.3390/cryst10090815 - 15 Sep 2020

Abstract This review of the current state of magnetocalorics is focused on materials exhibiting a giant magnetocaloric response near room temperature. To be economically viable for industrial applications and mass production, materials should have desired useful properties at a reasonable cost and should be [...] Read more.

(This article belongs to the Special Issue Magnetocalorics)

► Show Figures

Open Access Article

Convective Transport of Fluid–Solid Interaction: A Study between Non-Newtonian Casson Model with Dust Particles

by Abdul Rahman Mohd Kasim, Nur Syamilah Arifin, Syazwani Mohd Zokri, Mohd Zuki Salleh, Nurul Farahain Mohammad, Dennis Ling Chuan Ching, Sharidan Shafie and Noor Amalina Nisa Ariffin

Crystals 2020, *10*(9), 814; https://doi.org/10.3390/cryst10090814 - 15 Sep 2020

Abstract The Casson model is a fascinating model, which is genuinely recommended for use with fluids of a non-Newtonian type. The conventional model is not capable to represent the Casson model with the suspension of foreign bodies (dust particles). Due to this, the two-phase [...] Read more.

► Show Figures

Open Access Communication

Designer Synthesis of Ultra-Fine Fe-LTL Zeolite Nanocrystals

by Fen Zhang, Yunhong Luo, Lei Chen, Wei Chen, Yin Hu, Guihua Chen, Shengyong You and Weiguo Song

Crystals 2020, *10*(9), 813; https://doi.org/10.3390/cryst10090813 - 15 Sep 2020

Abstract Nanosized zeolites with larger external surface area and decreased diffusion pathway provide many potential opportunities in adsorption, diffusion, and catalytic applications. Herein, we report a designer synthesis of ultra-fine Fe-LTL zeolite nanocrystals under very mild synthesis conditions. We prepared Fe-LTL zeolite nanocrystals synthesized [...] Read more.

(This article belongs to the Special Issue Zeolites)

► Show Figures

Open Access Article

Synthesis, Crystal Structures and Characterization of Two Nonmetal Cation Tetrafluoroborates

by Noura Othman Alzamil, Ghareeba Mussad Al-Enzi, Aishah Hassan Alamri, Insaf Abdi and Amor BenAli

Crystals 2020, *10*(9), 812; https://doi.org/10.3390/cryst10090812 - 14 Sep 2020

Abstract Two new nonmetal cation tetrafluoroborate phases $[H_3tren](BF_4)_3$ (I) and $[H_3tren](BF_4)_3$ HF (II) were synthesized by microwave-assisted solvothermal and characterized by single crystal X-ray diffraction, IR spectroscopy and thermal analysis DTA-TGA. [H [...] Read more.

(This article belongs to the Special Issue Multifunctional Crystal Materials with Non-centrosymmetry: Piezoelectric and Nonlinear Optical Properties and Their Applications)

► Show Figures

Open Access Article

Prediction of Properties of FRP-Confined Concrete Cylinders Based on Artificial Neural Networks

by Afaq Ahmad, Vagelis Plevris and Qaiser-uz-Zaman Khan

Crystals 2020, *10*(9), 811; https://doi.org/10.3390/cryst10090811 - 14 Sep 2020

Abstract Recently, the use of fiber-reinforced polymers (FRP)-confinement has increased due to its various favorable effects on concrete structures, such as an increase in strength and ductility. Therefore, researchers have been attracted to exploring the behavior and efficiency of FRP-confinement for concrete structural elements [...] Read more.

(This article belongs to the Special Issue Numerical Study of Concrete)

► Show Figures

Open Access Article

Effects of CF_4 Plasma Treatment on Indium Gallium Oxide and Ti-doped Indium Gallium Oxide Sensing Membranes in Electrolyte–Insulator–Semiconductors

by Chyuan-Haur Kao, Yen-Lin Su, Wei-Jen Liao, Ming-Hsien Li, Wei-Lun Chan, Shang-Che Tsai and Hsiang Chen

Crystals 2020, *10*(9), 810; https://doi.org/10.3390/cryst10090810 - 14 Sep 2020

Abstract Electrolyte–insulator–semiconductor (EIS) sensors, used in applications such as pH sensing and sodium ion sensing, are the most basic type of ion-sensitive field-effect transistor (ISFET) membranes. Currently, some of the most popular techniques for synthesizing such sensors are chemical vapor deposition, reactive sputtering and [...] Read more.

► Show Figures

Open Access Article

Small-Polaron Hopping and Low-Temperature (45–225 K) Photo-Induced Transient Absorption in Magnesium-Doped Lithium Niobate

by Simon Messerschmidt, Andreas Krampf, Laura Vittadello, Mirco Imlau, Tobias Nörenberg, Lukas M. Eng and David Emin

Crystals 2020, *10*(9), 809; https://doi.org/10.3390/cryst10090809 - 14 Sep 2020

Abstract A strongly temperature-dependent photo-induced transient absorption is measured in 6.5 mol% magnesium-doped lithium niobate at temperatures ranging from 45 K to 225 K. This phenomenon is interpreted as resulting from the generation and subsequent recombination of oppositely charged small polarons. Initial two-photon absorptions [...] Read more.

(This article belongs to the Special Issue New Trends in Lithium Niobate: From Bulk to Nanocrystals)

► Show Figures

Open Access Article

Determination of Mohr-Coulomb Parameters for Modelling of Concrete

by Selimir Lelovic and Dejan Vasovic

Crystals 2020, *10*(9), 808; https://doi.org/10.3390/cryst10090808 - 13 Sep 2020

Abstract Cohesion is defined as the shear strength of material when compressive stress is zero. This article presents a new method for the experimental determination of cohesion at pre-set angles of shear deformation. Specially designed moulds are created to force deformation (close to τ-axis) [...] Read more.

(This article belongs to the Special Issue Numerical Study of Concrete)

► Show Figures

Open Access Editor's Choice Article

Large Angle Forward Diffraction by Chiral Liquid Crystal Gratings with Inclined Helical Axis

by Migle Stebryte, Inge Nys, Yera Ye. Ussembayev, Jeroen Beeckman and Kristiaan Neyts

Crystals 2020, *10*(9), 807; https://doi.org/10.3390/cryst10090807 - 12 Sep 2020

Abstract A layer of chiral liquid crystal (CLC) with a photonic bandgap in the visible range has excellent reflective properties. Recently, two director configurations have been proposed in the literature for CLC between two substrates with periodic photo-alignment: one with the director parallel to [...] Read more.

(This article belongs to the Special Issue Nematic Liquid Crystals)

► Show Figures

Open Access Article

Characterization and Luminescence of Eu^{3+}- and Gd^{3+}-Doped Hydroxyapatite

and Thickness on SOFC Performances

by Lara Bouleau, Noelia Coton, Pierre Coquoz, Raphael Ihringer, Alain Billard and Pascal Briois
Crystals 2020, 10(9), 759; https://doi.org/10.3390/cryst10090759 - 28 Aug 2020
Viewed by 433

Abstract Gadolinia-doped ceria (GDC) buffer layers were synthesized by reactive magnetron sputtering under different total pressures and different thickness. All as-deposited and after an annealing treatment during two hours under air at 1000 °C coating presents a face centered cubic (f.c.c) structure of ceria [...] Read more.
(This article belongs to the Special Issue Solid Oxide Fuel Cells and Electrolyzers)

► Show Figures

Open Access Editorial

Advanced LED Solid-State Lighting Optics

by Ching-Cherng Sun, Shih-Hsin Ma and Quang-Khoi Nguyen
Crystals 2020, 10(9), 758; https://doi.org/10.3390/cryst10090758 - 27 Aug 2020
Viewed by 546

Abstract Light-emitting diodes (LEDs) have been intensively studied for white-light lighting since their luminous efficacy exceeds 50 lm/W. Currently, the luminous efficacy of an LED light tube/bulb is almost above 100 lm/W. LED solid-state lighting (SSL) has unequivocally become the major light source in [...] Read more.
(This article belongs to the Special Issue Advanced LED Solid-state Lighting Optics)

Open Access Article

The Prediction of Stiffness of Bamboo-Reinforced Concrete Beams Using Experiment Data and Artificial Neural Networks (ANNs)

by Mehtar, Amri Gunasti, Suhardi, Nursaid, Irawati, Ilanka Cahya Dewi, Moh. Dasuki, Sofia Ariyani, Fitriana, Idris Mahmudi, Taufan Abadi, Miftahur Rahman, Syarif Hidayatullah, Agung Nilogiri, Senki Desta Galuh, Ari Eko Wardoyo and Rofi Budi Hamduwibawa
Crystals 2020, 10(9), 757; https://doi.org/10.3390/cryst10090757 - 27 Aug 2020
Cited by 3 | Viewed by 506

Abstract Stiffness is the main parameter of the beam's resistance to deformation. Based on advanced research, the stiffness of bamboo-reinforced concrete beams (BRC) tends to be lower than the stiffness of steel-reinforced concrete beams (SRC). However, the advantage of bamboo-reinforced concrete beams has enough [...] Read more.
(This article belongs to the Special Issue Numerical Study of Concrete)

► Show Figures

Open Access Article

Carbonate and Oxalate Crystallization by Interaction of Calcite Marble with *Bacillus subtilis* and *Bacillus subtilis–Aspergillus niger* Association

by Katerina V. Sazanova (nee Barinova), Olga V. Frank-Kamenetskaya, Dmitry Yu. Vlasov, Marina S. Zelenskaya, Alexey D. Vlasov, Aleksei V. Rusakov and Maya A. Petrova
Crystals 2020, 10(9), 756; https://doi.org/10.3390/cryst10090756 - 27 Aug 2020
Cited by 2 | Viewed by 487

Abstract Rock surfaces in natural systems are inhabited by multispecies communities of microorganisms. The biochemical activity of microorganisms and the patterns of microbial crystallization in these communities are mostly unexplored. Patterns of calcium carbonate and calcium oxalate crystallization induced by bacteria *Bacillus subtilis* and [...] Read more.
(This article belongs to the Special Issue Biominerals: Formation, Function, Properties)

► Show Figures

Open Access Review

Structural Biology of Calcium Phosphate Nanoclusters Sequestered by Phosphoproteins

by Samuel Lenton, Qian Wang, Tommy Nylander, Susana Teixeira and Carl Holt
Crystals 2020, 10(9), 755; https://doi.org/10.3390/cryst10090755 - 27 Aug 2020
Cited by 3 | Viewed by 995

Abstract Biofluids that contain stable calcium phosphate nanoclusters sequestered by phosphopeptides make it possible for soft and hard tissues to co-exist in the same organism with relative ease. The stability diagram of a solution of nanocluster complexes shows how the minimum concentration of phosphopeptide [...] Read more.
(This article belongs to the Special Issue Proteins and Biomineralisation)

► Show Figures

Open Access Article

Ablation of $BaWO_4$ Crystal by Ultrashort Laser Pulses

by Igor Kinyaevskiy, Pavel Danilov, Nikita Smirnov, Sergey Kudryashov, Andrey Koribut, Elizaveta Dunaeva, Irina Voronina, Yury Andreev and Andrey Ionin
Crystals 2020, 10(9), 754; https://doi.org/10.3390/cryst10090754 - 27 Aug 2020
Viewed by 489

Abstract Ablation of $BaWO_4$ Raman crystals with different impurity concentrations by ultrashort laser pulses was experimentally studied. Laser pulses with duration varying from 0.3 ps to 1.6 ps at wavelengths of 515 nm and 1030 nm were applied. A single-pulse optical damage threshold [...] Read more.
(This article belongs to the Special Issue Multifunctional Optical Crystals for Raman Lasers)

► Show Figures

Open Access Article

Research on Performance Improvement of Photovoltaic Cells and Modules Based on Black Silicon

by Zijian Chen, Haoyuan Jia, Yunfeng Zhang, Leilei Fan, Haina Zhu, Hong Ge, Baowen Cao and Shiyu Wang
Crystals 2020, 10(9), 753; https://doi.org/10.3390/cryst10090753 - 26 Aug 2020
Viewed by 421

Abstract This paper mainly studied the electrical performance improvement of black silicon photovoltaic (PV) cells and modules. The electrical performance of the cells and modules matched with black silicon was optimized through three different experiments. Firstly, in the pre-cleaning step, the effect of lotion [...] Read more.
(This article belongs to the Special Issue Growth and Evaluation of Crystalline Silicon (Volume II))

► Show Figures

Open Access Article

Influence of Carbon Cap on Self-Diffusion in Silicon Carbide

by Marianne Etzelmüller Bathen, Margareta Linnarsson, Misagh Ghezellou, Jawad Ul Hassan and Lasse Vines
Crystals 2020, 10(9), 752; https://doi.org/10.3390/cryst10090752 - 26 Aug 2020
Cited by 2 | Viewed by 597

Abstract Self-diffusion of carbon (C and C) and silicon (Si and Si) in 4H silicon carbide has been investigated by utilizing a structure containing an isotope purified 4H-SiC epitaxial layer grown on an n-type [...] Read more.
(This article belongs to the Special Issue Development and Investigation of SiC and SiC-based devices)

► Show Figures

Open Access Article

Multifunctional Electrochemical Properties of Synthesized Non-Precious Iron Oxide Nanostructures

by Ruby Phul, M. A. Majeed Khan, Maryam Sardar, Jahangeer Ahmed and Tokeer Ahmad
Crystals 2020, 10(9), 751; https://doi.org/10.3390/cryst10090751 - 26 Aug 2020
Cited by 4 | Viewed by 549

Abstract Magnetic Fe_3O_4 nanostructures for electrochemical water splitting and supercapacitor applications were synthesized by low temperature simple wet-chemical route. The crystal structure and morphology of as-acquired nanostructures were examined by powder X-ray diffraction and transmission electron microscopy. Magnetic measurements indicate that [...] Read more.
(This article belongs to the Special Issue Nanomaterials for Energy and Recycling)

► Show Figures

Open Access Communication

The Crystallization Process of Vaterite Microdisc Mesocrystals via Proto-Vaterite Amorphous Calcium Carbonate Characterized by Cryo-X-ray Absorption Spectroscopy

by Li Qiao, Ivo Zizak, Paul Zaslansky and Yurong Ma
Crystals 2020, 10(9), 750; https://doi.org/10.3390/cryst10090750 - 26 Aug 2020
Viewed by 380

Abstract Investigation on the formation mechanism of crystals via amorphous precursors has attracted a lot of interests in the last years. The formation mechanism of thermodynamically meta-stable vaterite in pure alcohols in the absence of any additive is less known. Herein, the crystallization process [...] Read more.

Abstract In this work, we studied inverted organic solar cells based on bulk heterojunction using poly(3-hexylthiophene-2,5-diyl):[6,6]-phenyl-C71-butyric acid methyl ester (P3HT:PCBM) as an active layer and a novel cathode buffer bilayer consisting of tin dioxide (SnO_2) combined with polyethylenimine-ethoxylated (PEIE) to overcome the [...] Read more.
(This article belongs to the Special Issue Organic Photovoltaic)

► Show Figures

Open Access Article

Terahertz Birefringence and Dichroism of KTA Crystal

by Jingguo Huang, Yang Li, Yanqing Gao, Zhaming Huang, Nazar Nikolaev, Alexander Mamrashev, Grigory Lanskii and Yury Andreev
Crystals 2020, 10(9), 730; https://doi.org/10.3390/cryst10090730 - 20 Aug 2020

Abstract For the first time, we present the spectra of all three components of the refractive index and absorption coefficient of the $KTiOAsO_4$ (KTA) crystal measured by the means of terahertz time-domain spectroscopy in the range of 0.3–2.1 THz. The dispersion of the [...] Read more.

► Show Figures

Open Access Article

Simulation of Porous Magnetite Deposits on Steam Generator Tubes in Circulating Water at 270 °C

by Soon-Hyeok Jeon, Hae-Sang Shim, Ji-Min Lee, Jeoh Han and Do Haeng Hur
Crystals 2020, 10(9), 729; https://doi.org/10.3390/cryst10090729 - 20 Aug 2020

Abstract In the secondary side of pressurized water reactors (PWRs), the main corrosion product accumulated on the steam generator (SG) tubes is magnetite, which has a porous structure. The purpose of this work is to simulate the porous magnetite deposited to the SG tubes [...] Read more.
(This article belongs to the Special Issue Stress Corrosion in Magnetite)

► Show Figures

Open Access Article

In Situ Electric-Field Study of Surface Effects in Domain Engineered $Pb(In_{1/2}Nb_{1/2})O_3$-$Pb(Mg_{1/3}Nb_{2/3})O_3$-$PbTiO_3$ Relaxor Crystals by Grazing Incidence Diffraction

by Markys G. Cain, Margo Staruch, Paul Thompson, Christopher Lucas, Didier Wermeille, Yves Kayser, Burkhard Beckhoff, Sam E. Lofland and Peter Finkel
Crystals 2020, 10(9), 728; https://doi.org/10.3390/cryst10090728 - 20 Aug 2020

Abstract In this work, we present a grazing incidence X-ray diffraction study of the surface of a $0.24Pb(In_{1/2}Nb_{1/2})O_3$-$Pb(Mg_{1/3}Nb_{2/3})O_3$-$PbTiO_3$ (PIN-PMN-PT) [011] poled rhombohedral single crystal. The near surface microstructure (the top several [...] Read more.
(This article belongs to the Special Issue A 10 Years Journey: Chemical, Physical, and Biological Properties and Applications of Crystals)

► Show Figures

Open Access Communication

All-Inkjet Printed Organic Thin-Film Transistors with and without Photo-Sensitivity to Visible Lights

by Chen Jiang
Crystals 2020, 10(9), 727; https://doi.org/10.3390/cryst10090727 - 20 Aug 2020

Abstract Printable organic thin-film transistors have enabled flexible low-cost electronics, which has the potential for a lot of emerging electronic applications. Despite the excellent dark performance of advanced all-inkjet printed organic thin-film transistors, their photoresponse is less explored and needs to be investigated, especially [...] Read more.
(This article belongs to the Special Issue Advances in Thin Film Materials and Devices)

► Show Figures

Open Access Article

Polarization Control with Helical Metasurfaces

by Ihar Faniayeu, Viktar Asadchy and Ivan Fanyaev
Crystals 2020, 10(9), 726; https://doi.org/10.3390/cryst10090726 - 20 Aug 2020

Abstract The ability to fully control the polarization of light using chiral metadevices has drawn considerable attention in various applications of integrated photonics, communication systems, and life sciences. In this work, we propose a comprehensive approach for the design of metasurfaces with desired polarization [...] Read more.
(This article belongs to the Special Issue Polarization-Handling Metasurfaces)

► Show Figures

Open Access Review

Making NSCLC Crystal Clear: How Kinase Structures Revolutionized Lung Cancer Treatment

by Juliana F. Vilachã, Sarah C. Mitchel, Muluembet Z. Akele, Stephen Evans and Matthew R. Groves
Crystals 2020, 10(9), 725; https://doi.org/10.3390/cryst10090725 - 20 Aug 2020

Abstract The parallel advances of different scientific fields provide a contemporary scenario where collaboration is not a differential, but actually a requirement. In this context, crystallography has had a major contribution on the medical sciences, providing a "face" for targets of diseases that previously [...] Read more.
(This article belongs to the Special Issue A 10 Years Journey: Chemical, Physical, and Biological Properties and Applications of Crystals)

► Show Figures

Open Access Article

The Sensitivity of the Pair-Angle Distribution Function to Protein Structure

by Patrick Adams, Jack Binns, Tamar L. Greaves and Andrew V. Martin
Crystals 2020, 10(9), 724; https://doi.org/10.3390/cryst10090724 - 20 Aug 2020

Abstract The continued development of X-ray free-electron lasers and serial crystallography techniques has opened up new experimental frontiers. Nanoscale dynamical processes such as crystal growth can now be probed at unprecedented time and spatial resolutions. Pair-angle distribution function (PADF) analysis is a correlation-based technique [...] Read more.
(This article belongs to the Special Issue Time Resolved Crystallography)

► Show Figures

Open Access Article

Flow Stability, Convective Heat Transfer and Chemical Reactions in Ammonothermal Autoclaves—Insights by In Situ Measurements of Fluid Temperatures

by Saskia Schimmel, Ines Kobelt, Lukas Heinlein, Anna-Carina L. Kimmel, Thomas G. Steigerwald, Eberhard Schlücker and Peter Wellmann
Crystals 2020, 10(9), 723; https://doi.org/10.3390/cryst10090723 - 20 Aug 2020

Abstract A variety of functional nitride materials, including the important wide bandgap semiconductor GaN, can be crystallized in exceptionally good structural quality by the ammonothermal method. However, the further development of this method is hindered by a lack of access to internal process parameters [...] Read more.
(This article belongs to the Section Inorganic Crystalline Materials)

► Show Figures

Open Access Article

Bulk Cyclotron Resonance in the Topological Insulator Bi_2Te_3

by Dmytro L. Kamenskyi, Artem V. Pronin, Hadj M. Benia, Victor P. Martovitskii, Kirill S. Pervakov and Yurii G. Selivanov
Crystals 2020, 10(9), 722; https://doi.org/10.3390/cryst10090722 - 20 Aug 2020

Abstract We investigated magneto-optical response of undoped Bi_2Te_3 films in the terahertz frequency range (0.3–5.1 THz, 10–170 cm^{-1}) in magnetic fields up to 10 T. The optical transmission, measured in the Faraday geometry, is dominated by a broad Lorentzian-shaped [...] Read more.
(This article belongs to the Special Issue Advances in Topological Materials)

► Show Figures

Open Access | Editorial

σ- and π-Hole Interactions

by Antonio Frontera

Crystals 2020, *10*(9), 721; https://doi.org/10.3390/cryst10090721 - 19 Aug 2020

Abstract
Supramolecular chemistry is a very active research field that was initiated in the last century [...] Full article

(This article belongs to the Special Issue σ- and π-Hole Interactions)

Open Access | Article

Preparation and Electrochemical Properties of Co_3O_4 Supercapacitor Electrode Materials

by Xuelei Wang, Jiawei Fu, Qiufeng Wang, Zhaojun Dong, Xiaoliang Wang, Anyu Hu, Wei Wang and Shaobin Yang

Crystals 2020, *10*(9), 720; https://doi.org/10.3390/cryst10090720 - 19 Aug 2020

Abstract A special gas-phase diffusion precipitation method with ammonia as the gas-phase diffusion precipitant was adopted. After fully reacting with different cobalt sources in a sealed space, the liquid funnel was separated and dried, and calcined at different temperatures for 2 h. The prepared [...] Read more.

(This article belongs to the Section Inorganic Crystalline Materials)

► Show Figures

Open Access | Article

Forbidden Reflections in TeO_2 in the Vicinity of the Te L_1 Absorption Edge

by Elena Ovchinnikova, Dmitri Novikov, Matthias Zschornak, Anton Kulikov, Ksenia Kozlovskaya, Vladimir Dmitrienko, Alexey Oreshko, Alexander Blagov, Enver Mukhamedzhanov, Nikita Marchenkov, Mickhail Borisov, Azat Khadiev, Arsen Petrenko and Yury Pisarevsky

Crystals 2020, *10*(9), 719; https://doi.org/10.3390/cryst10090719 - 19 Aug 2020

Abstract Examining forbidden reflections provides valuable information on electronic states and the local environment of resonant atoms in crystals. Experimental studies of two forbidden reflections 002 and 100 in TeO single crystals were performed at photon energies close to the tellurium [...] Read more.

(This article belongs to the Special Issue Synchrotron-Based X-Ray Techniques for the Study of New Crystalline Materials)

► Show Figures

Open Access | Article

The Future of Carbon: An Update on Graphene's Dermal, Inhalation, and Gene Toxicity

by Nima Moghimian and Soroush Nazarpour

Crystals 2020, *10*(9), 718; https://doi.org/10.3390/cryst10090718 - 19 Aug 2020

Abstract Recent studies on gene, inhalation and dermal toxicity of few-layer graphene have revealed much lower health risk than expected. This could pave the way for graphene as a young member of the nanocarbons family to become the "heir presumptive" to the long-reigning carbon [...] Read more.

(This article belongs to the Special Issue Graphene-Based Nanocomposites and Manufacturing)

Show export options ⌄

Displaying articles 1-134

Crystals

COUNTRY

Switzerland

Universities and research institutions in Switzerland

SUBJECT AREA AND CATEGORY

Chemical Engineering
- Chemical Engineering (miscellaneous)

Chemistry
- Inorganic Chemistry

Materials Science
- Materials Science (miscellaneous)

Physics and Astronomy
- Condensed Matter Physics

PUBLISHER

MDPI Multidisciplinary Digital Publishing Institute

H-INDEX

37

PUBLICATION TYPE

Journals

ISSN

20734352

COVERAGE

2010-2020

INFORMATION

Homepage

How to publish in this journal

helmut.coelfen@uni-konstanz.de

SCOPE

Crystals (ISSN 2073-4352) is an open access journal that covers all aspects of crystalline material research. Crystals provides a forum for the advancement of our understanding of the nucleation, growth, processing, and characterization of crystalline and liquid crystalline materials. Their mechanical, chemical, electronic, magnetic, and optical properties, and their diverse applications, are all considered to be of importance. Additionally, we encourage contributors to send articles focused on crystals research (of small and high molecular weight). Their characterization by using modern techniques for crystal growth and high resolution characterization such as synchrotron radiation and modern methods for the growth of crystals for X-ray free electron lasers (XFELS) would also be welcome. Crystals can be used as a reference and publication source for the crystalline research community. Crystals publishes reviews, regular research articles and short communications. Our aim is to encourage scientists to publish their experimental, theoretical and computational results in as much detail as possible so that results can be reproduced. Therefore, there is no restriction on article length.

Join the conversation about this journal

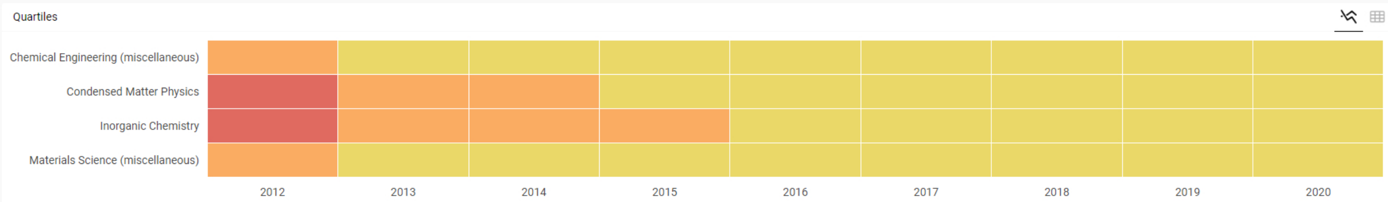

FIND SIMILAR JOURNALS

options

#	Journal	Country	Similarity
1	Beilstein Journal of Nanotechnology	DEU	61% similarity
2	Progress in Materials Science	GBR	60% similarity
3	MRS Communications	GBR	60% similarity
4	Rengong Jingti Xuebao/Journal of Synthetic	CHN	59% similarity
5	Science and Technology of Advanced Materials	GBR	58% similarity

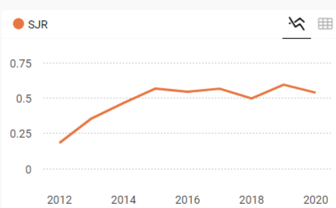

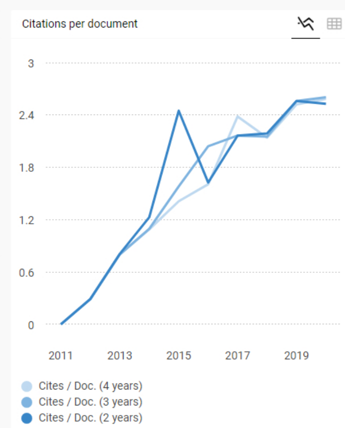

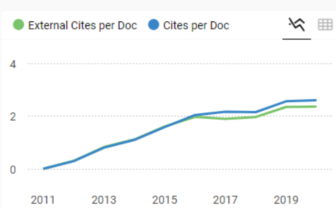

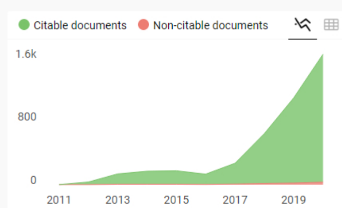

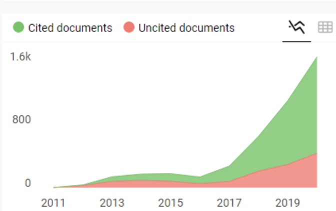

← Show this widget in your own website

Just copy the code below and paste within your html code:

<a href="https://www.scimag

Metrics based on Scopus® data as of April 2021

Y

Yuni Krisnandi 1 year ago

Hi there,

Could you inform us, when usually the SJR and other statistical data is released every year? I am looking forward for the 2019 score.

Thank you!
Yuni

reply

Melanie Ortiz 1 year ago SCImago Team

Dear Yuni,
Thank you for contacting us. Our data come from Scopus, they annually send us an update of the data. This update is sent to us around April / May every year. Thus, the indicators for 2019 will be available in June 2020. Best Regards, SCImago Team

Leave a comment

Name

Email
(will not be published)

I'm not a robot
reCAPTCHA
Privacy - Terms

Submit

The users of Scimago Journal & Country Rank have the possibility to dialogue through comments linked to a specific journal. The purpose is to have a forum in which general doubts about the processes of publication in the journal, experiences and other issues derived from the publication of papers are resolved. For topics on particular articles, maintain the dialogue through the usual channels with your editor.

crystals
an Open Access Journal by MDPI

CITESCORE 2.9 SCOPUS

IMPACT FACTOR 2.404

CERTIFICATE OF PUBLICATION

Certificate of publication for the article titled:

The Prediction of Stiffness of Bamboo-Reinforced Concrete Beams Using Experiment Data and Artificial Neural Networks (ANNs)

Authored by:

Muhtar; Amri Gunasti; Suhardi; Nursaid; Irawati; Ilanka Cahya Dewi; Moh. Dasuki; Sofia Ariyani; Fitriana; Idris Mahmudi; Taufan Abadi; Miftahur Rahman; Syarif Hidayatullah; Agung Nilogiri; Senki Desta Galuh; Ari Eko Wardoyo; Rofi Budi Hamduwibawa

Published in:

Crystals 2020, Volume 10, Issue 9, 757

MDPI Academic Open Access Publishing since 1996

Basel, November 2020

crystals

Article

The Prediction of Stiffness of Bamboo-Reinforced Concrete Beams Using Experiment Data and Artificial Neural Networks (ANNs)

Muhtar [1,*], Amri Gunasti [1], Suhardi [2], Nursaid [1], Irawati [1], Ilanka Cahya Dewi [1], Moh. Dasuki [1], Sofia Ariyani [1], Fitriana [1], Idris Mahmudi [1], Taufan Abadi [1], Miftahur Rahman [1], Syarif Hidayatullah [1], Agung Nilogiri [1], Senki Desta Galuh [1], Ari Eko Wardoyo [1] and Rofi Budi Hamduwibawa [1]

1 Faculty of Engineering, University of Jember, Jember Indonesia 68121, Indonesia; amrigunasti@unmuhjember.ac.id (A.G.); nursaid@unmuhjember.ac.id (N.); irawati@unmuhjember.ac.id (I.); ilankadewi@unmuhjember.ac.id (I.C.D.); moh.dasuki22@unmuhjember.ac.id (M.D.); sofia.ariyani@unmuhjember.ac.id (S.A.); fitriana@unmuhjember.ac.id (F.); idrismahmudi@unmuhjember.ac.id (I.M.); taufan.abadi@unmuhjember.ac.id (T.A.); miftahurrahman@unmuhjember.ac.id (M.R.); syarifhidayatullah@unmuhjember.ac.id (S.H.); agungnilogiri@unmuhjember.ac.id (A.N.); senki.desta@unmuhjember.ac.id (S.D.G.); arieko@unmuhjember.ac.id (A.E.W.); rofi.hamduwibawa@unmuhjember.ac.id (R.B.H.)

2 Faculty of Agricultural Technology, University of Jember, Jember Indonesia 68121, Indonesia; hardi.ftp@unej.ac.id

* Correspondence: muhtar@unmuhjember.ac.id

Received: 3 August 2020; Accepted: 19 August 2020; Published: 27 August 2020

Abstract: Stiffness is the main parameter of the beam's resistance to deformation. Based on advanced research, the stiffness of bamboo-reinforced concrete beams (BRC) tends to be lower than the stiffness of steel-reinforced concrete beams (SRC). However, the advantage of bamboo-reinforced concrete beams has enough good ductility according to the fundamental properties of bamboo, which have high tensile strength and high elastic properties. This study aims to predict and validate the stiffness of bamboo-reinforced concrete beams from the experimental results data using artificial neural networks (ANNs). The number of beam test specimens were 25 pieces with a size of 75 mm × 150 mm × 1100 mm. The testing method uses the four-point method with simple support. The results of the analysis showed the similarity between the stiffness of the beam's experimental results with the artificial neural network (ANN) analysis results. The similarity rate of the two analyses is around 99% and the percentage of errors is not more than 1%, both for bamboo-reinforced concrete beams (BRC) and steel-reinforced concrete beams (SRC).

Keywords: bamboo-reinforced concrete (BRC); stiffness prediction; artificial neural network (ANN)

1. Introduction

Some of the advantages of bamboo include having high tensile strength [1], easy to split, cut, elastic fibers, optimal in bearing loads, and it is not a pollutant. At the same time, the weakness of bamboo as a construction material is easily attacked by insects, because the starch content in bamboo is quite high. Therefore, bamboo as a building material requires treatment, such as immersion in water [2,3] and the application of adhesives and waterproof layers [3]. The application of adhesive and waterproof coating has increased the load capacity and stiffness of the BRC beam [4]. Bamboo as a reinforcement of concrete structural elements has been widely used, among other things, as beam reinforcement [2,5–7], bridge frame reinforcement [8], plate or panel reinforcement [9–11], and column reinforcement [12,13].

The most important mechanical properties of bamboo-reinforced concrete beams are stress, strain, and stiffness. Some previous researchers concluded that bamboo-reinforced concrete beams have lower stiffness compared to steel reinforced concrete beams but have elastic properties and high ductility, so that they are effective in absorbing earthquake energy [14,15]. However, low rigidity will lead to reduced construction integrity and excessive structural deformation. The behavior of materials and construction elements, especially the stiffness parameters can be known through the relationship of load and deflection, as shown in Figure 1.

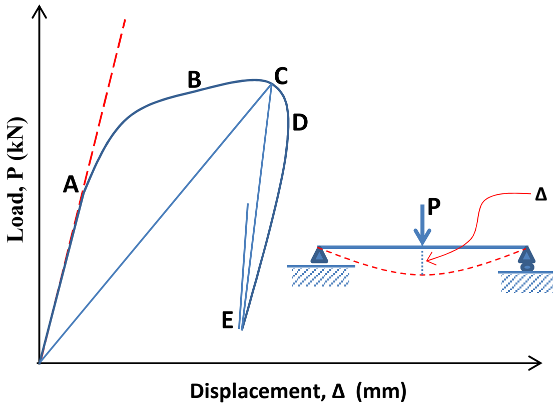

Figure 1. The load vs. deflection relationships of the reinforced concrete beam [15].

The stiffness of bamboo-reinforced concrete beams (*EI*) is the main factor of structural resistance to the bending deformation of BRC beams. Beam stiffness is a function of the modulus of elasticity of the material (*E*) and the moment of inertia (*I*). Moments of inertia before cracking use I_g, and after cracking they use I_{cr}. The effective inertia moment is the value between I_g and I_{cr}. This understanding can be seen from the behavior of the load vs. deflection relationship in Figure 1. In general, the determination of beam stiffness is based on the results of the beam flexural test, while the calculation of elasticity modulus (*E*) of BRC beams for testing beams with two load points can follow Equations (1) and (2) [15].

$$E = \frac{23PL^3}{648\Delta I}(N/mm^2) \quad (1)$$

$$\Delta = \frac{23PL^3}{648EI}(mm) \quad (2)$$

where *E* is the elasticity modulus, Δ is the initial crack, *P* is the initial crack load, *L* is the span, and *I* is the inertia moment of the cross-section.

Making conclusions from the results of research on the behavior of bamboo-reinforced concrete beams (BRC) is not easy to take. Correct conclusions must go through data validation and data analysis with other methods, such as statistical analysis, the finite element method [16], or the artificial neural network (ANN) method [17]. The determination of the stiffness of bamboo-reinforced concrete beams (BRC) from the experimental results must be validated by other methods, such as the artificial neural network (ANN) method.

Artificial neural networks (ANNs) consist of many neurons. Neurons are grouped into several layers. Neurons in each layer are connected with neurons in other layers. This does not apply to the input and output layers but only to the layers in between. Information received at the input layer is continued to the layers in ANN one by one until it reaches the output layer. The layer that lies between the input and output is called the hidden layer. However, not all ANNs have a hidden layer; some are only input and output layers.

Artificial neural networks (ANNs) are a powerful tool for solving complex problems in the field of civil engineering. Many researchers have used the ANN method for many structural engineering studies, such as predicting the compressive strength of concrete [18], axial strength of composite columns [19], and determination of displacement of concrete reinforcement (RC) buildings [20]. Determination and control of BRC beam stiffness are based on load vs. deflection diagrams. Load data and deflection of experimental results are used as input data and target data in the analysis of artificial neural networks (ANNs).

Some previous researchers have concluded that artificial neural networks (ANNs) can be an alternative in calculating deflection in a reinforced concrete beam. The results of deflection calculations on reinforced concrete using ANN proved to be very effective [21]. ANN is also very well used to predict deflection in the concrete beam with a very strong correlation level of 97.27% to the test data [22]. Likewise, the use of ANN to predict deflection in cantilever beams produces very accurate outcomes [23]. In this paper, we use uniform load input data, while the target data are the deflection of laboratory test results. Distribution of ANN model data composition consists of 70% training, 15% validation, and 15% testing. The schematic of ANN architecture for rectangular beams is shown in Figure 2.

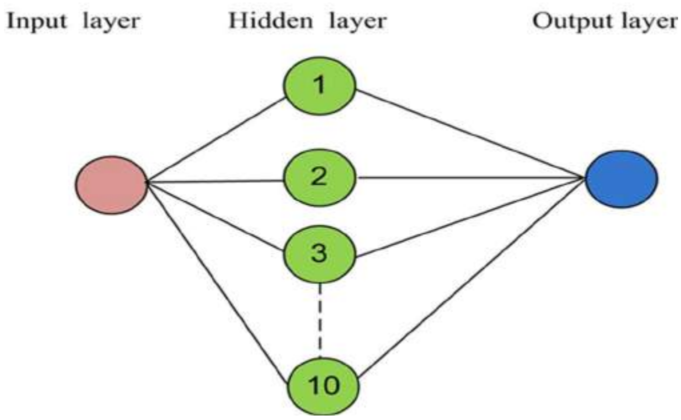

Figure 2. Schematic of ANN architecture for rectangular beams.

The purpose of this study is to validate the behavior and stiffness of the BRC beam experimental results with the artificial neural network (ANN) method. Errors resulting from experimental data are usually caused by some things, such as human errors, calibration of tools that have expired, test method errors, and test items that do not match. Therefore, the experimental data are evaluated and compared with the results of the artificial neural network (ANN) method. In this study, the experimental data are thought to have a large deviation from the results of the artificial neural network (ANN) method. Then, an efficient ANN-based computational technique is presented to estimate the load vs. deflection of bamboo-reinforced concrete blocks (BRC). Furthermore, stiffness observations are made at the same loading point.

2. Materials and Methods

Experimental data were obtained from a single reinforced BRC beam bending test with two load points based on ASTM C 78-02 [24]. The size of bamboo reinforcement is 15 mm × 15 mm, which is treated first through immersion, drying, and the waterproof coating using Sikadur®-752 [3]. As a strengthening of bamboo reinforcement used diameter hose-clamps $\frac{3}{4}$″ [8]. The number of beam test specimens were 25 pieces with a size of 75 mm × 150 mm × 1100 mm consisting of 24 BRC beams and 1 SRC beam with steel reinforcement. The detailed image of the BRC beam specimen is shown in Figure 3. The design of the concrete mixture in this study was Portland Pozzolana Cement (PPC), sand, coarse aggregate, and water with a proportion of 1:1.81:2.82:0.52. The average compressive strength of concrete at the age of 28 days is 31.31 MPa. The steel used is plain steel with f_y = 240 MPa.

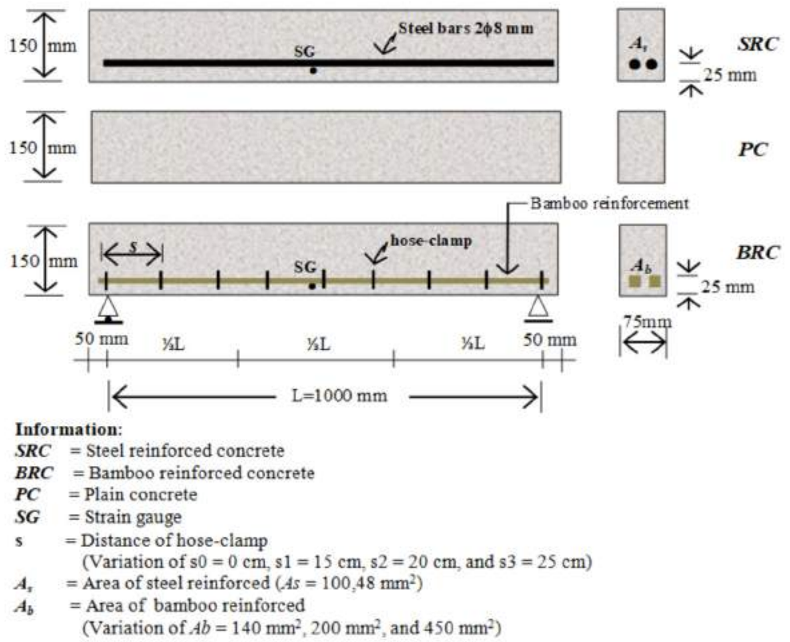

Figure 3. Geometry and details of bamboo-reinforced concrete beams.

The beam flexural test is carried out on two simple supports, namely joint support and roller support. Load in the form of a centralized load divided into two load points with a distance of $^1/_3$L from the support. The strain gauge is mounted on the bamboo reinforcement with a distance of $\frac{1}{2}$L from the support to determine the strain that is occurring. To detect deflection, a linear variable differential transformer is installed at a distance of $\frac{1}{2}$L from the support. To get the stages of loading from zero until the beam collapses, a hydraulic jack and load cell are used that are connected to the load indicator. Loading is carried out slowly at a speed of 8 kg/cm^2–10 kg/cm^2. Load reading on the load indicator is used to control the hydraulic jack pump, deflection, and strain according to the planned loading stage. However, when the test specimen reaches the ultimate load, deflection readings become the control of readings of the strain and load. Hydraulic jack pumping continues to take place slowly according to the deflection reader command. The collapse pattern is observed and identified through cracks that occur, starting from the first crack until the beam collapses. The BRC beam test setting is shown in Figure 4.

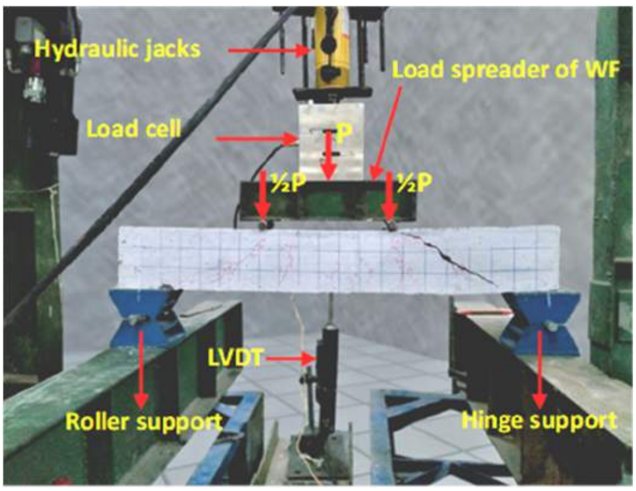

Figure 4. Test arrangement of bamboo-reinforced concrete beams.

3. Results

Mechanical properties and stress–strain characteristics of steel and bamboo materials are the dominant factors that influence the shape of the load vs. deflection relationship behavior models. The difference in the stress and strain relationship pattern of steel and bamboo is seen in the difference in melting point and fracture stress, as shown in Figures 5 and 6. Steel reinforcement shows a clear melting point, whereas bamboo reinforcement does not show a clear melting point. Both of them show a clear stress fracture point, but in bamboo reinforcement, after fracture stress occurs, the strain–stress relationship pattern tends to return to zero, as shown in Figure 5. This shows that bamboo has good elastic properties.

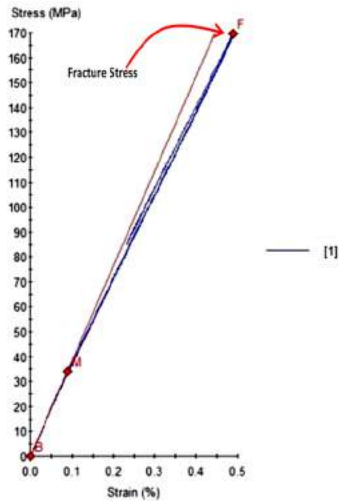

Figure 5. The stress–strain relationship of normal bamboo reinforcement.

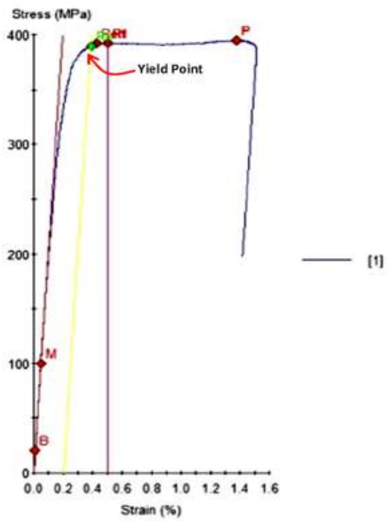

Figure 6. The stress–strain relationship of steel reinforcement.

Figure 7 shows the relation between load vs. deflection of the BRC beam and SRC beam from the analysis of experimental data, while Figure 8 shows the relationship between load vs. deflection of BRC beams and SRC beams resulting from the analysis of artificial neural network (ANN) methods. The BRC beam tends to have a large deflection, but when the maximum load is reached, the deflection tends to return to zero if the load is released, as shown in Figure 9. Documentation of the gradual load discharge after the ultimate load has been reached can be seen in the following link: https://goo.gl/6AVWmP [14] and the BRC beam flat back. This shows its compatibility with bamboo strain–stress behavior. The load vs. deflection relationship of the SRC beam shows the existence of an elastic limit, elasto-plastic limit, and plastic, as shown in Figure 7. While the relationship of load vs. deflection of the BRC beam shows a linear line until the maximum load limit and after the peak load, the deflection returns to zero, as shown in Figure 9.

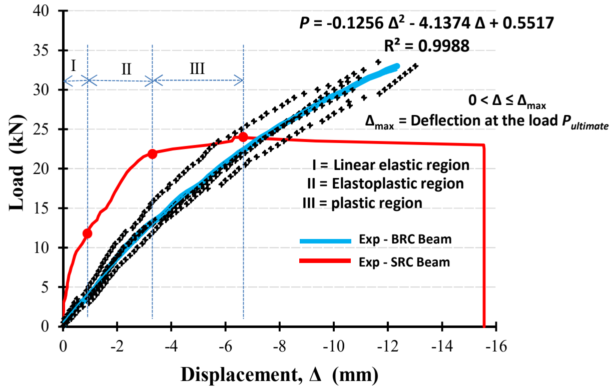

Figure 7. The load vs. deflection relationship of the BRC beam from experiment [14].

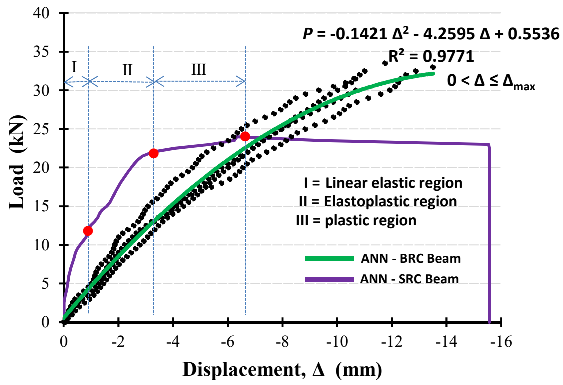

Figure 8. The load vs. deflection relationship of the BRC beam from the ANN method.

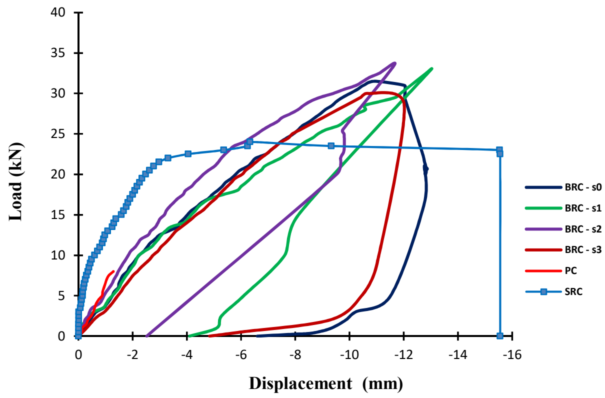

Figure 9. The load vs. deflection relationship of the BRC beam and the SRC beam until the gradual release of the load.

In this case, the ANN studies the network to diagnose the shape and distribution of data from the deflection of BRC beams and SRC beams with different loads. After reaching small and acceptable variations of errors, training in neural networks is stopped. Then, the neural network model is tested, and the results are validated by comparing it with the results of the analysis of experimental data. Every network created in the ANN is trained, tested, and validated for all data samples to identify the best technique. The data input for the network used is the deflection data from the experimental results of the BRC beam and the SRC beam. The deflection data file of the experimental results is saved in the form of MS Excel. Data are distributed into training (70%), testing (15%), and validation (15%).

Figures 10–13 show the prediction of the load vs. deflection relationship of the BRC beam and Figure 14 shows the prediction of the relationship of load vs. deflection of the SRC beam from the ANN method analysis. The correlation value of laboratory data by using ANN shows an average value of R Square of 0.999. The results of predictions by the ANN method show that the percentage of errors is very small, with a maximum error of 0.26%. Overall, the comparison of experimental data with the results of the ANN method predictions shows no more than a 1% error. From the data results of the two analyses and the pattern of load vs. deflection relationships, it can be concluded that the stiffness of the BRC beams is similar. Then, the stiffness prediction with the elasticity modulus parameter can be calculated based on the load vs. deflection relationship graph, as shown in Figure 15.

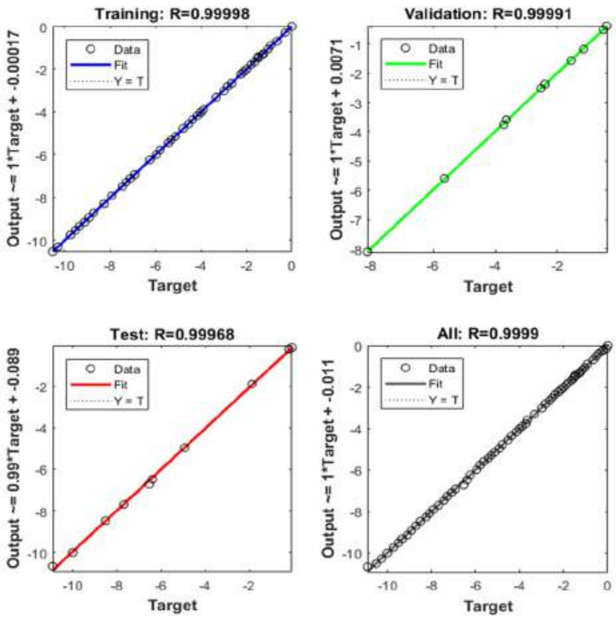

Figure 10. The correlation value of laboratory data and the ANN method (BRC-1 beam).

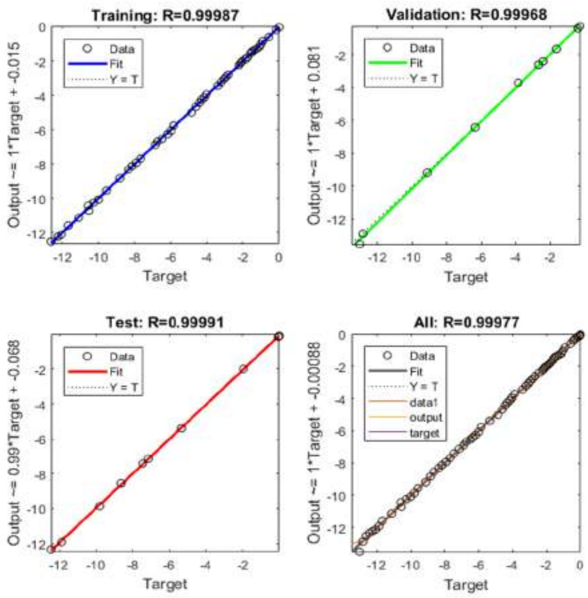

Figure 11. The correlation value of laboratory data and the ANN method (BRC-2 beam).

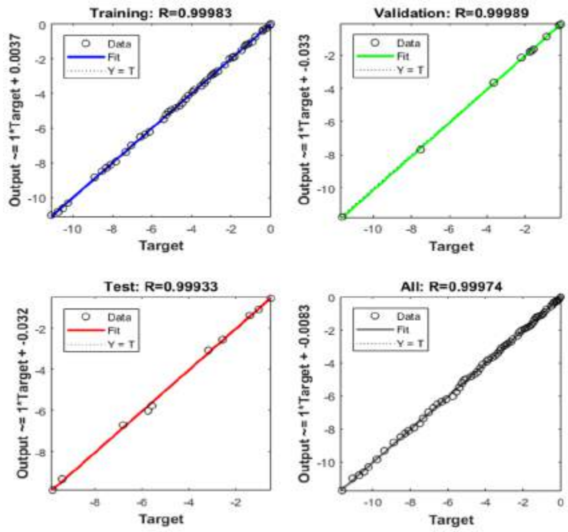

Figure 12. The correlation value of laboratory data and the ANN method (BRC-3 beam).

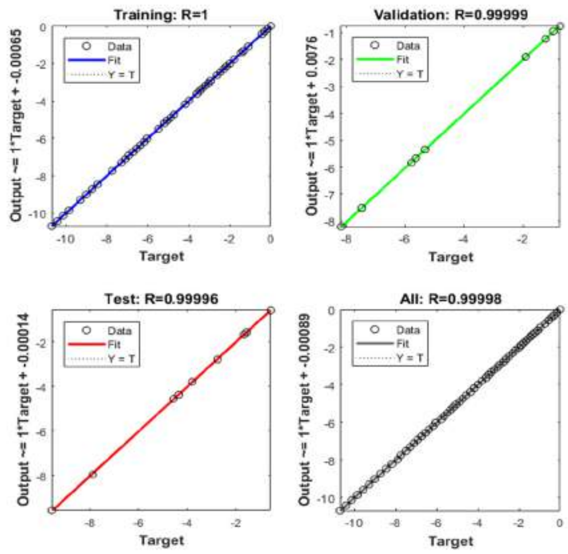

Figure 13. The correlation value of laboratory data and the ANN method (BRC-4 beam).

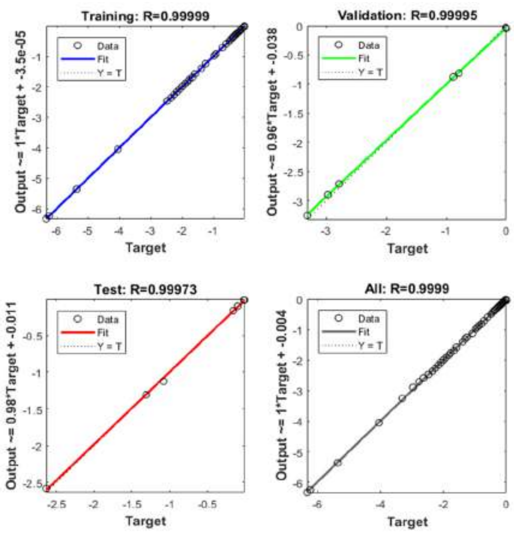

Figure 14. The correlation value of laboratory data and the ANN method (SRC beam).

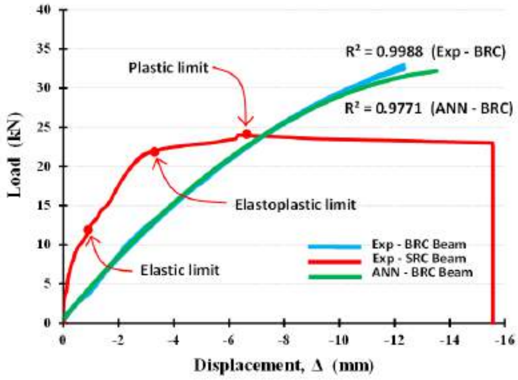

Figure 15. The load vs. deflection relationship the experimental results and ANN analysis.

Figure 15 shows the combined relationship of the load vs. deflection beam of the experimental BRC beam and the ANN analysis results. Figure 15 shows a graph that is coincidental with an error rate of not more than 1%, so that the combined graph of the load vs. deflection relationship can be used to determine the modulus of elasticity or the stiffness of the BRC beam.

4. Discussion

Figure 16 shows the results of the two methods of data analysis being a load vs. deflection pattern. From this load vs. deflection pattern, the stiffness of bamboo-reinforced concrete beams can be predicted. Prediction of stiffness with the elasticity modulus parameters can be calculated based on the load vs. deflection relationship graph. The graph of load vs. deflection relationship shows that at 40% ultimate load, the stiffness of the BRC beam has a stiffness lower to 44% than the SRC beam. Meanwhile, if viewed from the graph load vs. deflection relationship, ANN analysis results with experimental results show the same stiffness value up to 80% ultimate load. The stiffness of BRC beams at loads above 80% indicates a difference, namely the stiffness of the ANN analysis results is lower than the experimental results, as shown in Figure 16.

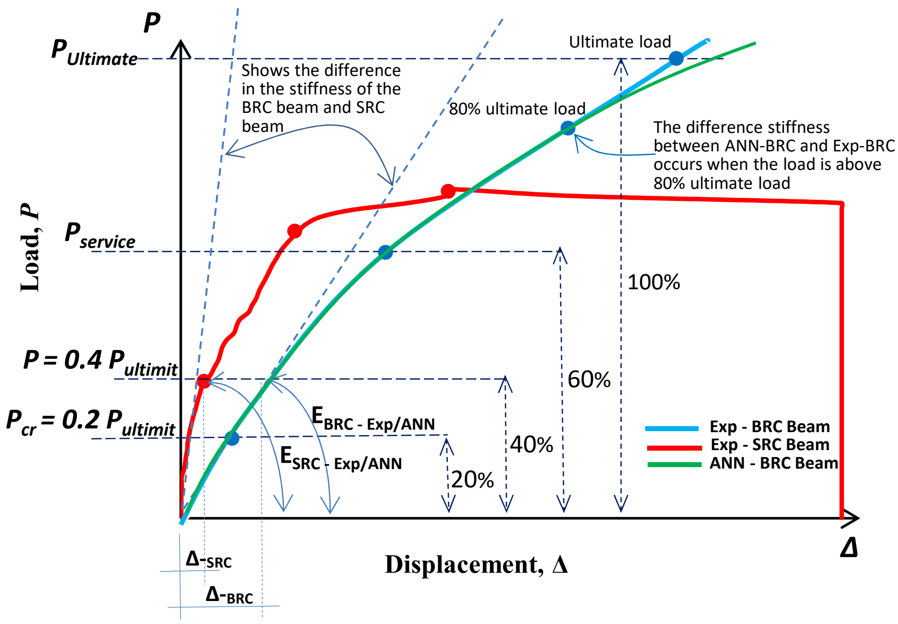

Figure 16. The difference in stiffness between the SRC beam, BRC beam, and BRC beam of ANN analysis result.

Table 1 shows that the initial crack (elastic region) of the BRC beam is in the range of 20% of the ultimate load and 40% of the ultimate load for the SRC beam. Whereas the effect of installing hose-clamps on bamboo reinforcement on the ultimate load of BRC beams is optimum at a distance of 20 cm (BRC-s2) and decreases at a distance of 25 cm, this indicates that installing hose-clamps that are too tight will reduce the elastic properties of bamboo reinforcement and decrease its ductility, as shown in Figure 17. Installation of hoses that are too tight does not increase the stiffness of the BRC beam but instead reduces the load capacity. The control of the load vs. deflection relationship with the ANN method is taken from the results of the regression analysis of six beam samples in each group, namely the BRC-s0, BRC-s1, BRC-s2, and BRC-s3 groups, plus one SRC beam, as shown in Figures 7 and 8. The ANN analysis results for each group are regressed back and used as the final result to determine the stiffness of the BRC beam, as shown in Figure 15. The ANN analysis results for each group are shown in Figures 10–13.

Table 1. The value of the average initial crack loads and ultimate loads based on theoretical calculations and experimental.

Specimens	Theoretical Calculations		Flexural Test Results		
	First Crack Load (kN)	Ultimate Load (kN)	Average First Crack Load (kN)	Average Failure Load (kN)	Average Deflection at Failure (mm)
(a) BRC-s0	6.87	32.19	8.25	30.25	11.41
(b) BRC-s1	6.87	32.19	7.25	32.00	12.60
(c) BRC-s2	6.87	32.19	8.00	33.25	12.01
(d) BRC-s3	6.87	32.19	7.50	29.75	9.15
(e) SRC	6.51	16.14	10.00	24.00	6.33

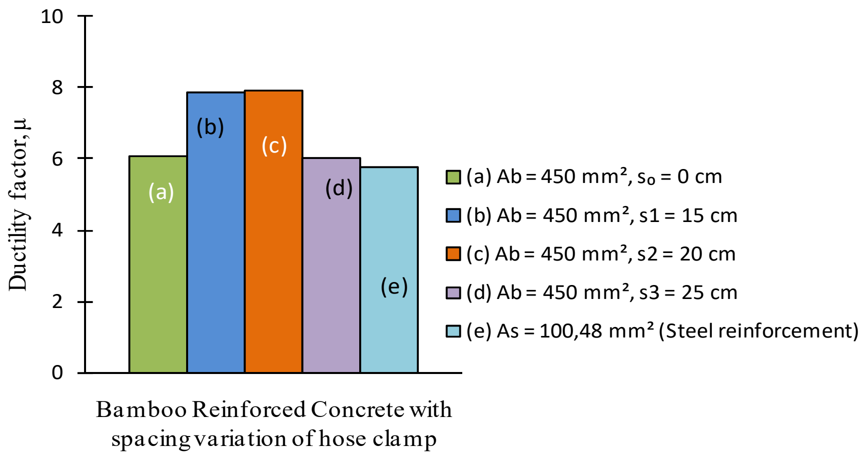

Figure 17. The effect of hose-clamp distance on the ductility value.

Stiffness (*EI*) is the main parameter of the resistance of structural elements to bending deformation. The basic properties and behavior of stress–strain material are the dominant factors determining the size of the rigidity of structural elements. SRC beam stiffness has a greater stiffness than the BRC beam stiffness. This is due to the steel reinforcement having an elasticity modulus greater than the elasticity modulus of bamboo. However, the BRC beam has good elastic properties, in harmony with the pattern of stress–strain relationships of bamboo. This proves that bamboo material has good earthquake energy absorption. The behavior of elastic on the BRC beam can be seen in the video at the following link: https://goo.gl/6AVWmP [14].

Integrity and rigidity in a structure are essential. Therefore, the low stiffness of the BRC beam is essential to find a solution. Solutions to solve the low stiffness of the BRC beam, such as the graph diagram in Figure 16, can be done in two ways, namely giving strength to bamboo reinforcement and applying the principle of confined concrete [7]. Strengthening of bamboo reinforcement can be achieved by using adhesive, increasing surface roughness, installing hose-clamps that function as hooks and shear connectors, and so on. An equally important solution is to increase the strength of the concrete to support increasing the stiffness of the BRC beam. Previous studies showed that the cause of the majority of BRC beam collapse is by slippage [14] and shear collapse [14]. The principle of confined concrete is fundamental to do by giving shear reinforcement to the BRC beam.

5. Conclusions

Predictions of bamboo-reinforced concrete beam stiffness based on experimental results and analysis results of artificial neural network (ANN) methods show very close similarities or with an error prediction of no more than 1%.

Bamboo-reinforced concrete (BRC) beams have a lower stiffness of up to 40% when compared to steel reinforced concrete (SRC) beams.

The stiffness of the BRC beam of experimental result and the artificial neural network (ANN) analysis results have in common up to 80% of the ultimate load and, afterward, show differences.

The coatings of adhesives, modification of bamboo reinforcement roughness, and the use of shear reinforcement are solutions to increase the stiffness and capacity of the BRC beam.

Installation of a hose-clamp that is too tight does not increase the stiffness of the BRC beam but reduces its elastic properties and reduces its load capacity.

Author Contributions: Conceptualization, M., S., and A.G.; methodology, M., S., and A.N.; software, S., S.A., A.N., and A.E.W.; validation, M., I., and I.C.D.; formal analysis, M., S., and M.D.; investigation, N., and T.A.; resources, N.; data curation, M., and S.; writing—original draft preparation, A.N. and F.; writing—review and editing, M. and S.D.G.; visualization, M.R. and S.H.; supervision, N.; project administration, R.B.H.; funding acquisition, N. and I.M. All authors have read and agreed to the published version of the manuscript.

Funding: APC was financed entirely by the DPRM Republic of Indonesia and LPPM of the University of Muhammadiyah, Jember, Indonesia.

Acknowledgments: Funding Research is fully borne by the research Program, Directorate of Research and Community Service, Directorate General of Research and Technology Strengthening and Development of the Ministry of Research, Technology, and Higher Education of the Republic of Indonesia.

Conflicts of Interest: The authors declare no conflict of interest.

References

1. Ghavami, K. Bamboo as reinforcement in structural concrete elements. *Cem. Concr. Compos.* **2005**, *27*, 637–649. [CrossRef]
2. Agarwal, A.; Nanda, B.; Maity, D. Experimental investigation on chemically treated bamboo reinforced concrete beams and columns. *Constr. Build. Mater.* **2014**, *71*, 610–617. [CrossRef]
3. Muhtar, M. Experimental data from strengthening bamboo reinforcement using adhesives and hose-clamps. *Data Brief* **2019**, *27*, 104827. [CrossRef] [PubMed]
4. Muhtar, M. Cracked Pattern of Bamboo Reinforced Concrete Beams Using Double Reinforcement with the Strengthening on Tensile Reinforcement. *Int. J. Eng. Res. Technol.* **2020**, *13*, 608–612.
5. Rahman, M.M.; Rashid, M.H.; Hossain, M.A.; Hasan, M.T.; Hasan, M.K. Performance evaluation of bamboo reinforced concrete beam. *Int. J. Eng. Res. Technol. IJET-IJENS* **2011**, *11*, 113–118.
6. Dewi, S.M.; Nuralinah, D.; Munawir, A.; Wijaya, M.N. Crack behavior study of bamboo reinforced concrete beam with additional pegs in reinforcing. *Int. J. Civ. Eng. Technol.* **2018**, *9*, 1632–1640.
7. Dewi, S.M. The flexural behavior model of bamboo reinforced concrete beams using a hose clamp. *Proc. Mater. Sci. Eng. Chem.* **2019**, *276*, 1033.
8. Muhtar, A.; Gunasti Manggala, A.S.; Nusant, A.F.P.; Hanafi, A.N. Effect of reinforcement details on precast bridge frames of bamboo reinforced concrete to load capacity and crack patterns. *Int. J. Eng. Res. Technol.* **2020**, *13*, 631–636.
9. Puri, V.; Chakrabortty, P.; Anand, S.; Majumdar, S. Bamboo reinforced prefabricated wall panels for low-cost housing. *J. Build. Eng.* **2017**, *9*, 52–59. [CrossRef]
10. Maruthupandian, G.; Saravanan, R.; S Suresh, K.S.; Sivakumar, B.G. A Study on Bamboo Reinforced Concrete Slabs. *J. Chem. Pharm. Sci. A* **2016**, *9*, 978–980.

11. Daud, N.M.; Nor, N.M.; Yusof, M.A.; Yahya, M.A.; Munikanan, V. Axial and flexural load test on untreated bamboocrete multi-purpose panel. *Int. J. Integr. Eng.* **2018**, *10*, 28–31.
12. Tripura, D.D.; Singh, K.D. Mechanical behavior of rammed earth column: A comparison between unreinforced, steel and bamboo reinforced columns. *Mater. Constr.* **2018**, *68*, 174. [CrossRef]
13. Rameshwar, S.; Kale, A.; Rashmirana, P. Suitability of Bamboo as Reinforcement in Column. *Int. J. Recent Innov. Trends Comput. Commun.* **2016**, *4*, 270–272.
14. Dewi, S.M. Enhancing bamboo reinforcement using a hose-clamp to increase bond-stress and slip resistance. *J. Build. Eng.* **2019**, *26*, 100896.
15. Dewi, S.M. The Stiffness and Cracked Pattern of Bamboo Reinforced Concrete Beams Using a Hose Clamp. *Int. J. Civ. Eng. Technol.* **2018**, *9*, 273–284.
16. Muhtar, M. Numerical validation data of tensile stress zones and crack zones in bamboo reinforced concrete beams using the Fortran PowerStation 4.0 program. *Data Brief* **2020**, *29*, 105332. [CrossRef]
17. Suryanita, R.; Maizir, H.; Jingga, H. Prediction of Structural Response due to Earthquake Load using Artificial Prediction of Structural Response due to Earthquake Load using Artificial Neural Networks. In Proceedings of the International Conference on Engineering & Technology, Computer, Basic & Applied Sciences, Bangkok, Thailand, 20–21 June 2016.
18. Naderpour, H.; Kheyroddin, A.; Amiri, G.G. Prediction of FRP-confined compressive strength of concrete using artificial neural networks. *Compos. Struct.* **2010**, *92*, 2817–2829. [CrossRef]
19. Ahmadi, M.; Naderpour, H.; Kheyroddin, A. Utilization of artificial neural networks to prediction of the capacity of CCFT short columns subject to short term axial load. *Arch. Civ. Mech. Eng.* **2014**, *14*, 510–517. [CrossRef]
20. Khademi, F.; Akbari, M.; Nikoo, M. Displacement determination of concrete reinforcement building using data-driven models. *Int. J. Sustain. Built Environ.* **2017**, *6*, 400–411. [CrossRef]
21. Kaczmarek, M.; Szymanska, A. application of artificial neural networks to predict the deflections of reinforced concrete beams. *Stud. Geotech. Mech.* **2016**, *38*, 37–46. [CrossRef]
22. Abd, A.M.; Salman, W.D.; Ahmed, Q.W. Ann and statistical modelling to predict the deflection of continuous reinforced concrete. *Diyala J. Eng. Sci.* **2015**, 134–143.
23. Ya, T.T.; Alebrahim, R.; Fitri, N.; Alebrahim, M. Analysis of Cantilever Beam Deflection under Uniformly Distributed Load using Artificial Neural Networks. *MATEC Web Conf.* **2019**, *4*, 06004.
24. ASTM C78/C78M-02. *Standard Test Method for Flexural Strength of Concrete (Using Simple Beam with Third-Point Loading)*; ASTM International: Sikangshihoken, PA, USA, 2002.

The Prediction of Stiffness of Bamboo-Reinforced Concrete Beams Using Experiment Data and Artificial Neural Networks (ANNs)

by Muhtar [1,*], Amri Gunasti [1], Suhardi [2], Nursaid [1], Irawati [1], Ilanka Cahya Dewi [1], Moh. Dasuki [1], Sofia Anyani [1], Fitriana [1], Idris Mahmudi [1], Taufan Abadi [1], Miftahur Rahman [1], Syarif Hidayatullah [1], Agung Nilogiri [1], Senki Desta Galuh [1], Ari Eko Wardoyo [1] and Rofi Budi Hamduwibawa [1]

1 Faculty of Engineering, University of Jember, Jember Indonesia 68121, Indonesia
2 Faculty of Agricultural Technology, University of Jember, Jember Indonesia 68121, Indonesia
* Author to whom correspondence should be addressed.

Crystals 2020, *10*(9), 757; https://doi.org/10.3390/cryst10090757

Received: 3 August 2020 / Revised: 18 August 2020 / Accepted: 19 August 2020 / Published: 27 August 2020

(This article belongs to the Special Issue Numerical Study of Concrete)

Abstract

Stiffness is the main parameter of the beam's resistance to deformation. Based on advanced research, the stiffness of bamboo-reinforced concrete beams (BRC) tends to be lower than the stiffness of steel-reinforced concrete beams (SRC). However, the advantage of bamboo-reinforced concrete beams has enough good ductility according to the fundamental properties of bamboo, which have high tensile strength and high elastic properties. This study aims to predict and validate the stiffness of bamboo-reinforced concrete beams from the experimental results data using artificial neural networks (ANNs). The number of beam test specimens were 25 pieces with a size of 75 mm × 150 mm × 1100 mm. The testing method uses the four-point method with simple support. The results of the analysis showed the similarity between the stiffness of the beam's experimental results with the artificial neural network (ANN) analysis results. The similarity rate of the two analyses is around 99% and the percentage of errors is not more than 1%, both for bamboo-reinforced concrete beams (BRC) and steel-reinforced concrete beams (SRC). View Full-Text

Keywords: bamboo-reinforced concrete (BRC); stiffness prediction; artificial neural network (ANN)

▼ Show Figures

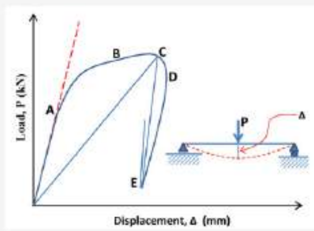

Figure 1

Share and Cite

MDPI and ACS Style
Muhtar; Gunasti, A.; Suhardi; Nursaid; Irawati; Dewi, I.C.; Dasuki, M.; Anyani, S.; Fitriana; Mahmudi, I.; Abadi, T.; Rahman, M.; Hidayatullah, S.; Nilogiri, A.; Desta Galuh, S.; Eko Wardoyo, A.; Budi Hamduwibawa, R. The Prediction of Stiffness of Bamboo-Reinforced Concrete Beams Using Experiment Data and Artificial Neural Networks (ANNs). *Crystals* **2020**, *10*, 757. https://doi.org/10.3390/cryst10090757

AMA Style
Muhtar, Gunasti A, Suhardi, Nursaid, Irawati, Dewi IC, Dasuki M, Anyani S, Fitriana, Mahmudi I, Abadi T, Rahman M, Hidayatullah S, Nilogiri A, Desta Galuh S, Eko Wardoyo A, Budi Hamduwibawa R. The Prediction of Stiffness of Bamboo-Reinforced Concrete Beams Using Experiment Data and Artificial Neural Networks (ANNs). *Crystals*. 2020; 10(9):757. https://doi.org/10.3390/cryst10090757

Chicago/Turabian Style
Muhtar, Gunasti, Amri; Suhardi; Nursaid; Irawati; Dewi, Ilanka C.; Dasuki, Moh.; Anyani, Sofia; Fitriana; Mahmudi, Idris; Abadi, Taufan; Rahman, Miftahur; Hidayatullah, Syarif; Nilogiri, Agung; Desta Galuh, Senki; Eko Wardoyo, Ari; Budi Hamduwibawa, Rofi. 2020. "The Prediction of Stiffness of Bamboo-Reinforced Concrete Beams Using Experiment Data and Artificial Neural Networks (ANNs)" Crystals 10, no. 9: 757. https://doi.org/10.3390/cryst10090757

Find Other Styles
Type a publisher, journal or format name

Note that from the first issue of 2016, MDPI journals use article numbers instead of page numbers. See further details here.

Article Metrics

Citations

Crossref	Scopus	Web of Science	Google Scholar
2	2	3	[click to view]

Article Access Statistics

Article access statistics
800

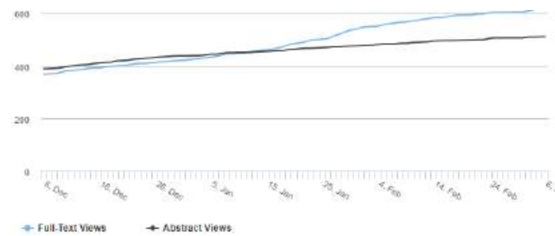
600
400
200
0
6. Dec
16. Dec
26. Dec
5. Jan
15. Jan
25. Jan
4. Feb
14. Feb
24. Feb
Full-Text Views
Abstract Views

crystals

MDPI

Article

The Prediction of Stiffness of Bamboo-Reinforced Concrete Beams Using Experiment Data and Artificial Neural Networks (ANNs)

Muhtar [1,*], Amri-Gunasti [1], Suhardi [2], Nursaid [1], Irawati [1], Ilanka-Cahya Dewi [1], Moh.-Dasuki [1], Sofia-Ariyani [1], Fitriana [1], Idris-Mahmudi [1], Taufan-Abadi [1], Miftahur-Rahman [1], Syarif-Hidayatullah [1], Agung-Nilogiri [1], Senki-Desta Galuh [1], Ari Eko Wardoyo [1] and Rofi-Budi Hamduwibawa [1]

[1] University of Muhammadiyah Jember, Jember, 68121, Indonesia; amrigunasti@unmuhjember.ac.id (A.-G.); nursaid@unmuhjember.ac.id (N.); irawati@unmuhjember.ac.id (I.); ilankadewi@unmuhjember.ac.id (I.-C.D.); moh.dasuki22@unmuhjember.ac.id (M.-D.); sofia.ariyani@unmuhjember.ac.id (S.-A.); fitriana@unmuhjember.ac.id (F.); idrismahmudi@unmuhjember.ac.id (I.-M.); taufan.abadi@unmuhjember.ac.id (T.-A.); miftahurrahman@unmuhjember.ac.id (M.-R.); syarifhidayatullah@unmuhjember.ac.id (S.-H.); agungnilogiri@unmuhjember.ac.id (A.-N.); senki.desta@unmuhjember.ac.id (S.-D.G.); arieko@unmuhjember.ac.id (A.-E.W.); rofi.hamduwibawa@unmuhjember.ac.id (R.-B.H.)

[2] University of Jember, Jember, 68121, Indonesia; hardi.ftp@unej.ac.id (S.)

* Correspondence: muhtar@unmuhjember.ac.id

Received: 3 August 2020; Accepted: 19 August 2020; Published: date

Abstract: Stiffness is the main parameter of the beam's resistance to deformation. Based on advanced research, the stiffness of bamboo-reinforced concrete beams (BRC) tends to be lower than the stiffness of steel-reinforced concrete beams (SRC). However, the advantage of bamboo-reinforced concrete beams has enough good ductility according to the fundamental properties of bamboo, which have high tensile strength and high elastic properties. This study aims to predict and validate the stiffness of bamboo-reinforced concrete beams from the experimental results data using artificial neural networks (ANNs). The number of beam test specimens were 25 pieces with a size of 75 mm × 150 mm × 1100 mm. The testing method uses the four-point method with simple support. The results of the analysis showed the similarity between the stiffness of the beam's experimental results with the artificial neural network (ANN) analysis results. The similarity rate of the two analyses is around 99% and the percentage of errors is not more than 1%, both for bamboo-reinforced concrete beams (BRC) and steel-reinforced concrete beams (SRC).

Keywords: bamboo-reinforced concrete (BRC); stiffness prediction; artificial neural network (ANN)

1. Introduction

Some of the advantages of bamboo include having high tensile strength [1], easy to split, cut, elastic fibers, optimal in bearing loads, and it is not a pollutant. At the same time, the weakness of bamboo as a construction material is easily attacked by insects, because the starch content in bamboo is quite high. Therefore, bamboo as a building material requires treatment, such as immersion in water [2,3] and the application of adhesives and waterproof layers [3]. The application of adhesive and waterproof coating has increased the load capacity and stiffness of the BRC beam [4]. Bamboo as a reinforcement of concrete structural elements has been widely used, among other things, as beam reinforcement [2,5–7], bridge frame reinforcement [8], plate or panel reinforcement [9–11], and column reinforcement [12,13].

Commented [GD1]: Attention AE/ME. The following layout issues have not been checked by the English Editing Department and must be carefully verified by the AE/Layout Department: All callout issues, bold usage of callouts, and references to callouts in the text. Correct callout usage in figures. Figure and Table layout issues. Footnote formatting and Glossaries have not been checked. En dash usage for negative values, en dash usage to indicate relationships, en dash usage to indicate bonds (especially in chemistry). The English Editing Department is not responsible for correct italic usage for genes, proteins and technical terminology. This responsibility belongs to the authors. The following are also not checked: spacing between numbers and units of measurement, ratios, en dashes for ranges, date and time formats, punctuation in equation lines, and less than/more than spacing (< >). Finally, capitalization and layout of titles/headings must be properly checked as well as ensuring ... [1]

Deleted:

Commented [M2]: Please carefully check the accuracy of ... [2]

Deleted:

Deleted: But

Deleted:

Deleted: ,

Deleted:

Deleted: A

Deleted: N

Deleted: N

Commented [M3]: Changed by multiplication sign, please ... [3]

Deleted: A

Deleted: N

Deleted: N

Deleted: s

Deleted: z

Deleted: or

Deleted: bamboo r

Deleted: bamboo r

Commented [GD4]: Define if appropriate.

Deleted: The use of b

Deleted: ve

Deleted: s

The most important mechanical properties of bamboo-reinforced concrete beams are stress, strain, and stiffness. Some previous researchers concluded that bamboo-reinforced concrete beams have lower stiffness compared to steel reinforced concrete beams but have elastic properties and high ductility, so that they are effective in absorbing earthquake energy [14,15]. However, low rigidity will lead to reduced construction integrity and excessive structural deformation. The behavior of materials and construction elements, especially the stiffness parameters can be known through the relationship of load and deflection, as shown in Figure 1.

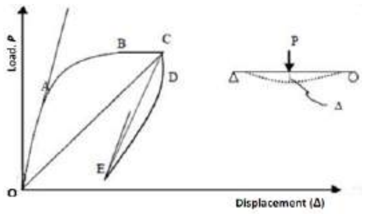

Figure 1. The load vs. deflection relationships of the reinforced concrete beam [15].

The stiffness of bamboo-reinforced concrete beams (*EI*) is the main factor of structural resistance to the bending deformation of BRC beams. Beam stiffness is a function of the modulus of elasticity of the material (*E*) and the moment of inertia (*I*). Moments of inertia before cracking use I_g, and after cracking they use I_{cr}. The effective inertia moment is the value between I_g and I_{cr}. This understanding can be seen from the behavior of the load vs. deflection relationship in Figure 1. In general, the determination of beam stiffness is based on the results of the beam flexural test, while the calculation of elasticity modulus (*E*) of BRC beams for testing beams with two load points can follow Equations (1,2) [15].

$$E = \frac{23PL^3}{648\Delta I}(N/mm^2) \quad (1)$$

$$\Delta = \frac{23PL^3}{648EI}(mm) \quad (2)$$

where *E* is the elasticity modulus, *Δ* is the initial crack, *P* is the initial crack load, *L* is the span, and *I* is the inertia moment of the cross-section.

Making conclusions from the results of research on the behavior of bamboo-reinforced concrete beams (BRC) is not easy to take. Correct conclusions must go through data validation and data analysis with other methods, such as statistical analysis, the finite element method [16], or the artificial neural network (ANN) method [17]. The determination of the stiffness of bamboo-reinforced concrete beams (BRC) from the experimental results must be validated by other methods, such as the artificial neural network (ANN) method.

Artificial neural networks (ANNs) consist of many neurons. Neurons are grouped into several layers. Neurons in each layer are connected with neurons in other layers. This does not apply to the input and output layers but only to the layers in between. Information received at the input layer is continued to the layers in ANN one by one until it reaches the output layer. The layer that lies between the input and output is called the hidden layer. However, not all ANNs have a hidden layer; some are only input and output layers.

Artificial neural networks (ANNs) are a powerful tool for solving complex problems in the field of civil engineering. Many researchers have used the ANN method for many structural engineering studies, such as predicting the compressive strength of concrete [18], axial strength of composite columns [19], and determination of displacement of RC buildings [20]. Determination and control of BRC beam stiffness are based on load vs. deflection diagrams. Load data and deflection of

Deleted: bamboo r
Deleted: bamboo r
Deleted: ,
Deleted: ,
Commented [M5]: Please confirm if there is any copyright issue with this figure. For any reused figures or tables, permission shall be obtained from the copyright holder.
Deleted: bamboo r
Deleted: are used
Deleted: ing
Deleted: .
Deleted: W
Deleted: Which one
Deleted: bamboo r
Deleted: A
Deleted: N
Deleted: N
Deleted: s
Deleted: bamboo r
Deleted: A
Deleted: N
Deleted: N
Deleted: s
Deleted: N
Deleted: N
Deleted: s
Deleted: ,
Deleted: ,
Deleted: N
Deleted: N
Deleted: is
Commented [GD6]: Define if appropriate.

experimental results are used as input data and target data in the analysis of artificial neural networks (ANNs).

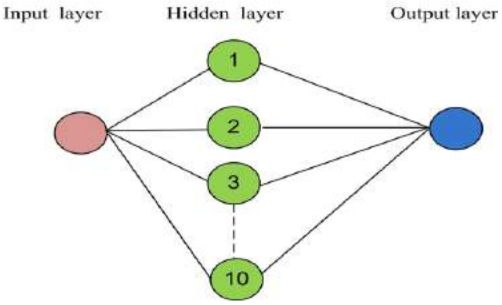

Figure 2. Schematic of ANN architecture for rectangular beams.

Some previous researchers have concluded that artificial neural networks (ANNs) can be an alternative in calculating deflection in a reinforced concrete beam. The results of deflection calculations on reinforced concrete using ANN proved to be very effective [21]. ANN is also very well used to predict deflection in the concrete beam with a very strong correlation level of 97.27% to the test data [22]. Likewise, the use of ANN to predict deflection in cantilever beams produces very accurate outcomes [23]. In this paper, we use uniform load input data, while the target data are the deflection of laboratory test results. Distribution of ANN model data composition consists of 70% training, 15% validation, and 15% testing. The schematic of ANN architecture for rectangular beams is shown in Figure 2.

The purpose of this study is to validate the behavior and stiffness of the BRC beam experimental results with the artificial neural network (ANN) method. Errors resulting from experimental data are usually caused by some things, such as human errors, calibration of tools that have expired, test method errors, and test items that do not match. Therefore, the experimental data are evaluated and compared with the results of the artificial neural network (ANN) method. In this study, the experimental data are thought to have a large deviation from the results of the artificial neural network (ANN) method. Then, an efficient ANN-based computational technique is presented to estimate the load vs. deflection of bamboo-reinforced concrete blocks (BRC). Furthermore, stiffness observations are made at the same loading point.

2. Materials and Methods

Experimental data were obtained from a single reinforced BRC beam bending test with two load points based on ASTM C 78-02 [24]. The size of bamboo reinforcement is 15 mm × 15 mm, which is treated first through immersion, drying, and the waterproof coating using Sikadur®-752 [3]. As a strengthening of bamboo reinforcement used diameter hose-clamps ¾" [8]. The number of beam test specimens were 25 pieces with a size of 75 mm × 150 mm × 1100 mm consisting of 24 BRC beams and 1 SRC beam with steel reinforcement. The detailed image of the BRC beam specimen is shown in Figure 3. The design of the concrete mixture in this study was Portland Pozzolana Cement (PPC), sand, coarse aggregate, and water with a proportion of 1:1.81:2.82:0.52. The average compressive strength of concrete at the age of 28 days is 31.31 MPa. The steel used is plain steel with f_y = 240 MPa.

The beam flexural test is carried out on two simple supports, namely joint support and roller support. Load in the form of a centralized load divided into two load points with a distance of ⅓L from the support. The strain gauge is mounted on the bamboo reinforcement with a distance of ½L from the support to determine the strain that is occurring. To detect deflection, a linear variable differential transformer is installed at a distance of ½L from the support. To get the stages of loading from zero until the beam collapses, a hydraulic jack and load cell are used that are connected to the

Deleted: A
Deleted: N
Deleted: N
Commented [GD7]: Define if appropriate.
Deleted: s
Deleted: A
Deleted: N
Deleted: N
Deleted: is
Deleted: s
Deleted: A
Deleted: N
Deleted: N
Deleted: s
Deleted: A
Deleted: N
Deleted: N
Deleted: s
Deleted: is
Deleted: A
Deleted: N
Deleted: N
Deleted: s
Deleted: bamboo r
Commented [GD8]: Define if appropriate.
Deleted:
Deleted:
Deleted:
Deleted: L
Deleted: V
Deleted: D
Deleted: T

load indicator. Loading is carried out slowly at a speed of 8 kg/cm^2–10 kg/cm^2. Load reading on the load indicator is used to control the hydraulic jack pump, deflection, and strain according to the planned loading stage. However, when the test specimen reaches the ultimate load, deflection readings become the control of readings of the strain and load. Hydraulic jack pumping continues to take place slowly according to the deflection reader command. The collapse pattern is observed and identified through cracks that occur, starting from the first crack until the beam collapses. The BRC beam test setting is shown in Figure 4.

Deleted: But

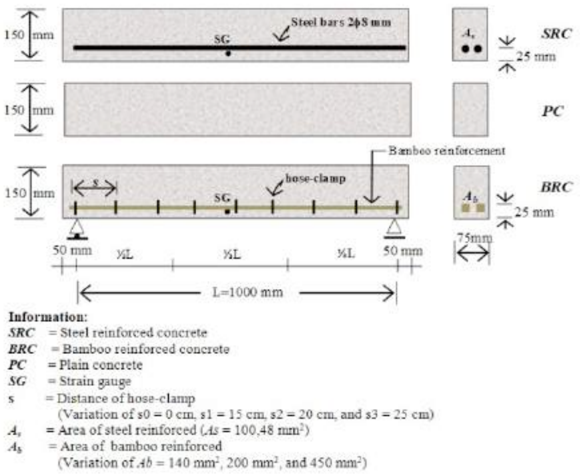

Figure 3. Geometry and details of bamboo-reinforced concrete beams.

Deleted: bamboo r

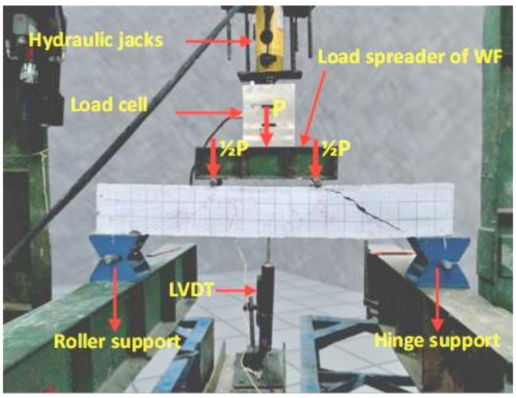

Figure 4. Test arrangement of bamboo-reinforced concrete beams.

Deleted: bamboo r

3. Results

Mechanical properties and stress–strain characteristics of steel and bamboo materials are the dominant factors that influence the shape of the load vs. deflection relationship behavior models. The difference in the stress and strain relationship pattern of steel and bamboo is seen in the difference in melting point and fracture stress, as shown in Figure 5 and Figure 6. Steel reinforcement shows a

Deleted: -

clear melting point, whereas bamboo reinforcement does not show a clear melting point. Both of them show a clear stress fracture point, but in bamboo reinforcement, after fracture stress occurs, the strain–stress relationship pattern tends to return to zero, as shown in Figure 5. This shows that bamboo has good elastic properties.

Deleted:

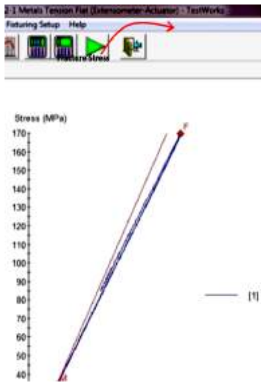

Figure 5. The stress–strain relationship of normal bamboo reinforcement

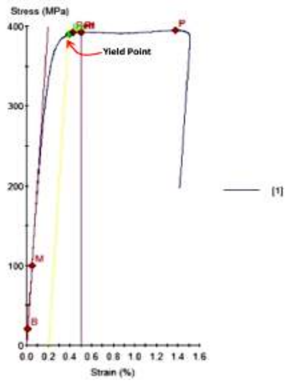

Figure 6. The stress–strain relationship of steel reinforcement.

Deleted: -

Deleted: -

Figure 7 shows the relation between load vs. deflection of the BRC beam and SRC beam from the analysis of experimental data, while Figure 8 shows the relationship between load vs. deflection of BRC beams and SRC beams resulting from the analysis of artificial neural network (ANN) methods. The BRC beam tends to have a large deflection, but when the maximum load is reached, the deflection tends to return to zero if the load is released, as shown in Figure 9. Documentation of the gradual load discharge after the ultimate load has been reached can be seen in the following link: https://goo.gl/6AVWmP [14] and the BRC beam flat back. This shows its compatibility with bamboo strain–stress behavior. The load vs. deflection relationship of the SRC beam shows the existence of an elastic limit, elasto-plastic limit, and plastic, as shown in Figure 7. While the relationship of load vs. deflection of the BRC beam shows a linear line until the maximum load limit and after the peak load, the deflection returns to zero, as shown in Figure 9.

Deleted: A

Deleted: N

Deleted: N

Deleted: s

Formatted: Highlight

Deleted: ,

Deleted:

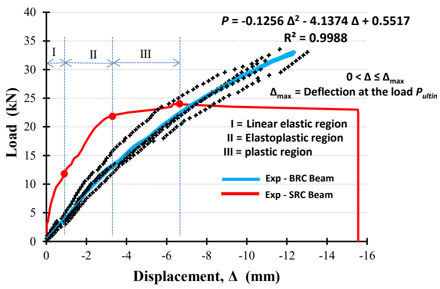

Figure 7. The load vs. deflection relationship of the BRC beam from experiment [14].

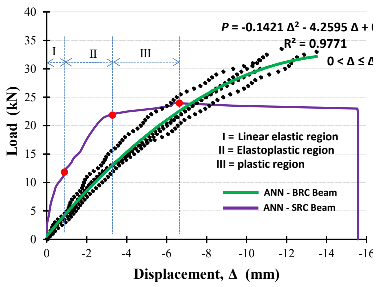

Figure 8. The load vs. deflection relationship of the BRC beam from the ANN method.

Commented [M9]: Please confirm if there is any copyright issue with this figure. For any reused figures or tables, permission shall be obtained from the copyright holder.

Deleted: al

Commented [GD10]: Define if appropriate.

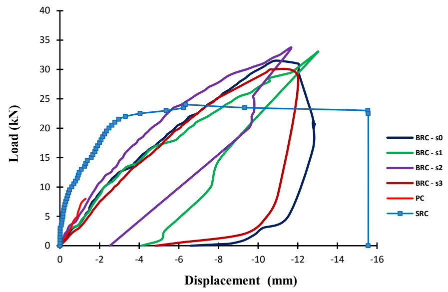

Figure 9. The load vs. deflection relationship of the BRC beam and the SRC beam until the gradual release of the load.

In this case, the ANN studies the network to diagnose the shape and distribution of data from the deflection of BRC beams and SRC beams with different loads. After reaching small and acceptable variations of errors, training in neural networks is stopped. Then, the neural network model is tested, and the results are validated by comparing it with the results of the analysis of experimental data. Every network created in the ANN is trained, tested, and validated for all data samples to identify the best technique. The data input for the network used is the deflection data from the experimental results of the BRC beam and the SRC beam. The deflection data file of the experimental results is saved in the form of MS Excel. Data are distributed into training (70%), testing (15%), and validation (15%).

Deleted: N

Deleted: N

Deleted: D

Deleted: i

Deleted: s

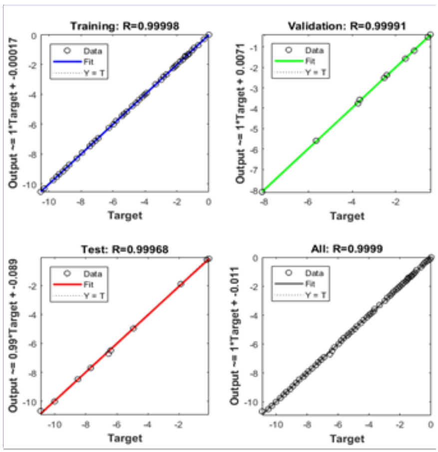

Figure 10. The correlation value of laboratory data and the ANN method (BRC-1 beam).

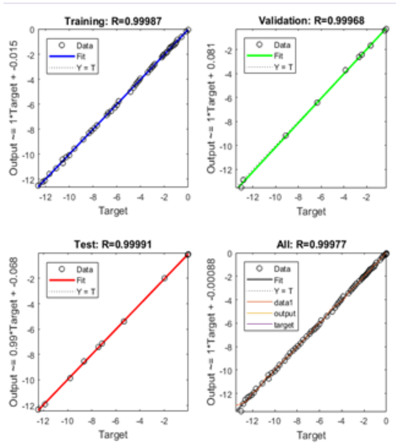

Figure 11. The correlation value of laboratory data and the ANN method (BRC-2 beam).

Commented [M11]: 1.Please provide sharper images for all your figures, Please use the original images.

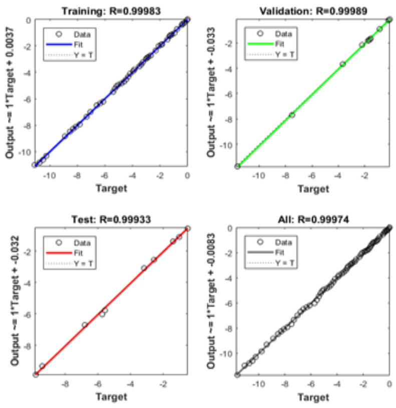

Figure 12. The correlation value of laboratory data and the ANN method (BRC-3 beam).

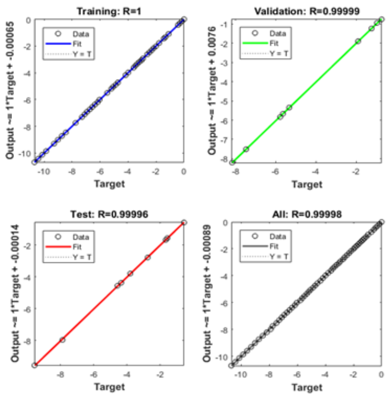

Figure 13. The correlation value of laboratory data and the ANN method (BRC-4 beam).

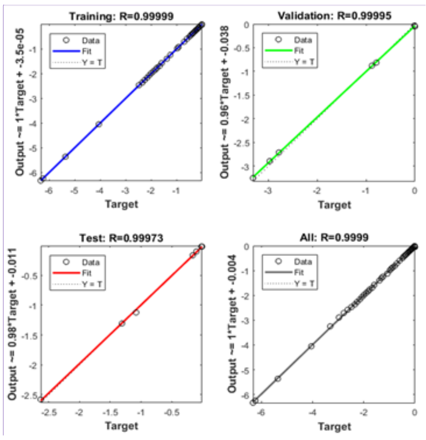

Figure 14. The correlation value of laboratory data and the ANN method (SRC beam).

Figures 10–13 show the prediction of the load vs. deflection relationship of the BRC beam and Figure 14 shows the prediction of the relationship of load vs. deflection of the SRC beam from the ANN method analysis. The correlation value of laboratory data by using ANN shows an average value of R Square of 0.999. The results of predictions by the ANN method show that the percentage of errors is very small, with a maximum error of 0.26%. Overall, the comparison of experimental data with the results of the ANN method predictions shows no more than a 1% error. From the data results of the two analyses and the pattern of load vs. deflection relationships, it can be concluded that the stiffness of the BRC beams is similar. Then, the stiffness prediction with the elasticity modulus parameter can be calculated based on the load vs. deflection relationship graph, as shown in Figure 15.

Figure 15 shows the combined relationship of the load vs. deflection beam of the experimental BRC beam and the ANN analysis results. Figure 15 shows a graph that is coincidental with an error

Commented [M12]: Please provide sharper images for all your figures, Please use the original images.

Deleted: and

Deleted: s

Deleted: z

Deleted: has

Deleted: ities

rate of not more than 1%, so that the combined graph of the load vs. deflection relationship can be used to determine the modulus of elasticity or the stiffness of the BRC beam.

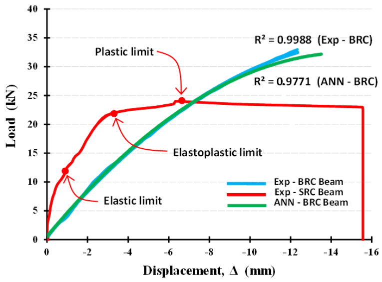

Figure 15. The load vs. deflection relationship the experimental results and ANN analysis.

4. Discussion

Figure 16 shows the results of the two methods of data analysis being a load vs. deflection pattern. From this load vs. deflection pattern, the stiffness of bamboo-reinforced concrete beams can be predicted. Prediction of stiffness with the elasticity modulus parameters can be calculated based on the load vs. deflection relationship graph. The graph of load vs. deflection relationship shows that at 40% ultimate load, the stiffness of the BRC beam has a stiffness lower to 44% than the SRC beam. Meanwhile, if viewed from the graph load vs. deflection relationship, ANN analysis results with experimental results show the same stiffness value up to 80% ultimate load. The stiffness of a BRC beam at a load above 80% ultimate load indicates a stiffness difference that is the stiffness of the BRC beam, so the ANN analysis results are lower than the experimental results, as shown in Figure 16.

Deleted: bamboo r

Commented [GD13]: Please check meaning retained.

Table 1. The value of the average initial crack loads and ultimate loads based on theoretical calculations and experimental.

Specimens	Theoretical Calculations		Flexural Test Results		
	First Crack Load (kN)	Ultimate Load (kN)	Average First Crack Load (kN)	Average Failure Load (kN)	Average Deflection at Failure (mm)
(a) BRC-s0	6,87	32,19	8,25	30,25	11,41
(b) BRC - s1	6,87	32,19	7,25	32,00	12,60
(c) BRC - s2	6,87	32,19	8,00	33,25	12,01
(d) BRC - s3	6,87	32,19	7,50	29,75	9,15
(e) SRC	6,51	16,14	10,00	24,00	6,33

Deleted: Ultimete

Table 1 shows that the initial crack (elastic region) of the BRC beam is in the range of 20% of the ultimate load and 40% of the ultimate load for the SRC beam. Whereas the effect of installing hose-clamps on bamboo reinforcement on the ultimate load of BRC beams is optimum at a distance of 20 cm (BRC-s2) and decreases at a distance of 25 cm, this indicates that installing hose-clamps that are too tight will reduce the elastic properties of bamboo reinforcement and decrease its ductility, as

Deleted: s

shown in Figure 17. Installation of hoses that are too tight does not increase the stiffness of the BRC beam but instead reduces the load capacity. The control of the load vs. deflection relationship with the ANN method is taken from the results of the regression analysis of six beam samples in each group, namely the BRC-s0, BRC-s1, BRC-s2, and BRC-s3 groups, plus one SRC beam, as shown in Figure 7 and Figure 8. The ANN analysis results for each group are regressed back and used as the final result to determine the stiffness of the BRC beam, as shown in Figure 15. The ANN analysis results for each group are shown in Figures 10–13.

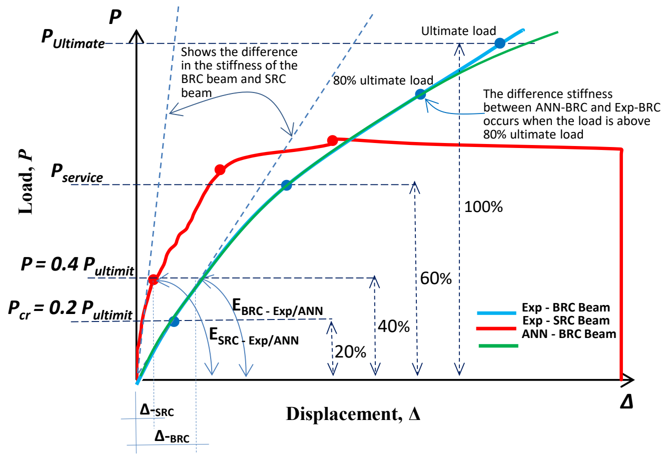

Figure 16. The difference in stiffness between the SRC beam, BRC beam, and BRC beam of ANN analysis result.

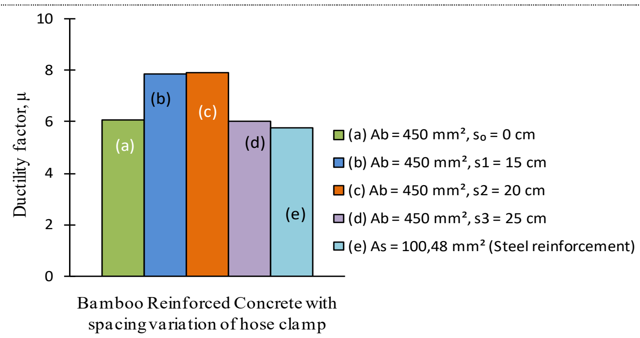

Figure 17. The effect of hose-clamp distance on the ductility value.

Stiffness (*EI*) is the main parameter of the resistance of structural elements to bending deformation. The basic properties and behavior of stress–strain material are the dominant factors determining the size of the rigidity of structural elements. SRC beam stiffness has a greater stiffness than the BRC beam stiffness. This is due to the steel reinforcement having an elasticity modulus greater than the elasticity modulus of bamboo. However, the BRC beam has good elastic properties, in harmony with the pattern of stress–strain relationships of bamboo. This proves that bamboo material has good earthquake energy absorption. The behavior of elastic on the BRC beam can be seen in the video at the following link: https://goo.gl/6AVWmP [14].

Deleted: 6

Deleted: 1

Deleted: -

Deleted: -

Formatted: Highlight

Integrity and rigidity in a structure are essential. Therefore, the low stiffness of the BRC beam is essential to find a solution. Solutions to solve the low stiffness of the BRC beam, such as the graph diagram in Figure 16, can be done in two ways, namely giving strength to bamboo reinforcement and applying the principle of confined concrete [7]. Strengthening of bamboo reinforcement can be achieved by using adhesive, increasing surface roughness, installing hose-clamps that function as hooks and shear connectors, and so on. An equally important solution is to increase the strength of the concrete to support increasing the stiffness of the BRC beam. Previous studies showed that the cause of the majority of BRC beam collapse is by slippage [14] and shear collapse [14]. The principle of confined concrete is fundamental to do by giving shear reinforcement to the BRC beam.

5. Conclusions

Predictions of bamboo-reinforced concrete beam stiffness based on experimental results and analysis results of artificial neural network (ANN) methods show very close similarities or with an error prediction of no more than 1%.

Bamboo-reinforced concrete (BRC) beams have a lower stiffness of up to 40% when compared to steel reinforced concrete (SRC) beams.

The stiffness of the BRC beam of experimental result and the artificial neural network (ANN) analysis results have in common up to 80% of the ultimate load and, afterward, show differences.

The coatings of adhesives, modification of bamboo reinforcement roughness, and the use of shear reinforcement are solutions to increase the stiffness and capacity of the BRC beam.

Installation of a hose-clamp that is too tight does not increase the stiffness of the BRC beam but reduces its elastic properties and reduces its load capacity.

Author Contributions: Conceptualization, M., S., and A.-G.; methodology, M., S., and A.-N.; software, S., S.-A., A.-N., and A.-E.W.; validation, M., I., and I.-C.D.; formal analysis, M., S., and M.-D.; investigation, N., and T.-A.; resources, N.; data curation, M., and S.; writing—original draft preparation, A.-N. and F.; writing—review and editing, M. and S.-D.G.; visualization, M.-R. and S.-H.; supervision, N.; project administration, R.-B.H.; funding acquisition, N. and I.-M. All authors have read and agreed to the published version of the manuscript.

Funding: APC was financed entirely by the DPRM Republic of Indonesia and LPPM of the University of Muhammadiyah Jember, Indonesia.

Acknowledgments: Funding Research is fully borne by the research Program, Directorate of Research and Community Service, Directorate General of Research and Technology Strengthening and Development of the Ministry of Research, Technology, and Higher Education of the Republic of Indonesia

Conflicts of Interest: The authors declare no conflict of interest.

References

1. 1. K. Ghavami. Bamboo as reinforcement in structural concrete elements. *Cement and Concrete Composites*. **2005**, 27, 6, 637–649.
2. 2. A. Agarwal; B. Nanda; D. Maity. Experimental investigation on chemically treated bamboo reinforced concrete beams and columns. *Construction and Building Materials*. **2014**, 71, 610–617.
3. 3. Muhtar. Experimental data from strengthening bamboo reinforcement using adhesives and hose-clamps. *Data in brief*. **2019**, 27, 104827.
4. 4. Muhtar. Cracked Pattern of Bamboo Reinforced Concrete Beams Using Double Reinforcement with the Strengthening on Tensile Reinforcement. *International Journal of Engineering Research and Technology*. 2020, 13, 3, 608–612.
5. 5. M. M. Rahman; M. H. Rashid; M. A. Hossain; M. T. Hasan; M. K. Hasan. Performance evaluation of bamboo reinforced concrete beam. *International Journal of Engineering & Technology IJET-IJENS*. **2011**, 11, 4, 113–118.
6. 6. S. M. Dewi; D. Nuralinah; A. Munawir; M. N. Wijaya. Crack Behavior Study of Bamboo Reinforced Concrete Beam with Additional Pegs in Reinforcing. *International Journal of Civil Engineering and Technology (IJCIET)*. **2018**, 9, 7, 1632–1640.
7. 7. Muhtar; S. M. Dewi; Wisnumurti; A. Munawir. The flexural behavior model of bamboo reinforced concrete beams using a hose clamp. *Proceedings in Materials Science, Engineering, and Chemistry*. **2019**, 1033.

Deleted: like
Deleted: ening
Deleted: bamboo r
Deleted: A
Deleted: N
Deleted: N
Deleted: s
Deleted: Bamboo r
Deleted:
Deleted: A
Deleted: N
Deleted: N
Deleted: s
Deleted: ,
Deleted: ,
Deleted: ,
Deleted: ,
Deleted: ,
Commented [M14]: Please check if the individual contribution of each co-author has been stated.
Deleted: ,
Deleted: financing

8. 8. Muhtar; A. Gunasti; A. S. Manggala; A. F. P. Nusant; Hanafi; A. Nilogiri. Effect of Reinforcement Details on Precast Bridge Frames of Bamboo Reinforced Concrete to Load Capacity and Crack Patterns. *International Journal of Engineering Research and Technology*. **2020**, 13, 4, 631–636.
9. 9. V. Puri; P. Chakrabortty; S. Anand; S. Majumdar. Bamboo reinforced prefabricated wall panels for low-cost housing. *Journal of Building Engineering*. **2017**, 9, 52–59.
10. 10. G. Maruthupandian; R. Saravanan; S. K. S; B. G. Sivakumar. A Study on Bamboo Reinforced Concrete Slabs. *Journal of Chemical and Pharmaceutical Sciences A*. **2016**, 9, 2, 978–980.
11. 11. N. M. Daud; N. M. Nor; M. A. Yusof; M. A. Yahya; V. Munikanan. Axial and Flexural Load Test on Untreated Bamboocrete Multi-Purpose Panel. *International Journal of Integrated Engineering*. **2018**, 10, 28–31.
12. 12. D. D. Tripura; K. D. Singh. Mechanical behavior of rammed earth column : A comparison between unreinforced, steel and bamboo reinforced columns. *Materiales de Construcción*. **2018**, 68, 332, 1–19.
13. 13. S. Rameshwar; A. Kale; P. Rashmirana. Suitability of Bamboo as Reinforcement in Column. *International Journal on Recent and Innovation Trends in Computing and Communication*. **2016**, 4, 4, 270–272.
14. 14. Muhtar; S. M. Dewi; Wisnumurti; A. Munawir. Enhancing bamboo reinforcement using a hose-clamp to increase bond-stress and slip resistance. *Journal of Building Engineering*. **2019**, 26, 100896.
15. 15. Muhtar; S. M. Dewi; Wisnumurti; A. Munawir. The Stiffness and Cracked Pattern of Bamboo Reinforced Concrete Beams Using a Hose Clamp. *International Journal of Civil Engineering and Technology (IJCIET)*. **2018**, 9, 8, 273–284.
16. 16. M. Muhtar. Numerical validation data of tensile stress zones and crack zones in bamboo reinforced concrete beams using the Fortran PowerStation 4.0 program. *Data in Brief*. **2020**, 29, 105332.
17. 17. R. Suryanita; H. Maizir; H. Jingga. Prediction of Structural Response due to Earthquake Load using Artificial Prediction of Structural Response due to Earthquake Load using Artificial Neural Networks. *International conference on "Engineering & Technology, Computer, Basic & Applied Sciences ECBA*, **2016**.
18. 18. H. Naderpour; A. Kheyroddin; G. G. Amiri. Prediction of FRP-confined compressive strength of concrete using artificial neural networks. *Composite Structures*. **2010**, 92, 12, 2817–2829.
19. 19. M. Ahmadi; H. Naderpour; A. Kheyroddin. Utilization of artificial neural networks to prediction of the capacity of CCFT short columns subject to short term axial load. *Archives of Civil and Mechanical Engineering*. **2014**, 14, 3, 510–517.
20. 20. F. Khademi; M. Akbari; M. Nikoo. Displacement determination of concrete reinforcement building using data-driven models. *International Journal of Sustainable Built Environment*, **2017**, 6, 2, 400–411.
21. 21. M. Kaczmarek; A. Szymanska. Application Of Artificial Neural Networks To Predict The Deflections Of Reinforced Concrete Beams. *Studia Geotechnica et Mechanica*. **2016**, 38, 2, 37-46.
22. 22. A. M. Abd; W. D. Salman; Q. W. Ahmed. Ann And Statistical Modelling To Predict The Deflection Of Continuous Reinforced Concrete. *Diyala Journal of Engineering Sciences*, **2015**, 134–143.
23. 23. T. M. Y. S. Tang Ya; R. Alebrahim; N. Fitri; M. Alebrahim. Analysis of Cantilever Beam Deflection under Uniformly Distributed Load using Artificial Neural Networks. *MATEC Web of Conferences*, 2019, 4, 1–5.
24. 24. ASTM C78/C78M-02. *Standard Test Method for Flexural Strength of Concrete (Using Simple Beam with Third-Point Loading)*. ASTM International, USA, **2002**.
25.

28.

Page 1: [1] Commented [GD1]	Georgia Dey	19/08/2020 09:33:00

Attention AE/ME. The following layout issues have not been checked by the English Editing Department and must be carefully verified by the AE/Layout Department: All callout issues, bold usage of callouts, and references to callouts in the text. Correct callout usage in figures. Figure and Table layout issues. Footnote formatting and Glossaries have not been checked. En dash usage for negative values, en dash usage to indicate relationships, en dash usage to indicate bonds (especially in chemistry). The English Editing Department is not responsible for correct italic usage for genes, proteins and technical terminology. This responsibility belongs to the authors. The following are also not checked: spacing between numbers and units of measurement, ratios, en dashes for ranges, date and time formats, punctuation in equation lines, and less than/more than spacing (< >). Finally, capitalization and layout of titles/headings must be properly checked as well as ensuring 'Eq.' and 'Fig.' are properly spelled out, as these are layout issues.

Page 1: [2] Commented [M2]	MDPI	19/08/2020 11:45:00

Please carefully check the accuracy of names and affiliations. Changes will not be possible after proofreading.

Page 1: [3] Commented [M3]	MDPI	19/08/2020 11:50:00

Changed by multiplication sign, please confirm.

crystals

MDPI

Article

The Prediction of Stiffness of Bamboo-Reinforced Concrete Beams Using Experiment Data and Artificial Neural Networks (ANNs)

Muhtar [1,]*, Amri-Gunasti [1], Suhardi [2], Nursaid [1], Irawati [1], Ilanka-Cahya Dewi [1], Moh.-Dasuki [1], Sofia-Ariyani [1], Fitriana [1], Idris-Mahmudi [1], Taufan-Abadi [1], Miftahur-Rahman [1], Syarif-Hidayatullah [1], Agung-Nilogiri [1], Senki-Desta Galuh [1], Ari Eko Wardoyo [1] and Rofi-Budi Hamduwibawa [1]

[1] University of Muhammadiyah Jember, Jember, 68121, Indonesia; amrigunasti@unmuhjember.ac.id (A.-G.); nursaid@unmuhjember.ac.id (N.); irawati@unmuhjember.ac.id (I.); ilankadewi@unmuhjember.ac.id (I.-C.D.); moh.dasuki22@unmuhjember.ac.id (M.-D.); sofia.ariyani@unmuhjember.ac.id (S.-A.); fitriana@unmuhjember.ac.id (F.); idrismahmudi@unmuhjember.ac.id (I.-M.); taufan.abadi@unmuhjember.ac.id (T.-A.); miftahurrahman@unmuhjember.ac.id (M.-R.); syarifhidayatullah@unmuhjember.ac.id (S.-H.); agungnilogiri@unmuhjember.ac.id (A.-N.); senki.desta@unmuhjember.ac.id (S.-D.G.); arieko@unmuhjember.ac.id (A.-E.W.); rofi.hamduwibawa@unmuhjember.ac.id (R.-B.H.)

[2] University of Jember, Jember, 68121, Indonesia; hardi.ftp@unej.ac.id

* Correspondence: muhtar@unmuhjember.ac.id

Received: 3 August 2020; Accepted: 19 August 2020; Published: date

Abstract: Stiffness is the main parameter of the beam's resistance to deformation. Based on advanced research, the stiffness of bamboo-reinforced concrete beams (BRC) tends to be lower than the stiffness of steel-reinforced concrete beams (SRC). However, the advantage of bamboo-reinforced concrete beams has enough good ductility according to the fundamental properties of bamboo, which have high tensile strength and high elastic properties. This study aims to predict and validate the stiffness of bamboo-reinforced concrete beams from the experimental results data using artificial neural networks (ANNs). The number of beam test specimens were 25 pieces with a size of 75 mm × 150 mm × 1100 mm. The testing method uses the four-point method with simple support. The results of the analysis showed the similarity between the stiffness of the beam's experimental results with the artificial neural network (ANN) analysis results. The similarity rate of the two analyses is around 99% and the percentage of errors is not more than 1%, both for bamboo-reinforced concrete beams (BRC) and steel-reinforced concrete beams (SRC).

Keywords: bamboo-reinforced concrete (BRC); stiffness prediction; artificial neural network (ANN)

1. Introduction

Some of the advantages of bamboo include having high tensile strength [1], easy to split, cut, elastic fibers, optimal in bearing loads, and it is not a pollutant. At the same time, the weakness of bamboo as a construction material is easily attacked by insects, because the starch content in bamboo is quite high. Therefore, bamboo as a building material requires treatment, such as immersion in water [2,3] and the application of adhesives and waterproof layers [3]. The application of adhesive and waterproof coating has increased the load capacity and stiffness of the BRC beam [4]. Bamboo as a reinforcement of concrete structural elements has been widely used, among other things, as beam

Comment [M1]: Please provide full name.

Comment [M2]: Please carefully check the accuracy of names and affiliations. Changes will not be possible after proofreading.

Comment [M3]: Please provide full names for authors.

Comment [M4]: Please provide full name.

Comment [M5]: The email addresses is not consistent with submission system, please revise.

Comment [M6]: Changed by multiplication sign, please confirm.

reinforcement [2,5–7], bridge frame reinforcement [8], plate or panel reinforcement [9–11], and column reinforcement [12,13].

The most important mechanical properties of bamboo-reinforced concrete beams are stress, strain, and stiffness. Some previous researchers concluded that bamboo-reinforced concrete beams have lower stiffness compared to steel reinforced concrete beams but have elastic properties and high ductility, so that they are effective in absorbing earthquake energy [14,15]. However, low rigidity will lead to reduced construction integrity and excessive structural deformation. The behavior of materials and construction elements, especially the stiffness parameters can be known through the relationship of load and deflection, as shown in Figure 1.

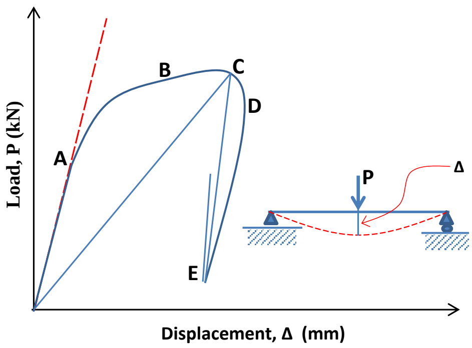

Figure 1. The load vs. deflection relationships of the reinforced concrete beam [15].

Comment [M7]: Please confirm if there is any copyright issue with this figure. For any reused figures or tables, permission shall be obtained from the copyright holder.

The stiffness of bamboo-reinforced concrete beams (*EI*) is the main factor of structural resistance to the bending deformation of BRC beams. Beam stiffness is a function of the modulus of elasticity of the material (*E*) and the moment of inertia (*I*). Moments of inertia before cracking use I_g, and after cracking they use I_{cr}. The effective inertia moment is the value between I_g and I_{cr}. This understanding can be seen from the behavior of the load vs. deflection relationship in Figure 1. In general, the determination of beam stiffness is based on the results of the beam flexural test, while the calculation of elasticity modulus (*E*) of BRC beams for testing beams with two load points can follow Equations (1,2) [15].

$$E = \frac{23PL^3}{648\Delta I}(N/mm^2) \quad (1)$$

$$\Delta = \frac{23PL^3}{648EI}(mm) \quad (2)$$

where *E* is the elasticity modulus, *Δ* is the initial crack, *P* is the initial crack load, *L* is the span, and *I* is the inertia moment of the cross-section.

Making conclusions from the results of research on the behavior of bamboo-reinforced concrete beams (BRC) is not easy to take. Correct conclusions must go through data validation and data analysis with other methods, such as statistical analysis, the finite element method [16], or the artificial neural network (ANN) method [17]. The determination of the stiffness of bamboo-reinforced concrete beams (BRC) from the experimental results must be validated by other methods, such as the artificial neural network (ANN) method.

Artificial neural networks (ANNs) consist of many neurons. Neurons are grouped into several layers. Neurons in each layer are connected with neurons in other layers. This does not apply to the input and output layers but only to the layers in between. Information received at the input layer is continued to the layers in ANN one by one until it reaches the output layer. The layer that lies between the input and output is called the hidden layer. However, not all ANNs have a hidden layer; some are only input and output layers.

Artificial neural networks (ANNs) are a powerful tool for solving complex problems in the field of civil engineering. Many researchers have used the ANN method for many structural engineering studies, such as predicting the compressive strength of concrete [18], axial strength of composite columns [19], and determination of displacement of RC buildings [20]. Determination and control of BRC beam stiffness are based on load vs. deflection diagrams. Load data and deflection of experimental results are used as input data and target data in the analysis of artificial neural networks (ANNs).

Comment [GD8]: Define if appropriate.

Some previous researchers have concluded that artificial neural networks (ANNs) can be an alternative in calculating deflection in a reinforced concrete beam. The results of deflection calculations on reinforced concrete using ANN proved to be very effective [21]. ANN is also very well used to predict deflection in the concrete beam with a very strong correlation level of 97.27% to the test data [22]. Likewise, the use of ANN to predict deflection in cantilever beams produces very accurate outcomes [23]. In this paper, we use uniform load input data, while the target data are the deflection of laboratory test results. Distribution of ANN model data composition consists of 70% training, 15% validation, and 15% testing. The schematic of ANN architecture for rectangular beams is shown in Figure 2.

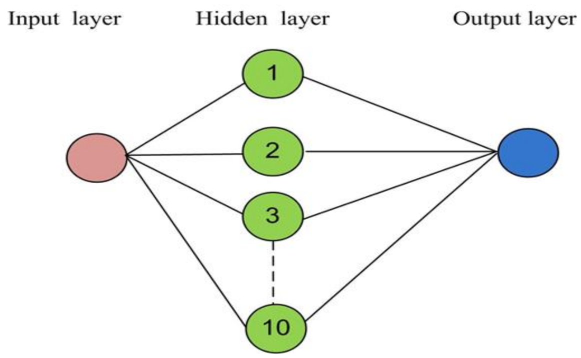

Figure 2. Schematic of ANN architecture for rectangular beams.

Comment [M9]: Position changed, please confirm.

The purpose of this study is to validate the behavior and stiffness of the BRC beam experimental results with the artificial neural network (ANN) method. Errors resulting from experimental data are usually caused by some things, such as human errors, calibration of tools that have expired, test method errors, and test items that do not match. Therefore, the experimental data are evaluated and compared with the results of the artificial neural network (ANN) method. In this study, the experimental data are thought to have a large deviation from the results of the artificial neural network (ANN) method. Then, an efficient ANN-based computational technique is presented to estimate the load vs. deflection of bamboo-reinforced concrete blocks (BRC). Furthermore, stiffness observations are made at the same loading point.

2. Materials and Methods

Experimental data were obtained from a single reinforced BRC beam bending test with two load points based on ASTM C 78-02 [24]. The size of bamboo reinforcement is 15 mm × 15 mm, which is treated first through immersion, drying, and the waterproof coating using Sikadur®-752 [3]. As a strengthening of bamboo reinforcement used diameter hose-clamps ¾" [8]. The number of beam test specimens were 25 pieces with a size of 75 mm × 150 mm × 1100 mm consisting of 24 BRC beams and 1 SRC beam with steel reinforcement. The detailed image of the BRC beam specimen is shown in Figure 3. The design of the concrete mixture in this study was Portland Pozzolana Cement (PPC), sand, coarse aggregate, and water with a proportion of 1:1.81:2.82:0.52. The average compressive strength of concrete at the age of 28 days is 31.31 MPa. The steel used is plain steel with f_y = 240 MPa.

The beam flexural test is carried out on two simple supports, namely joint support and roller support. Load in the form of a centralized load divided into two load points with a distance of ⅓L from the support. The strain gauge is mounted on the bamboo reinforcement with a distance of ½L from the support to determine the strain that is occurring. To detect deflection, a linear variable differential transformer is installed at a distance of ½L from the support. To get the stages of loading from zero until the beam collapses, a hydraulic jack and load cell are used that are connected to the load indicator. Loading is carried out slowly at a speed of 8 kg/cm²–10 kg/cm². Load reading on the load indicator is used to control the hydraulic jack pump, deflection, and strain according to the planned loading stage. However, when the test specimen reaches the ultimate load, deflection readings become the control of readings of the strain and load. Hydraulic jack pumping continues to take place slowly according to the deflection reader command. The collapse pattern is observed and identified through cracks that occur, starting from the first crack until the beam collapses. The BRC beam test setting is shown in Figure 4.

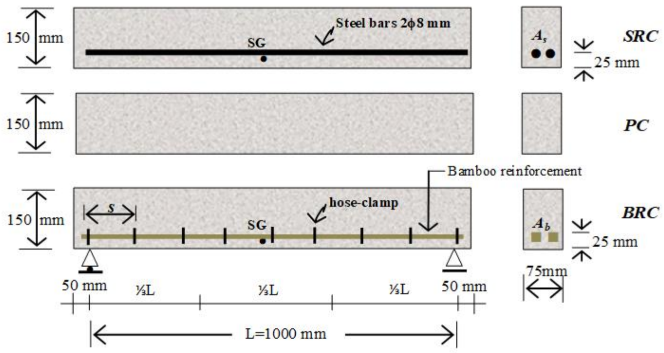

Information:
SRC = Steel reinforced concrete
BRC = Bamboo reinforced concrete
PC = Plain concrete
SG = Strain gauge
s = Distance of hose-clamp
(Variation of s0 = 0 cm, s1 = 15 cm, s2 = 20 cm, and s3 = 25 cm)
A_s = Area of steel reinforced (As = 100,48 mm²)
A_b = Area of bamboo reinforced
(Variation of Ab = 140 mm², 200 mm², and 450 mm²)

Figure 3. Geometry and details of bamboo-reinforced concrete beams.

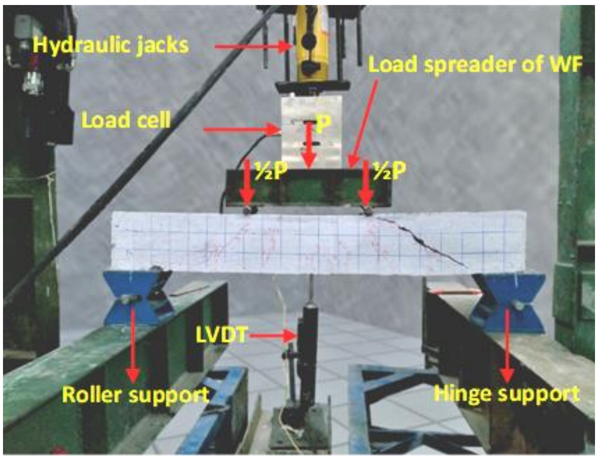

Figure 4. Test arrangement of bamboo-reinforced concrete beams.

3. Results

Mechanical properties and stress–strain characteristics of steel and bamboo materials are the dominant factors that influence the shape of the load vs. deflection relationship behavior models. The difference in the stress and strain relationship pattern of steel and bamboo is seen in the difference in melting point and fracture stress, as shown in Figures 5 and 6. Steel reinforcement shows a clear melting point, whereas bamboo reinforcement does not show a clear melting point. Both of them show a clear stress fracture point, but in bamboo reinforcement, after fracture stress occurs, the strain–stress relationship pattern tends to return to zero, as shown in Figure 5. This shows that bamboo has good elastic properties.

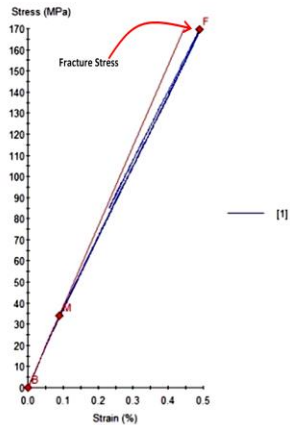

Figure 5. The stress–strain relationship of normal bamboo reinforcement.

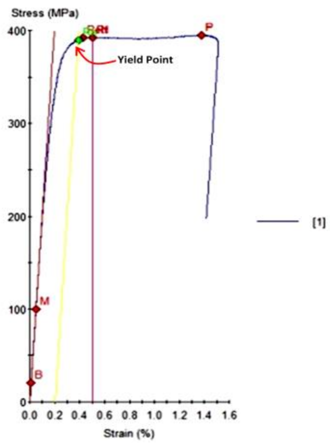

Figure 6. The stress–strain relationship of steel reinforcement.

Figure 7 shows the relation between load vs. deflection of the BRC beam and SRC beam from the analysis of experimental data, while Figure 8 shows the relationship between load vs. deflection of BRC beams and SRC beams resulting from the analysis of artificial neural network (ANN) methods. The BRC beam tends to have a large deflection, but when the maximum load is reached, the deflection tends to return to zero if the load is released, as shown in Figure 9. Documentation of the gradual load discharge after the ultimate load has been reached can be seen in the following link: https://goo.gl/6AVWmP [14] and the BRC beam flat back. This shows its compatibility with bamboo strain–stress behavior. The load vs. deflection relationship of the SRC beam shows the existence of an elastic limit, elasto-plastic limit, and plastic, as shown in Figure 7. While the relationship of load vs. deflection of the BRC beam shows a linear line until the maximum load limit and after the peak load, the deflection returns to zero, as shown in Figure 9.

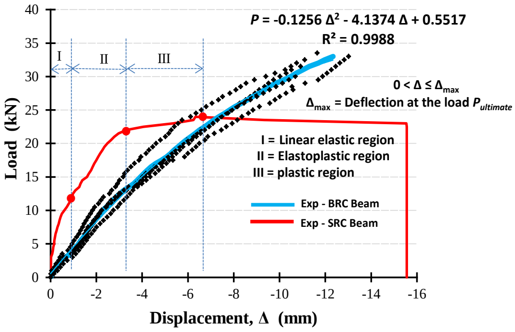

Figure 7. The load vs. deflection relationship of the BRC beam from experiment [14].

Comment [M10]: Please confirm if there is any copyright issue with this figure. For any reused figures or tables, permission shall be obtained from the copyright holder.

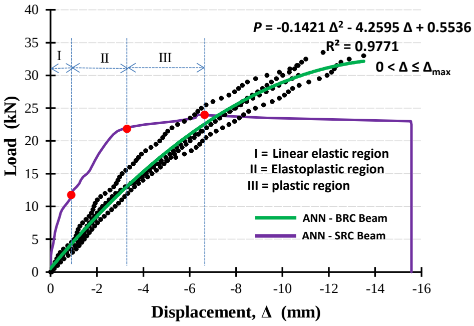

Figure 8. The load vs. deflection relationship of the BRC beam from the ANN method.

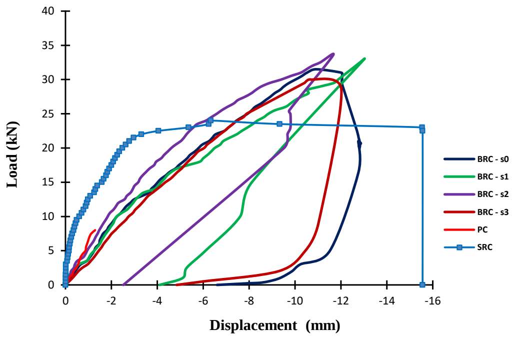

Figure 9. The load vs. deflection relationship of the BRC beam and the SRC beam until the gradual release of the load.

In this case, the ANN studies the network to diagnose the shape and distribution of data from the deflection of BRC beams and SRC beams with different loads. After reaching small and acceptable variations of errors, training in neural networks is stopped. Then, the neural network model is tested, and the results are validated by comparing it with the results of the analysis of experimental data. Every network created in the ANN is trained, tested, and validated for all data samples to identify the best technique. The data input for the network used is the deflection data from the experimental results of the BRC beam and the SRC beam. The deflection data file of the experimental results is saved in the form of MS Excel. Data are distributed into training (70%), testing (15%), and validation (15%).

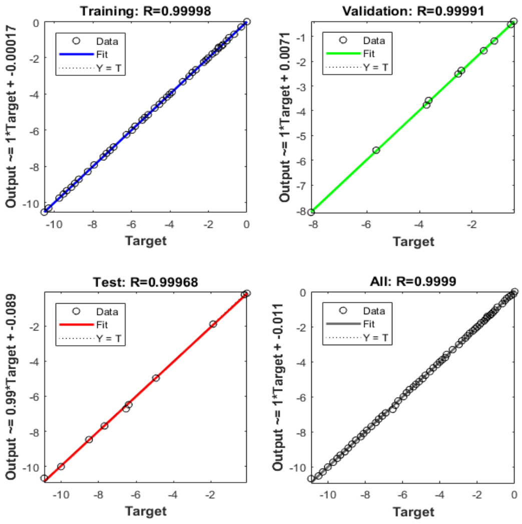

Figure 10. The correlation value of laboratory data and the ANN method (BRC-1 beam).

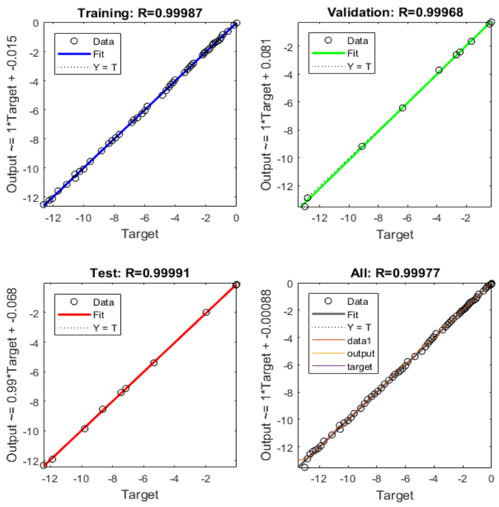

Figure 11. The correlation value of laboratory data and the ANN method (BRC-2 beam).

Comment [M11]: 1.Please provide sharper images for all your figures, Please use the original images.

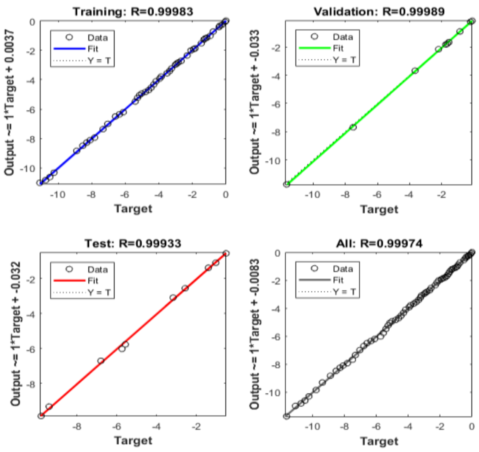

Figure 12. The correlation value of laboratory data and the ANN method (BRC-3 beam).

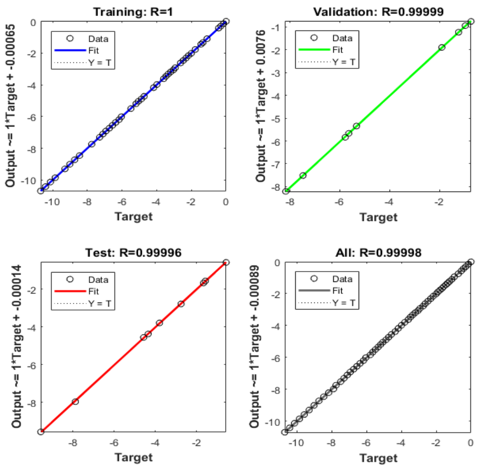

Figure 13. The correlation value of laboratory data and the ANN method (BRC-4 beam).

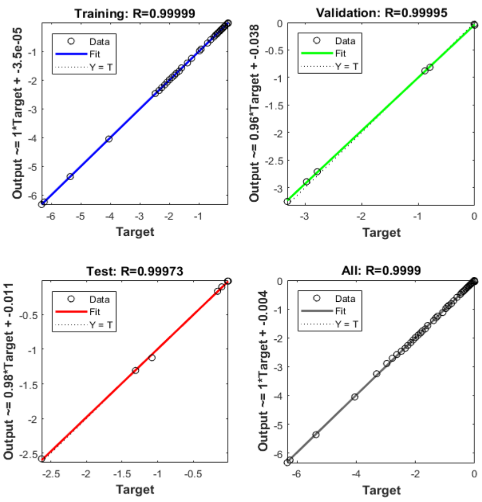

Figure 14. The correlation value of laboratory data and the ANN method (SRC beam).

Comment [M12]: Please provide sharper images for all your figures, Please use the original images.

Figures 10–13 show the prediction of the load vs. deflection relationship of the BRC beam and Figure 14 shows the prediction of the relationship of load vs. deflection of the SRC beam from the ANN method analysis. The correlation value of laboratory data by using ANN shows an average value of R Square of 0.999. The results of predictions by the ANN method show that the percentage of errors is very small, with a maximum error of 0.26%. Overall, the comparison of experimental data with the results of the ANN method predictions shows no more than a 1% error. From the data results of the two analyses and the pattern of load vs. deflection relationships, it can be concluded that the stiffness of the BRC beams is similar. Then, the stiffness prediction with the elasticity modulus parameter can be calculated based on the load vs. deflection relationship graph, as shown in Figure 15.

Figure 15 shows the combined relationship of the load vs. deflection beam of the experimental BRC beam and the ANN analysis results. Figure 15 shows a graph that is coincidental with an error rate of not more than 1%, so that the combined graph of the load vs. deflection relationship can be used to determine the modulus of elasticity or the stiffness of the BRC beam.

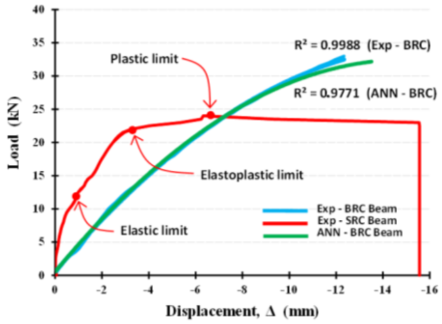

Figure 15. The load vs. deflection relationship the experimental results and ANN analysis.

4. Discussion

Figure 16 shows the results of the two methods of data analysis being a load vs. deflection pattern. From this load vs. deflection pattern, the stiffness of bamboo-reinforced concrete beams can be predicted. Prediction of stiffness with the elasticity modulus parameters can be calculated based on the load vs. deflection relationship graph. The graph of load vs. deflection relationship shows that at 40% ultimate load, the stiffness of the BRC beam has a stiffness lower to 44% than the SRC beam. Meanwhile, if viewed from the graph load vs. deflection relationship, ANN analysis results with experimental results show the same stiffness value up to 80% ultimate load. The stiffness of a BRC beam at a load above 80% ultimate load indicates a stiffness difference that is the stiffness of the BRC beam, so the ANN analysis results are lower than the experimental results, as shown in Figure 16.

Comment [GD13]: Please check meaning retained.

Table 1. The value of the average initial crack loads and ultimate loads based on theoretical calculations and experimental.

Specimens	Theoretical Calculations		Flexural Test Results		
	First Crack Load (kN)	Ultimate Load (kN)	Average First Crack Load (kN)	Average Failure Load (kN)	Average Deflection at Failure (mm)
(a) BRC-s0	6.87	32.19	8.25	30.25	11.41
(b) BRC - s1	6.87	32.19	7.25	32.00	12.60

(c) BRC - s2	6.87	32.19	8.00	33.25	12.01
(d) BRC - s3	6.87	32.19	7.50	29.75	9.15
(e) SRC	6.51	16.14	10.00	24.00	6.33

Comment [M14]: The comma are replaced with dot, please confirm whether it is correct.

Table 1 shows that the initial crack (elastic region) of the BRC beam is in the range of 20% of the ultimate load and 40% of the ultimate load for the SRC beam. Whereas the effect of installing hose-clamps on bamboo reinforcement on the ultimate load of BRC beams is optimum at a distance of 20 cm (BRC-s2) and decreases at a distance of 25 cm, this indicates that installing hose-clamps that are too tight will reduce the elastic properties of bamboo reinforcement and decrease its ductility, as shown in Figure 17. Installation of hoses that are too tight does not increase the stiffness of the BRC beam but instead reduces the load capacity. The control of the load vs. deflection relationship with the ANN method is taken from the results of the regression analysis of six beam samples in each group, namely the BRC-s0, BRC-s1, BRC-s2, and BRC-s3 groups, plus one SRC beam, as shown in Figures 7 and 8. The ANN analysis results for each group are regressed back and used as the final result to determine the stiffness of the BRC beam, as shown in Figure 15. The ANN analysis results for each group are shown in Figures 10–13.

Comment [M15]: The citation should be mentioned before table 1, please put it into the proper position.

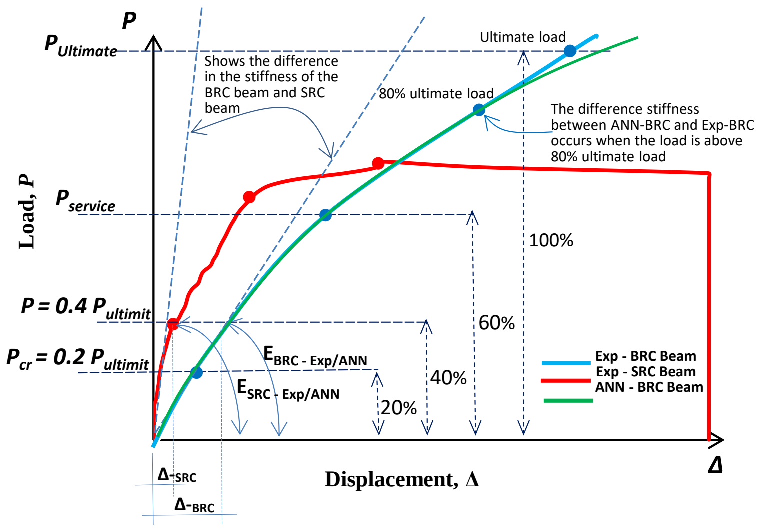

Figure 16. The difference in stiffness between the SRC beam, BRC beam, and BRC beam of ANN analysis result.

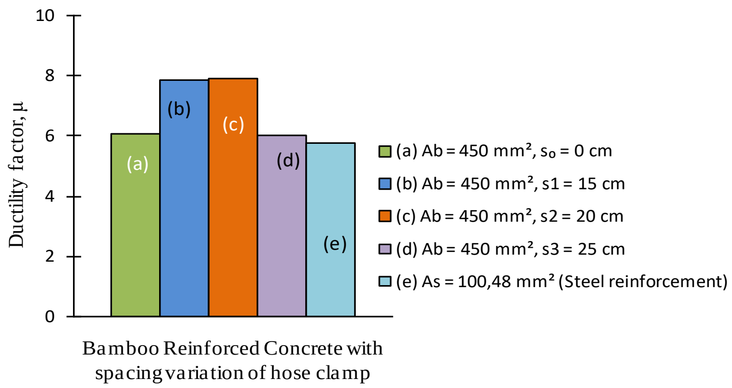

Figure 17. The effect of hose-clamp distance on the ductility value.

Stiffness (*EI*) is the main parameter of the resistance of structural elements to bending deformation. The basic properties and behavior of stress–strain material are the dominant factors determining the size of the rigidity of structural elements. SRC beam stiffness has a greater stiffness than the BRC beam stiffness. This is due to the steel reinforcement having an elasticity modulus greater than the elasticity modulus of bamboo. However, the BRC beam has good elastic properties, in harmony with the pattern of stress–strain relationships of bamboo. This proves that bamboo material has good earthquake energy absorption. The behavior of elastic on the BRC beam can be seen in the video at the following link: https://goo.gl/6AVWmP [14].

Integrity and rigidity in a structure are essential. Therefore, the low stiffness of the BRC beam is essential to find a solution. Solutions to solve the low stiffness of the BRC beam, such as the graph diagram in Figure 16, can be done in two ways, namely giving strength to bamboo reinforcement and applying the principle of confined concrete [7]. Strengthening of bamboo reinforcement can be achieved by using adhesive, increasing surface roughness, installing hose-clamps that function as hooks and shear connectors, and so on. An equally important solution is to increase the strength of the concrete to support increasing the stiffness of the BRC beam. Previous studies showed that the cause of the majority of BRC beam collapse is by slippage [14] and shear collapse [14]. The principle of confined concrete is fundamental to do by giving shear reinforcement to the BRC beam.

5. Conclusions

Predictions of bamboo-reinforced concrete beam stiffness based on experimental results and analysis results of artificial neural network (ANN) methods show very close similarities or with an error prediction of no more than 1%.

Bamboo-reinforced concrete (BRC) beams have a lower stiffness of up to 40% when compared to steel reinforced concrete (SRC) beams.

The stiffness of the BRC beam of experimental result and the artificial neural network (ANN) analysis results have in common up to 80% of the ultimate load and, afterward, show differences.

The coatings of adhesives, modification of bamboo reinforcement roughness, and the use of shear reinforcement are solutions to increase the stiffness and capacity of the BRC beam.

Installation of a hose-clamp that is too tight does not increase the stiffness of the BRC beam but reduces its elastic properties and reduces its load capacity.

Author Contributions: Conceptualization, M., S., and A.-G.; methodology, M., S., and A.-N.; software, S., S.-A., A.-N., and A.-E.W.; validation, M., I., and I.-C.D.; formal analysis, M., S., and M.-D.; investigation, N., and T.-A.; resources, N.; data curation, M., and S.; writing—original draft preparation, A.-N. and F.; writing—review and editing, M. and S.-D.G.; visualization, M.-R. and S.-H.; supervision, N.; project administration, R.-B.H.; funding acquisition, N. and I,-M. All authors have read and agreed to the published version of the manuscript.

Funding: APC was financed entirely by the DPRM Republic of Indonesia and LPPM of the University of Muhammadiyah, Jember, Indonesia.

Comment [M16]: Please check if the individual contribution of each co-author has been stated.

Acknowledgments: Funding Research is fully borne by the research Program, Directorate of Research and Community Service, Directorate General of Research and Technology Strengthening and Development of the Ministry of Research, Technology, and Higher Education of the Republic of Indonesia

Conflicts of Interest: The authors declare no conflict of interest.

References

1. Ghavami, K. Bamboo as reinforcement in structural concrete elements. *Cem. Concr. Compos*. **2005**, *27*, 637–649.
2. Agarwal, A.; Nanda, B.; Maity, D. Experimental investigation on chemically treated bamboo reinforced concrete beams and columns. *Constr. Build. Mater*. **2014**, *71*, 610–617.
3. Muhtar. Experimental data from strengthening bamboo reinforcement using adhesives and hose-clamps. *Data Brief*. **2019**, *27*, 104827.
4. Muhtar. Cracked Pattern of Bamboo Reinforced Concrete Beams Using Double Reinforcement with the Strengthening on Tensile Reinforcement. *Int. J. Eng. Res. Technol.* **2020**, *13*, 608–612.
5. Rahman, M.M.; Rashid, M.H.; Hossain, M.A.; Hasan, M.T.; Hasan, M.K. Performance evaluation of bamboo reinforced concrete beam. *Int. J. Eng. Res. Technol. IJET-IJENS*. **2011**, *11*, 113–118.
6. Dewi, S.M.; Nuralinah, D.; Munawir, A.; Wijaya, M.N. crack behavior study of bamboo reinforced concrete beam with additional pegs in reinforcing. *Int. J. Civ. Eng. Technol. (IJCIET).* **2018**, *9*, 1632–1640.
7. Muhtar; Dewi, S.M.; Wisnumurti; Munawir, A. The flexural behavior model of bamboo reinforced concrete beams using a hose clamp. *Proc. Mater. Sci. Eng. Chem*. **2019**, 1033.
8. Muhtar, A. Gunasti; Manggala, A.S.; Nusant, A.F.P.; Hanafi; Nilogiri, A. Effect of reinforcement details on precast bridge frames of bamboo reinforced concrete to load capacity and crack patterns. *Int. J. Eng. Res. Technol.* **2020**, *13*, 631–636.
9. Puri, V.; Chakrabortty, P.; Anand, S.; Majumdar, S. Bamboo reinforced prefabricated wall panels for low-cost housing. *J. Build. Eng.* **2017**, *9*, 52–59.
10. Maruthupandian, G.; Saravanan, R.; S Suresh,K.S.; Sivakumar, B.G. A Study on Bamboo Reinforced Concrete Slabs. *J. Chem. Pharm. Sci. A* **2016**, *9*, 978–980.
11. Daud, N.M.; Nor, N.M.; Yusof, M.A.; Yahya, M.A.; Munikanan, V. Axial and flexural load test on untreated bamboocrete multi-purpose panel. *Int. J. Integr. Eng*. **2018**, *10*, 28–31.
12. D. D. Tripura; K. D. Singh. Mechanical behavior of rammed earth column : A comparison between unreinforced, steel and bamboo reinforced columns. *Mater. Construcción* **2018**, *68*, 1–19.
13. S. Rameshwar; A. Kale; P. Rashmirana. Suitability of Bamboo as Reinforcement in Column. *Int. J. Recent Innov. Trends Comput. Commun.* **2016**, *4*, 270–272.
14. Muhtar; S. M. Dewi; Wisnumurti; A. Munawir. Enhancing bamboo reinforcement using a hose-clamp to increase bond-stress and slip resistance. *J. Build. Eng*. **2019**, *26*, 100896.
15. Muhtar; S. M. Dewi; Wisnumurti; A. Munawir. The Stiffness and Cracked Pattern of Bamboo Reinforced Concrete Beams Using a Hose Clamp. *Int. J. Civ. Eng. Technol. (IJCIET).* **2018**, *9*, 8, 273–284.
16. Muhtar, M. Numerical validation data of tensile stress zones and crack zones in bamboo reinforced concrete beams using the Fortran PowerStation 4.0 program. *Data Brief* **2020**, *29*, 105332.
17. Suryanita, R.; Maizir, H.; Jingga, H. Prediction of Structural Response due to Earthquake Load using Artificial Prediction of Structural Response due to Earthquake Load using Artificial Neural Networks. In *International Conference on "Engineering & Technology, Computer , Basic & Applied Sciences"*, Bangkok, Thailand, 20–21 June 2016.
18. Naderpour, H.; Kheyroddin, A.; Amiri, G.G. Prediction of FRP-confined compressive strength of concrete using artificial neural networks. *Compos. Struct.* **2010**, *92*, 2817–2829.
19. Ahmadi, M.; Naderpour, H.; Kheyroddin, A. Utilization of artificial neural networks to prediction of the capacity of CCFT short columns subject to short term axial load. *Arch. Civ. Mech. Eng.* **2014**, *14*, 510–517.
20. Khademi, F.; Akbari, M.; Nikoo, M. Displacement determination of concrete reinforcement building using data-driven models. *Int. J. Sustain. Built Environ.* **2017**, *6*, 400–411.
21. Kaczmarek, M.; Szymanska, A. application of artificial neural networks to predict the deflections of reinforced concrete beams. *Studia Geotech. Mech.* **2016**, *38*, 37–46.
22. Abd, A.M.; Salman, W.D.; Ahmed, Q.W. Ann and statistical modelling to predict the deflection of continuous reinforced concrete. *Diyala J. Eng. Sci.* **2015**, 134–143.

Comment [M17]: Newly added, please confirm.

23. Ya, T.M.Y.S.T.; Alebrahim, R.; Fitri, N.; Alebrahim, M. Analysis of Cantilever Beam Deflection under Uniformly Distributed Load using Artificial Neural Networks. *MATEC Web Conf.* **2019**, *4*, 1–5.
24. ASTM C78/C78M-02. *Standard Test Method for Flexural Strength of Concrete (Using Simple Beam with Third-Point Loading)*; ASTM International: Sikangshihoken, PA, USA, 2002.

Comment [Ma18]: Newly added information, please confirm.

3.